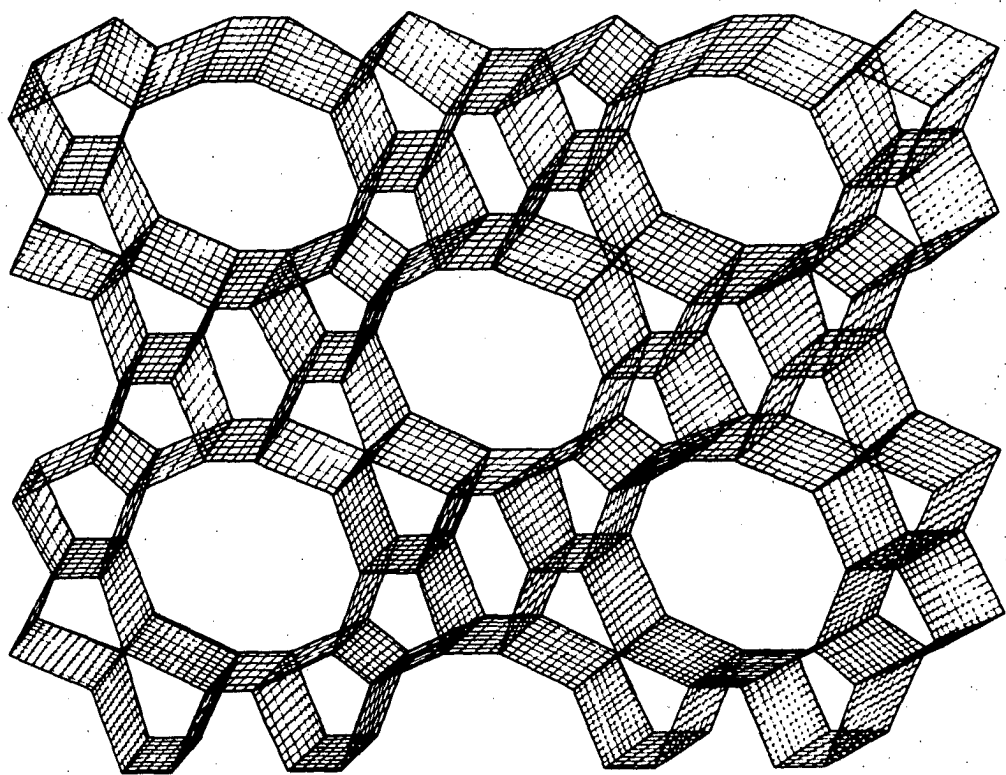# HIGH-SILICA ZEOLITES

and their use as catalyst in organic chemistry

R.A. le Febre
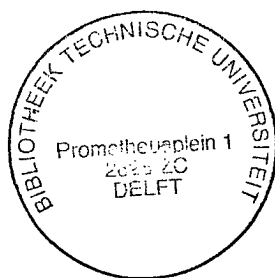
HIGH-SILICA ZEOLITES

and their use as catalyst in organic chemistry

HIGH-SILICA ZEOLITES

and their use as catalyst in organic chemistry

Proefschrift ter verkrijging van de graad van doctor

aan de Technische Universiteit Delft, op gezag van

de Rector Magnificus, Prof. drs. P.A. Schenck, in het

openbaar te verdedigen ten overstaan van een

commissie aangewezen door het College van Dekanen

op donderdag 23 maart 1989 te 16.00 uur, door

Robert Arie le Febre

geboren te Leiden

scheikundig doctorandus

Dit proefschrift is goedgekeurd door de promotor

Prof. dr. ir. H. van Bekkum

TABLE OF CONTENTS

Drawings: Mr. W.J. Jongeleen

Aan: Annelies
     Mijn ouders
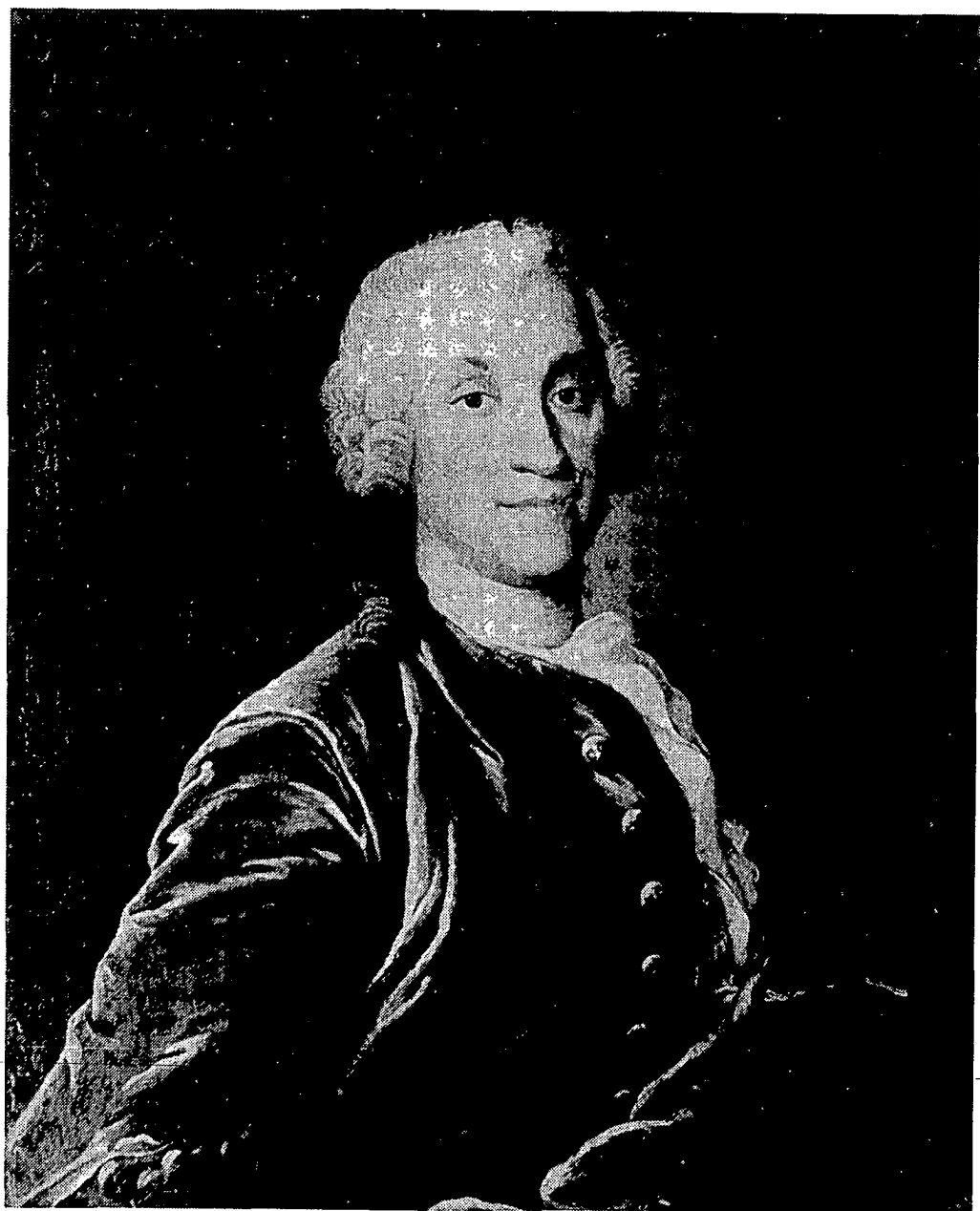
A.F. Crønstedt. 1722 – 1765. Courtesy of the Swedish Academy of Science.

CHAPTER I

ZEOLITES: AN INTRODUCTION

GENERAL OVERVIEW

The term zeolite was first mentioned in scientific literature by Cronstedt (see opposite page) in 1756 (1) as the name of an aluminosilicate mineral (stilbite) that seemed to steam when heated. The word zeolite was derived from the Greek words zeo and lithos meaning boiling stone. Since that time, 41 naturally occurring zeolites have been identified (2). The first ones were observed in basalts which had been altered by hydrothermal geological processes that sometimes formed crystals of museum display quality. Late in the 19th century zeolite occurrence in sedimentary tuffs and marine sediments was detected (3). Both before and after the second World War these reports became numerous, with zeolite formations often found in fairly large amounts, present in vitric tuffs, dry saline lake beds (in association with bentonites) and in low grade metamorphic rocks. For example, the city of Naples is underlain by a zeolitic deposit, some 200 km^2 in area, which is only five to ten thousand years old.

From the early 1940's onwards systematic synthesis studies on zeolites were started. Nowadays, thanks to successful laboratory syntheses, a large number (>200) of zeolite structures and compositions are available, most of them having no natural counterparts.

The broad present interest in zeolite science and technology has been fueled by the application of zeolite catalysts in several important oil refinery processes, resulting in an estimated annual zeolite usage of over
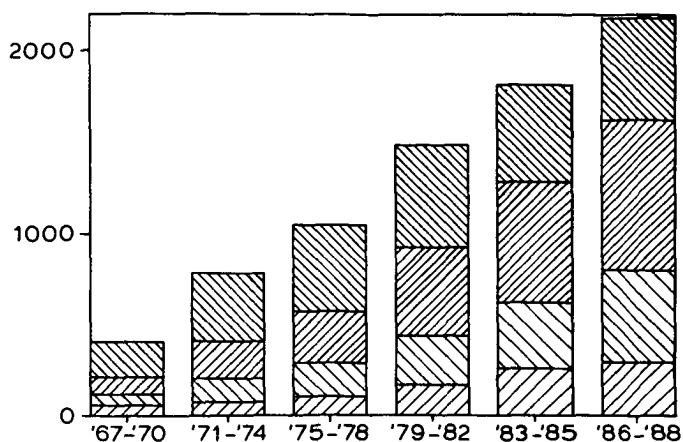
Figure 1. The yearly number of patents (▨, ▧) and publi-
cations (▨, ▧) regarding zeolites reported in the Chemical
Abstracts. Data are averaged over the given period.
Language English ▨, ▨; Language not English ▧, ▧.
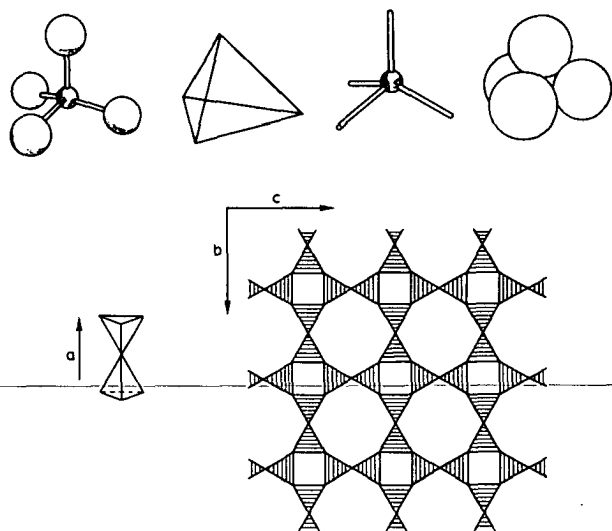
Figure 2. Top) different presentations of TO_4 tetrahedra.
Bottom) The structure of the zeolite phillipsite, built from
tetrahedra. The double tetrahedral unit shown left is pro-
jected in the zeolite structure as a single (equilateral)
triangle.

35,000 tonnes as catalysts, over 45,000 tonnes in detergents
and over 20,000 tonnes as adsorbents for 1987 (4).

The increase in zeolite investigations and applications
can be illustrated by comparing the yearly number of
publications and patents pertaining to zeolites. As shown
in Figure 1 the total number of publications and patents
reported in the Chemical Abstracts increased from an average
of about 400 per year over the period 1967-1970 to over 2000
per year over the period 1986-1988 and is still growing.

STRUCTURE

Zeolites are a class of framework aluminosilicates (other
classes include feldspars and feldspathoids) known as
tectosilicates (5), which are built from
corner-oxygen-sharing SiO_4^{4-} and AlO_4^{5-} tetrahedra. The
individual tetrahedra are always close to regular, but the
shared oxygen linkage can accommodate T-O-T angles (T stands
for T-atom, meaning tetrahedrally surrounded silicon or

S 4R   S6R   S 8R

D4R   D 6R

4-1   5-1   4-4-1
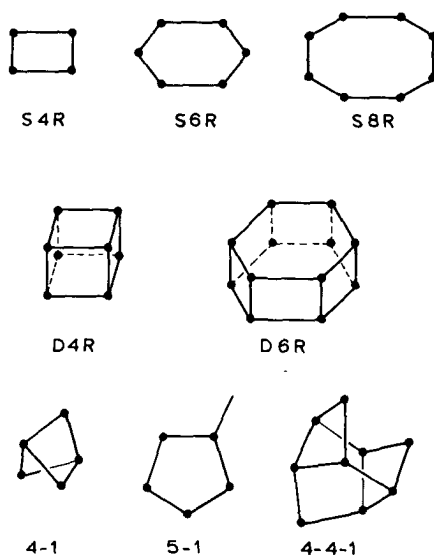
Figure 3. Secondary Building Units (SBU's) observed in zeo-
lite structures.
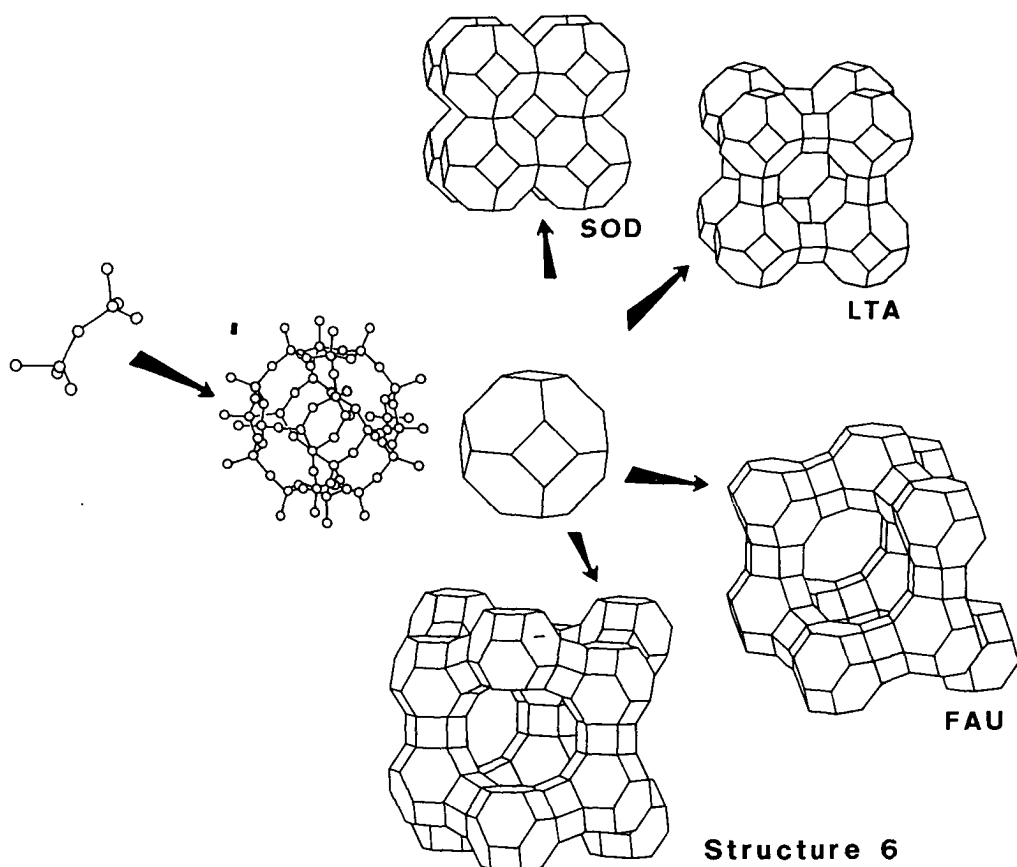
Figure 4. The figurative construction of four different zeo-
lite frameworks containing sodalite cages. A pair of TO_4
tetrahedra sharing one vertex is linked into a single soda-
lite cage.   In a less cluttered representation, the oxygen
atoms are omitted and the cage is represented by straight
lines connecting the tetrahedral units.   The sodalite cage
unit is found in the SOD. LTA and FAU frameworks.   Structure
6, a hypothetical framework related to that of FAU, is also
constructed from sodalite cages.

aluminum atom) from 130 to 180°. Figure 2 shows how TO_4
tetrahedra form the basic structure of phillipsite.   In
contrast to high-density species as quartz or cristobalite,
the aluminosilicate frameworks of zeolites exhibit high and
uniform porosities.
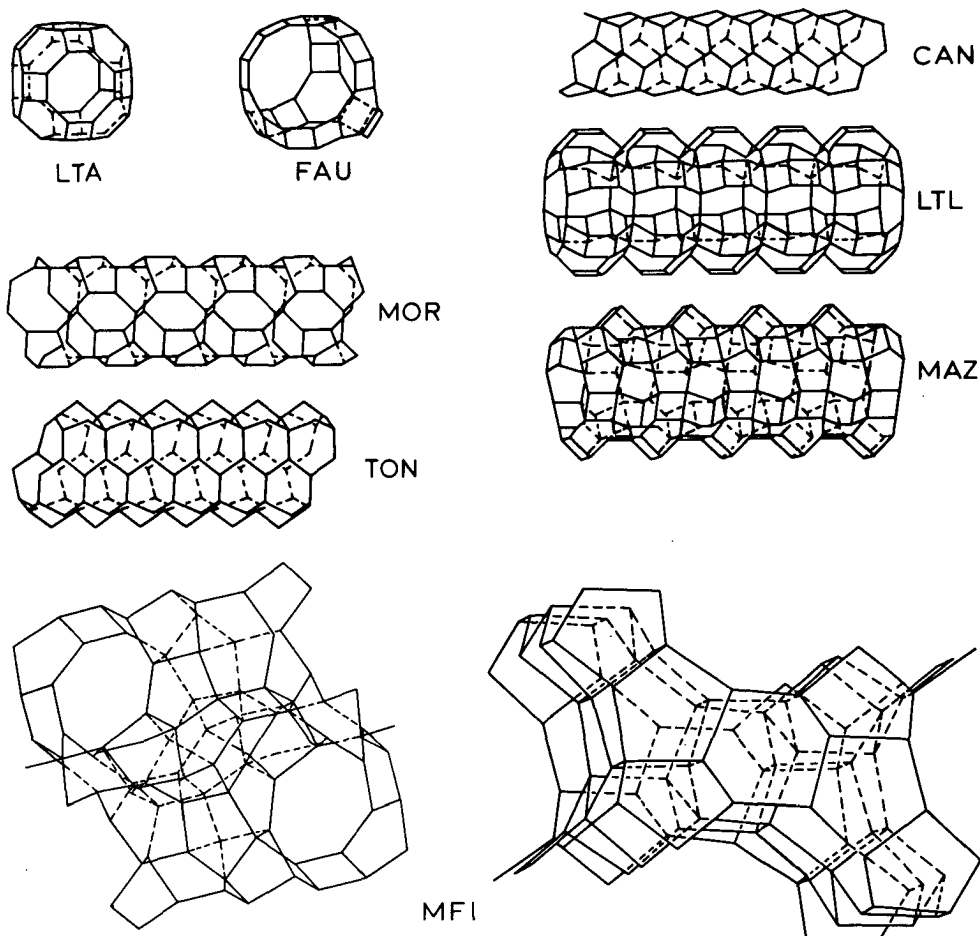
Figure 5. Representations of selected members of the zeolite
family, showing pores of various sizes, shapes and dimen-
sionalities. The outlines of the cages and channels are
drawn as straight lines connecting adjacent tetrahedral
sites (see Table 1).

   Zeolite structures can be formed by repeating so-called
Secondary Building Units (SBU's, depicted in Figure 3).
According to these SBU's zeolites can be classified into
eight groups. A selected list is presented in Table 1. The
TO_4 tetrahedra can be combined to yield a large variety of
framework structures (see Figure 4). In this way cage-
,chain-, layer- and tubular-like structures can be formed.

Table 1. Selected aluminosilicate frameworks (cf. 5). The nomenclature of the pore structure and the code is that of Meier and Olson (9). The underlined integers indicate the number of tetrahedral atoms (Si or Al) that define the aperture. The subsequent numbers indicate the size of the aperture (in nm). For structures with more than one channel system <> and | indicate whether or not the channels are interconnected, respectively.

Code	Examples	SBU	Typical Si/Al	Pore structure
ABW[1]	Li-A(BW)[2]	D4R	1	8 0.36x0.40
ANA	Analcime, Leucite, Pollucite, Viseite, Waisakite, Na-B	S4R,S6R	2	6-ring maximum aperture
CAN	Cancrinite	S6R	1	12 0.62
CHA	Chabazite, Herschelite, Linde D, Linde R	D6R	2	8 0.36x0.37
EDI	Edingtonite	4-1	1.5	8 0.35x0.39 <> 8 variable
ERI	Erionite	S6R	3	8 0.36x0.52
FAU	Faujasite, X, Y	D6R	2.3	12 0.74
GIS	Gismondine, Garronite, Gobbinsite, B, P	S4R	1	8 0.31x0.44 <> 8 0.28x0.49
HEU	Heulandite, Clinoptinolite	4-4-1	3.5	8 0.40x0.55 <> (10 0.44x 0.72 + 8 0.41x0.47)
KFI[1]	Ba-P, Ba-Q, ZK-5	D6R	2.2	8 0.39	8 0.39
LTA[1]	A, alpha, ZK-4, ZK-21, ZK-22, N-A	D4R	1	8 0.41
LTL[1]	L, (K,Ba)-G	S6R	2.6	12 0.71
MAZ[1]	Mazzite, Omega, ZSM-4	5-1	2.6	12 0.74
MEL[1]	ZSM-11, Silicalite-2	5-1	30 ∞	10 0.51x0.55
MFI[1]	ZSM-5, Silicalite-1	5-1	30 ∞	10 0.54x0.56 <> 10 0.51x0.55
MOR	Mordenite, Ptilorite	5-1	5	12 0.67x0.70 <> 8 0.29x0.57
OFF	Offretite, O	S6R	3.5	12 0.64 <> 8 0.36x0.52
PHI	Phillipsite, Harmotome	S4R	4	8 0.42x0.44 <> 8 0.28x0.48 <> 8 0.33
RHO[1]	Rho	D8R[3]	3	8 0.39x0.51	8 0.39x0.51
SOD[2]	Sodalite, Nosean, Tugtupite, Ultramarine	S6R	1	6-ring maximum aperture
TON[1]	Theta-1, Nu-10, KZ-2, ISI-1, ZSM-22	5-1	30	~~10~~ 0.47x0.55[4]

[1] This framework has not been found to occur naturally.
[2] Non-zeolite materials with this framework are also known.
[3] No official SBU.
[4] Silica-ZSM-22 (10).

In these structures the Loewenstein rule (8) is operative
which means that no Al—O—Al linkages are present in the
zeolite framework.

   The 39 different framework topologies that have,
up—to—date, been observed for aluminosilicate zeolites have
pores that vary in shape, size and dimensionality as
depicted in Figure 5. The naked LTA and FAU frameworks (for
code and explanation see Table 1), for example, have large
cages, 1.14 and 1.18 nm in diameter, which are
interconnected through smaller constrictions or windows of
0.41 and 0.74 nm in crystallographic diameter,
respectively. The naked CAN, LTL, MAZ and TON frameworks
have one—dimensional channels with diameters of 0.62, 0.71,
0.74 and 0.47 nm, respectively. The framework of ZSM—5
(MFI) has two orthogonal interconnected elliptical channel
systems with diameters about 0.55 nm (cf. Table 1).
Schematic representations of some three—dimensional zeolite
channel patterns are depicted in Figure 6.
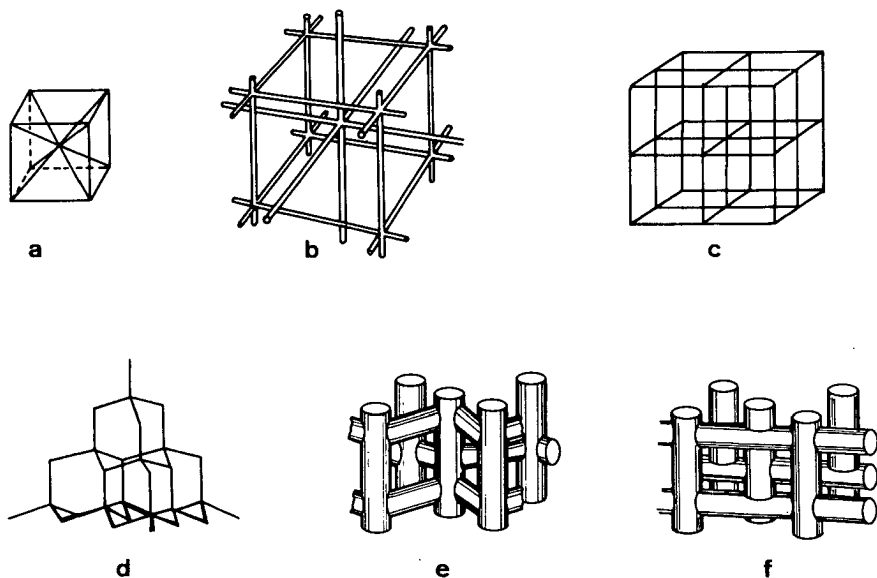
Figure 6. Formal representation of channel patterns in a)
sodalite hydrate, b) zeolite A, c) zeolite RHO, d) fauja-
site, e) ZSM—5 and f) ZSM—11.

CHEMICAL COMPOSITION

It is preferable to define a zeolite by its framework topology because its chemical composition may vary greatly. A general formula for the aluminosilicate zeolites can be written as

$$M_{x/m} \cdot Al_x Si_{2-x} O_4 \cdot n\, H_2O$$

Nonframe-   Framework   Sorbed
work atoms   components   water
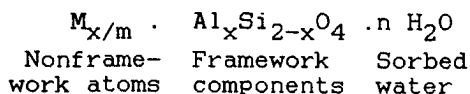
The presence of units with an overall formula of AlO_2^- in the framework provides the zeolite with a negative charge which is compensated by m-valent cations M. These nonframework cations are, at least in hydrated materials, usually mobile and can generally be replaced by a range of mono-, di- or trivalent cations through ion exchange in an appropriate solution under mild conditions.

Threedimensional frameworks based on linked $(Al,Si)O_4$ tetrahedra can cover the Si/Al range from 0 up to infinite. A convenient but arbitrary subdivision of phases in this range has been given by Barrer (3) and is listed in Table 2. Some specific or typical Si/Al ratios of zeolites are presented in Table 1. Table 3 shows the influence of the Si/Al ratio, which ranges from 1 to infinity, on some physical properties of zeolites.

Table 2. 3-dimensional frameworks based only on tetrahedra (aluminate, aluminosilicate, silica). Table was taken from reference 3.

Class	Si/Al ratio (x)	Examples
1	$0 < x < 1$	Aluminate sodalites; bicchulite
2	$1 < x < 5$	Feldspars (non-porous), feldspathoids (porous and non-porous), zeolites (porous)
3	$5 < x < 12$	Zeolites (ferrierite, svetlozarite; porous)
4	$x >= 12$	Zeolites (porous)
5	$x = \infty$	Crystalline silica's (porous and non-porous)

Table 3. Zeolite properties as a function of the Si/Al
ratio (12).

Zeolite	A	X	Y	Mordenite	ZSM-5	Silicalite-1
Si/Al	1	1.5	3	5	11-1000	∞

←——————————————— number of cations ——————————————→
——————————— framework stability towards acids ————————→
————————————— acidity zeolitic H-atoms ————————————→
————————————————— thermal stability ——————————————→
←——————————————— hydrophilic character ———————————
————————————— hydrophobic character ——————————————→
←—————————— affinity for polair molecules ——————————
——————————— affinity for non-polair molecules —————————→

SYNTHESIS

The synthesis of zeolites is usually performed under
hydrothermal conditions. The role of water as a
mineralizing catalyst, aided by alkaline conditions, was
first described by Schafheutl (13) in 1845 with regard to
the hydrothermal reaction of silica gel and water towards
quartz. The first hydrothermal zeolite synthesis is
credited to St. Claire Deville in 1862 (14). Solutions of K
and Na silicates heated to 170°C in sealed glass tubes gave
hexagonal, tubular, uniaxial crystals of levynite.
Pioneering work by Barrer in the 1940's and 1950's
demonstrated the synthesis of a wide range of zeolites from
aluminosilicate gels (15). An aqueous solution of alumina in
a base such as sodium hydroxide -present in excess- is mixed
intimately with a sol or solution of the silica component.
The highly alkaline mixture forms a thick gel that
crystallizes over a few hours/days when maintained at
100-180°C. The synthesis of the 'classical' zeolites A. X. Y
and mordenite still follows this path. Activation, i.e.
removal of adsorbed water, is achieved by heating the
as-synthesized zeolite up to ~400°C.

The addition of organic cations in zeolite synthesis was
introduced in the early 1960's by Barrer and Denny (16). The
presence of the tetramethylammonium cation in the synthesis
gel not only showed a structure directing effect towards the

synthesis of small cage-containing structures as sodalite or
gmelinite but also resulted in the preparation of new
siliceous materials as N-A, ZK-4 and alpha. These zeolites
are structural alike to zeolite A (LTA), but with a much
higher silica to alumina ratio than that of zeolite A made
in a solely NaOH-containing system (17).

   Exploration of a range of tetraalkylammonium compounds as
templating agents resulted, using the tetraethylammonium
cation, in the synthesis of zeolite beta, the first high
silica zeolite (Si/Al>20) (18), which structure was
elucidated recently (19). Shortly thereafter, a number of
high silica zeolites, i.e. ZSM-5 (20), ZSM-8 (21) and ZSM-11
(22) were reported in patent publications applying template
reagents as tetrapropyl-, tetraethyl- and tetrabutylammonium
compunds respectively, in the synthesis mixture. These
developments led in 1977 to the synthesis of Silicalite-1
(structural isomorphous to ZSM-5) by Flanigen et al. (23)
which was the first 'zeolite' having an infinite Si/Al
ratio. This success led to another class of crystalline
porous silica's including Silicalite-2 (ZSM-11 structure,
(24)), TEA-silicalite (25), Al-free ferrierite (26) and
silica-ZSM-22 (TON framework, (10)). These crystalline
porous silica's are named molecular sieves as the name
zeolite is restricted to compositions in which both Si and
Al appear as the framework metal ions.

   It seems that the presence of suitable organic species as
template in molecular sieve synthesis supports the
crystallization and stabilization of a particular
structure. The exact role of these molecules is as yet not
fully understood (17) as templates can be either locked up
or be desorbable. Thus during synthesis two
template-to-structure situations can be distinguished.
First, zeolite cages occupied by template; for example, the
tetramethylammonium which fits and is locked into sodalite
cages containing frameworks or intersecting channels
occupied by template, as exemplified by the presence of
tetrapropylammonium cations in ZSM-5 (12,27) situated at
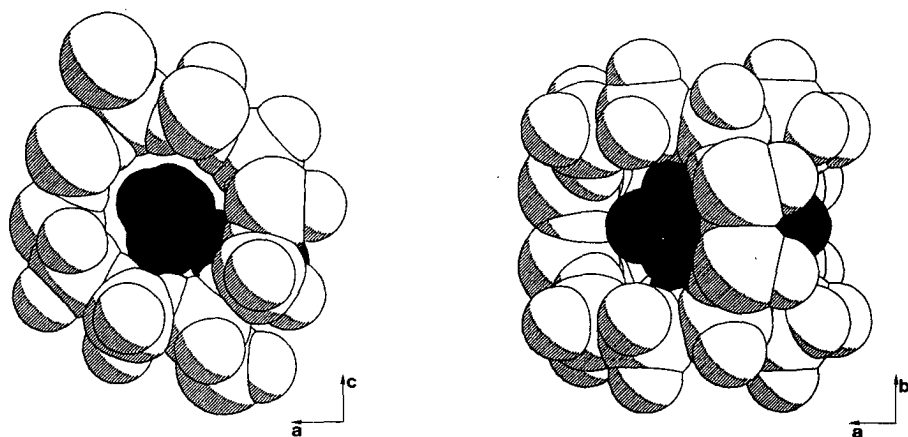
Figure 7. The geometry of the tetrapropylammonium ions in
zeolite ZSM-5. Space filled drawings looking into the
straight (left) and sinusoidal (right) channels of the
zeolite.

channel crossings as depicted in Figure 7. Secondly
desorbable templates might be present, as for instance
triethylenetetramine (TETA) in the synthesis of the channel
zeolite Nu-10 (Chapter IV). The template trapped within the
voids of the zeolite product must be removed before the
zeolite can be effectively used as a sorbent or catalyst.
This is achieved by calcination in air or oxygen at
temperatures between 400 and 600°C to degrade the template
and burn any 'deposited' carbon (28). Alternatively an
oxygen plasma technique may be used at lower temperature
(29).

The importance of templates in zeolite synthesis is
underlined by the large amount of literature published on
this subject (i.e. references 3, 17, 30-32, see also Chapter
IV, Table 2 (33)) occasionally leading to the
crystallization of new zeolites. As an example we mention
the synthesis of Sigma-1 by Stewart and Johnson (32) using
1-aminoadamantane as the template molecule.

CATION EXCHANGE

As mentioned earlier mobile, non-framework cations like Na^I are present in the as synthesized classical zeolites to compensate the negative AlO_2^- species. In 1850 Way (34) and Thompson (35) clarified the nature of ion exchange in soils which led to investigations on zeolites from 1870 onwards (36). The cation-exchange process occurs when ions from solution replace counterions within the crystal structure. The effective cation-exchange percentage of a zeolite when subjected to a certain ion is not only influenced by the concentration of the competing ions in solution and in the zeolite itself, but also by the inherent selectivity of that zeolite for the cations under consideration. The total cation-exchange capacity of a zeolite is often difficult to measure because certain cation positions sometimes require enhanced temperatures to replace the cation from these locations. Therefore by convention, cation selectivity is always measured relative to the ion being released by the zeolite. In the cation exchange process between a zeolite particle and an aqueous solution cations move from the bulk solution to a zeolite dependant stagnant waterlayer which surrounds the zeolite particle. After diffusion through this film the cations often have to dehydrate partly in order to enter the zeolites pores and channels. The exchange process itself is usually very rapid with the restriction made above. Concomitantly other cations are released from the zeolite to the solution (37).

A detailed description on this subject has been published by Nieuwenhuizen et al. (38). These authors show that Mg^{II} ion exchange in zeolite NaA is 300 times slower than Ca^{II} ion exchange at 32°C and pH=9. As both divalent ions, in the hydrated form, are too large to enter the zeolite partial disruption of the hydration sphere of the cation has to take place. Since the activation energy of dehydration of Ca^{II} is lower than that of the smaller Mg^{II}, Ca^{II} ion exchange will be faster as dehydration is the rate limiting

step. The leaving Na^I ion will diffuse faster than the
incoming divalent ions. The Ca—exchange properties of NaA
are applied in the detergent industry where NaA nowadays
plays an important role in detergent compositions as
phosphate substitute (39).

Besides modification of the accessibility of the zeolites
(see paragraph Adsorption, (40)), cation exchange in
zeolites can also lead to the incorporation of catalytically
active species in the zeolite (41) to be discussed later in
this Chapter. Finally cation exchange sometimes increases
the zeolite's stability (42).

ADSORPTION

Following quantitative measurements of water vapour ⟷
zeolite equilibria by Tamman (43), Grandjean (44) made some
notable early studies on the sorption of heavy vapours as
I_2, Br_2, Cl_2 and Hg in chabazite in 1910. McBain (45)
introduced the term 'molecular sieve' to describe the
selectivity of some micro—porous carbons and zeolites in the
uptake of molecules according to size. Molecules too large
to enter the micropores were sorbed much less than smaller
ones which could enter.

small   medium   large pore
A   ZSM-5   X,Y,L
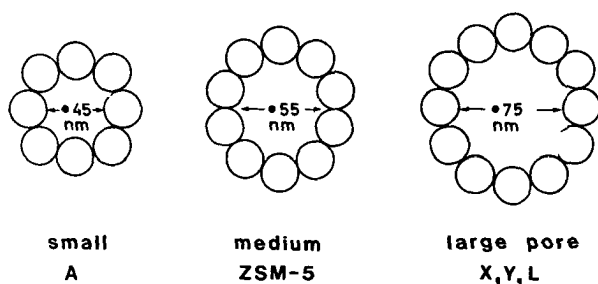
Figure 8. 8—, 10— and 12—membered rings of oxygen, showing
the maximum pores of some zeolites.
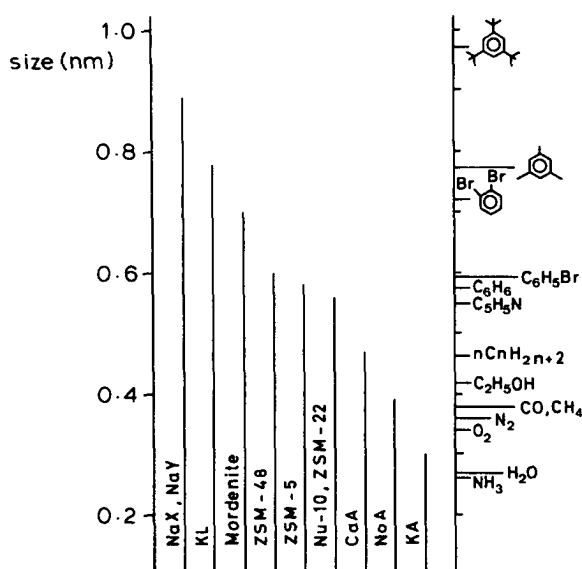
Figure 9. Chart showing a correlation between the pore size of some zeolites together with the critical diameter of various molecules.

Based on their adsorption properties, zeolites can be classified as small pore, medium pore or large pore. In general, these classifications have been related to the presence of 8-, 10- and 12-membered rings respectively, in the oxygen sub-lattices. determining the maximum accessibility as shown in Figure 8. Recent structural data on high silica zeolites (i.e. ZSM-5 (27), ZSM-22 (10). ZSM-23 (46) and ZSM-48 (47)) indicate a variety of pores and shapes (circular, elliptical etc.) within the classifications. Thus. subtle differences in the adsorption of various molecules may result from small differences in shape. The accessibility of several zeolites is presented in Figure 9 along with some typical molecular dimensions.

The recent discovery of the 18-ring alumino-phosphate molecular sieve VPI-5 (see paragraph on isomorphous substitution) by Davis et al. (48) can be seen as an important breakthrough that will restimulate the search for new large pore molecular sieves, previously only covered by

pillared clays.   The VPI-5 molecular sieve seems to be
structurally closely related to the MCM-9 SAPO molecular
sieve patented (49) but not recognized as superlarge pore
zeolite.

The actual pore size of a zeolite sometimes depends on the
type of cation present.   Type A zeolites have a cubic
structure with pore windows just big enough to allow normal
paraffins and other linear organic molecules to pass.
Monovalent cations (e.g. sodium. potassium) in zeolite A
occupy -amongst other sites- positions in the 8-membered
ring and therefore reduce the actual pore size to below 0.4
nm.   Divalent cations. however. require only 50% of the
cationic sites of monovalent cations and leave enough
8-membered rings free to allow normal paraffins to diffuse
through.   Isoparaffins and other branched alkanes are more

Methane   Ethane

Propane

Isobutane

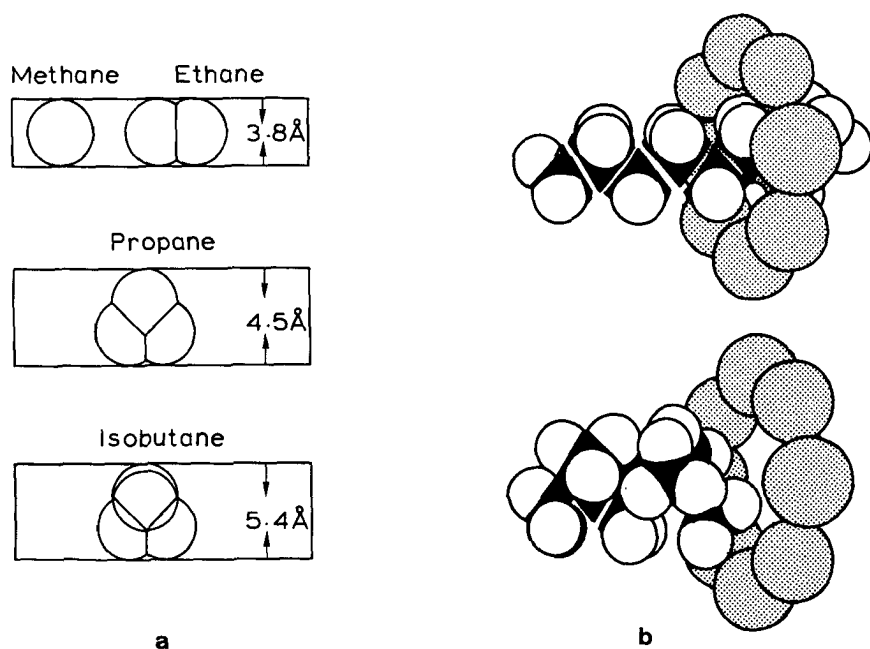a   b

Figure 10. a) Some molecular diameters.   b) Schematic
illustration of the entry of octane into a 8-ring pore and
blockage of an iso-octane hydrocarbon at a channel aperture
in a zeolite.

bulky than normal alkanes and therefore cannot enter CaA
(see Figure 10). An important industrial process (Isosieve;
Union Carbide) regarding the separation of branched and
linear hydrocarbons is based on this ability of zeolite CaA.

Another shape-selective adsorption is the separation of
p-isomers from mixtures of disubstituted benzenes by means
of zeolites as ZSM-5 and Nu-10. Some data on the adsorption
of organic molecules into these zeolites are presented in
Table 4. A comparison of the adsorption data for ZSM-5,
Silicalite-1 and Nu-10 reveals that the intracrystalline
pore volume of Nu-10 is smaller than that of ZSM-5 and
Silicalite-1 which cannot only be accounted for by the
absence of channel intersections in the intracrystalline
pore structure of Nu-10 (52) but is to be ascribed to the
slightly smaller pore diameter of Nu-10 as well (see Table
1). Table 4 shows furthermore that competitive adsorption of
xylenes, from the liqiud phase, into ZSM-5 results in a high
p-selectivity.

At higher temperatures the pores enlarge slightly and the
kinetic energy and molecular vibrations of the diffusing
molecules overcome repulsion forces at pore entrances
allowing molecules to wiggle through somewhat narrower pores
than expected on the basis of X-Ray dimensions whereafter
(catalytic) conversion is possible (54). However, not only

Table 4. Intracrystalline sorption capacity of ZSM-5 (49),
Silicalite-1 (50) and Nu-10 (51) for different sorbates for
single adsorption on outgassed samples by low sorbate
pressures (upper half) and competitive adsorption (52) for a
mixture containing 0.5 g o-xylene, 0.5 g m-xylene and 0.5 g
p-xylene in 2 ml 1,3,5-triisopropylbenzene (lower half).

Adsorbent (Si/Al ratio)	Adsorption Temp. (K)	Amount of material adsorbed (mg/g)				
		o-xylene	m-xylene	p-xylene	ben-zene	n-hexane
Silicalite-1 (∞)	298	54.1	73.1	112.4	110.8	122.1
H-ZSM-5 (38)	303	93.3	94.3	127.2	104.5	117.0
H-Nu-10 (60)	296	6.6	13.7	41.8	30.7	52.5
H-ZSM-5 (49)	283	0.1	0.0	67.0		
H-ZSM-5 (49)	298	2.2	2.4	61.0		
H-ZSM-5 (49)	313	2.2	6.0	58.0		

the pore size determines the adsorption characteristics.
The Si/Al ratio is an important factor as well (see Table 3)
amongst others because it is related to the amount of
cations present. A zeolite as CaA (Si/Al=1) highly prefers
water whereas Silicalite-1 (Si/Al=∞) prefers organics over
water.

ISOMORPHOUS SUBSTITUTION

Until 1982, the scope for the incorporation of framework
cations other than silicon and aluminum into the zeolite was
believed to be rather limited. Nowadays such limitations
have been largely dispelled by the discoveries of new
families of molecular sieves. Important examples towards
the preparation of molecular sieves having
non-aluminosilicate frameworks include aluminophosphates
discovered by Flanigen et al. ($Al^{III}:P^V=1$) (55),
iron^{III}-silicates (56) and boronsilicates (57). These
aluminophosphates led to the development of known as well as
of unknown lattice structures (cf. 48,49,55) whereas the
iron- and boronsilicates have an analogon in the families of
aluminosilicate zeolites.

A further expansion is isomorphous substitution in
aluminophosphate (AlPO) materials. Partial substitution of
aluminum and/or phosphorous by silicon leads to the so
called SAPO molecular sieves (58). Apart from Si various
other metal ions (as Co, Mg, Mn, Zn, As, Ti) can be
incorporated into the AlPO and SAPO frameworks, which then
are described as MeAPO- and MeAPSO molecular sieves
respectively (59-61). Therefore, a more general formula for
zeolite type materials based on 4-connected networks is the
following (62)

$$M_x M'_y N_z [T_m T'_n \cdot \cdot O_{2(m+n+..)a} {}^{(OH)}{}_{2a}]^{(OH)}{}_{br} {}^{(aq)}{}_p \cdot qO$$
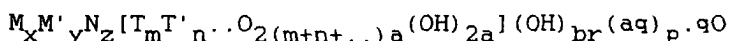
with Be, B, Al, Si, P, Ga, Ge. etc. as tetrahedral lattice
atoms (T). M and M' are exchangeable and nonexchangeable
metal cations, respectively. N non-metallic cations (e.g.
generally removable upon heating), (aq) chemically bonded
water (or other strongly held ligands of T-atoms), and q

sorbate molecules which need not to be water. The essential
part in square brackets denotes the 4-connected framework
which is anionic or neutral. (OH) represents the presence
of interrupted frameworks or hydroxobridges. Although only
main group elements are listed among the T-atoms other
possible T-atoms should not be excluded as referred to
earlier.

Undoubtedly, these new molecular sieve materials (no
zeolites according to the definition which is restricted to
Si/Al systems), as well as zeolites themselves. are a
promising and rapidly growing field of investigation and
application.

CATALYSIS

Zeolites have a number of properties which make them
interesting and valuable for heterogeneous catalysis: (a)
they have exchangeable cations. allowing the introduction of
different cations or combinations thereof with various
catalytic properties; (b) if the cationic sites are
exchanged directly or indirectly to H^+, a spectrum of
Bronsted acidity up to very strong acid sites can be
obtained. Apart from a (c) high internal surface area (>600
m^2/g) they (d) have pore diameters with usually a discrete
accessibility and (e) these pore diameters are in the order
of molecular dimensions (63). Further, the incorporation of
various (f) metal^0 clusters or (g) metal-complexes is
possible. Because of their high thermal stability (h)
regeneration/reactivation by high temperature treatment is
often possible. Therefore, the interior of a zeolite can be
transformed into an unique catalytic environment for
chemical transformations (cf. 64).

Molecular shape-selectivity in zeolite catalysis was first
reported by Weisz and Frilette (65) in 1960. In a subsequent
article Weisz et al. (66) defined two basic types of shape
selectivity (see Figure 11): reactant selectivity, where
certain molecules are admitted into the zeolite and others
excluded by virtue of their size and shape (kinetic
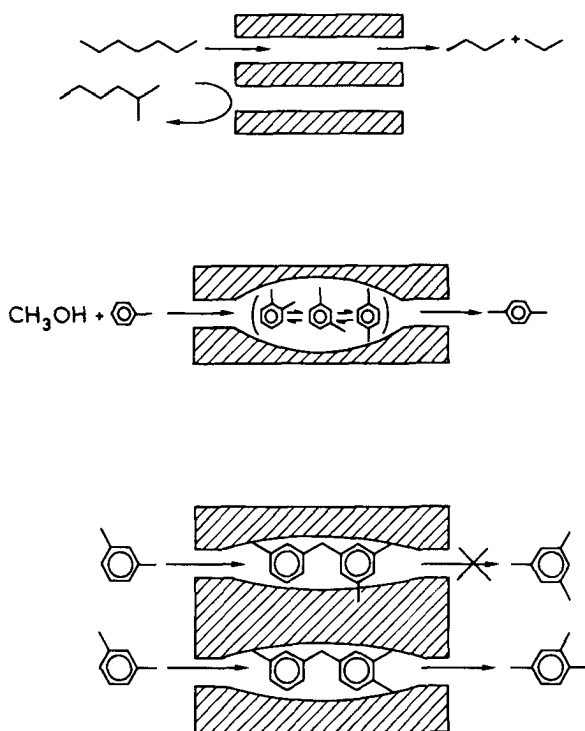
Figure 11. Reactant (top) and product (middle) selectivities
as exemplified by the selective cracking of n-heptane and
the preferred formation of p-xylene, respectively.   Restric-
ted transition state seletcivity (bottom). Because of its
large reaction intermediate the formation of 1.3.5 tri-
methylbenzene is prevented.

diameter); and product selectivity, which applies to
molecules formed -in equilibrium- within the zeolite where
escape from the zeolite is dictated by similar steric
considerations.   This general definition was later extended
by Csicsery (67) who added categories of cage effects and
restricted transition state selectivity (Figure 11), and by
Shabtai (68) who proposed that a zeolite may constrain
reactant molecules in preferred conformation and/or
orientation prior to reaction.

reactant selectivity

product selectivity

reaction selectivity
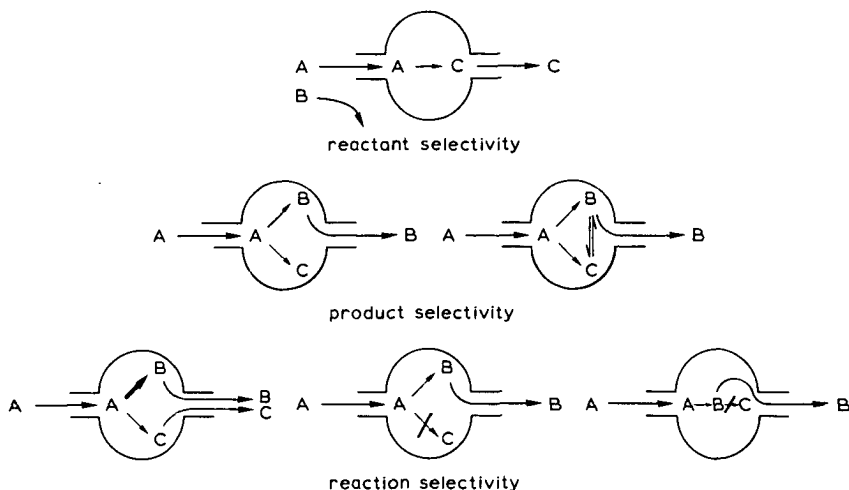
Figure 12. Schematic representations of zeolite reactant
selectivity, product selectivity and reaction selectivity.

   These selectivities can be combined under the name
reaction selectivity covering selectivity in parallel
reactions as well as in consecutive reactions (cf. Figure
12).

   Reactant selectivity occurs when part of the reactant
molecules are too large to diffuse through the catalyst
pores. To these molecules just the outer zeolite surface is
available then. Examples of reactant selectivity include
dehydration of alcohols: n-butanol dehydrates at 260°C over
both CaA and CaX whereas sec-butanol and isobutanol only
dehydrate over CaX (63); cracking of paraffins (69)
(industrially applied in the Mobil Selectoforming process
(70)); and selective hydrogenation of unsaturated organics
over M^O loaded zeolites as Rh^{O}NaY (71) or Pt^{O}ZSM-5 (72).

   Product selectivity occurs when some of the product(s)
formed within the pores are too bulky to diffuse out as
observed products. They are either converted to less bulky
molecules (e.g. by equilibration or cracking) or eventually
deactivate the catalyst by blocking the pores (Figure 11a).
Product selectivity has been observed, for example in the

para-selective methylation of toluene (73) over ZSM-5
zeolites modified by the introduction of Fe, B or P
species.   The high para-selectivity is attributed to the
relatively strong adsorption of o- and m-xylene on the
acidic reaction sites.   The p-isomer is more rapidly
desorbed because of its difference in size, shape and
polarity when compared to the m- and o-isomers.   Product
selectivity can also be observed in the bromination of
halobenzenes (74).

   In reaction selectivity certain reactions are prevented or
retarded because the transition state is too large for the
space available inside the molecular sieve.   In the ideal
case, both the reactants and the potential products are free
to diffuse through the zeolite's pores, but the formation of
the transition state of undesired reactions is inhibited
because it is too large (cf. Figure 12). An example is the
acid-catalyzed transalkylation of dialkylbenzenes (see
Figure 11). In this reaction one of the alkyl groups is
transferred from one molecule to another which involves a
bulky diphenylmethane-type transition state.   Over HY
zeolite and amorphous silica-alumina symmetrical
trialkylbenzenes are formed together with the other isomers,
while over H-mordenite the symmetrical trialkylbenzene is
almost absent from the reaction product (63). Reaction
selectivity has also been observed in bromination (75),
acylation (76) and oxidation reactions (77).

INDUSTRIAL USE

   Since their introduction as a new class of commercial
adsorbents in 1954, molecular sieve zeolites have grown into
an estimated quarter of a billion dollar industry and have
led to the creation of a new branch of chemical technology.
Commercial utilization of these materials in the fields of
drying, cation exchange, selective adsorption and catalysis
has been developed in most areas of the chemical industry
with major applications in detergents as cation exchanger,
in petroleum refining and in petrochemical processing as

catalysts and adsorbents. Zeolites are widely used in the
drying and purification of natural gas, cracked gas and
liquid paraffins; in desulfurization processes: for the
separations of normal and branched paraffins, the
separations of various mixtures of aromatic organic
compounds and for oxygen/nitrogen separation. Major
catalytic applications are as conversion catalysts in
cracking, hydrocracking, alkylation and paraffin
isomerization (78).

The interest for zeolites in catalytic reactions has
started in the early sixties with the observation that small
quantities of zeolites incorporated in the then used
petroleum cracking catalysts as silica-alumina and
silicaclay materials significantly improved their catalytic
properties (79). A breakthrough in this application was the
use of rare earth cation exchanged zeolite X and Y
because,along with its increased cracking ability, increased
gasoline production at the expense of both light gas and
coke could be achieved (4). The zeolites enhanced hydrogen
transfer activity is an important factor here. Nowadays,
the fluidized catalyst cracking application is the largest
as well as the oldest application of zeolite catalysts in
which dealuminated ultra-stable faujasite (US-Y) is used as
the cracking catalyst promotor to enhance octane yields and
as a hydrocracking catalyst (28).

The main industrial applications of zeolites are
summarized in Table 5. Application of both adsorption and
catalysis is found in the Shell/Union Carbide Total
Isomerization Process (TIP). This process is a combination
of the Shell Hysomer process (Pt-mordenite: C_5-C_6
isomerization) and the Union Carbide Isosieve process and
results in gasolines having a highly improved research
octane numbers (RON) (81).

Recently Holderich et al. (82) and van Bekkum and
Kouwenhoven (83) published reviews upon the use of zeolites
as a catalyst for the preparation of organic compounds,
including fine chemicals.

Table 5. Main commercial processes involving zeolites
(cf. 28,80).

Process	Catalyst	Products
Catalytic cracking	RE-Y, US-Y	gasoline, fuel oil
Hydrocracking	Co, Mo, W, Ni on faujasite, mordenite, erionite	kerosine, jet fuel benzene,toluene, xylene
Alkylation of aromatics	ZSM-5	p-xylene, ethyl-benzene, styrene
Xylene isomerization	ZSM-5	p-xylene
Dewaxing	Ni/ZSM-5 mordenite	increase in octane number
Selectoforming	Ni/erionite	LPG production
Methanol to gasoline	ZSM-5	gasoline with high octane number
Hydroisomerization	Pt or Pd on mordenite	i-hexane, heptane
Olefin drying	K-A	olefins
Iso/n-paraffin separation	Ca-A	pure n-paraffins, branched paraffins

Natural zeolites (having no constant composition) find
industrial fields of applications without necessarily
conflicting with the synthetic ones, especially when large
quantities are used. World utilization of natural zeolites
presently reaches 230-250,000 tons per year, resulting in a
total (natural + synthetic) yearly demand of over 300,000
tonnes (4,84) of zeolitic material for catalytic as well as
for non-catalytic applications. An overview on the
utilization of natural zeolites for 1985 is given in Table
6. Considering the exceptionally large but obviously often
impure deposits, natural zeolites are preferable over
synthetic ones in utilizations requiring a massive use of
zeolite material.

SCOPE OF THIS THESIS

In this laboratory the modification and characterization
of zeolites together with their (catalytic) use in organic
chemistry have been studied by Roelofsen (85), Wortel (86)
and Oudejans (87) who mainly investigated the selective

Table 6. Picture of the world utilization of natural zeo-
lites for 1985 (Approximate consumption values in ton/year).
Table was taken from reference 84.

	Japan	USA	Europe
<u>Building industry</u> (zeolitic tuffs)	8,000	+	140,000
<u>Industry/Agriculture</u>			
Insulation/Protection	1-2,000	+	+
Paper filler	57,000		
Soil conditioner	10,000	+	+
Additions to animal diets	5-6,000	+	+
Chelating agents (NH_4)	2.5-5,000	2-3,000	+
Chelating agent (metal ions, radionuclides, etc.)	+	+	+
Fish cultural systems			
Deodorizing animal excr.	200	+	+
Municipal waste waters			
O_2 air enrichment	+		
Natural gas cleaning	+	+	
Exhausted gas (SO_2) treatment		+	
Energy storage	+	+	+
Gas and water adsorption	25,000 (World)		

(+) utilization verified but data unavailable.

catalytic properties of zeolites in organic reactions and by
van der Gaag (88) who also studied the synthesis and
characterisation of the high silica zeolite ZSM-5 together
with isomorphous substitution on ZSM-5 type materials.

   Chapters II, III and VIII of this Thesis deal with the
zeolite ZSM-5. Chapter II describes an improvement on the
IR-characterization of ZSM-5 as reported by van der Gaag et
al. (89). Chapter III shows that the Al-gradient present in
ZSM-5 influences the rate and selectivity of its dissolution
in NaOH and HF. In Chapter VIII the geometry and
conformation of the tetrapropylammonium (TPA) template in
zeolite ZSM-5 was compared with other TPA-containing crystal
structures.

   The synthesis of the relatively new high silica zeolite
Theta-1/Nu-10, with Si/Al ratios in the same order of
magnitude as of ZSM-5, has been described in Chapter IV.
Several templates were studied and optimal synthesis
conditions were determined.

A good catalytic test for this Nu-10 zeolite is the
reaction of aqueous ammonia and ethanol towards pyridines
(Chapter V) as reported earlier by van der Gaag (88,90,91)
and Oudejans (87,90). An improved reaction scheme for this
reaction together with a relatively high selectivity towards
pyridines is described in Chapter VI.

Some exploratory work has been performed upon the
catalytic synthesis of hydroxymandelic acid from phenol and
glyoxylic acid. The dealuminating properties of glyoxylic
acid in an aqueous medium led to a publication of this
laboratory describing the homogeneously catalyzed formation
of hydroxymandelic acid (93) and to Chapter VII in which
experimental work on dealumination of zeolites by glyoxilic
acid is presented.

REFERENCES

1.   Cronstedt, A.F. Kongl. Svenska Vetenkaps Acad.
     Handlingen 1756, <u>17</u>, 120.
2.   'Natural Zeolites: Occurence, Properties, Use' Eds.
     L.B. Sand and F.A. Mumpton, Pergamon Press, Oxford
     1978.
3.   Barrer, R.M. 'Zeolites (Synth. Struct. Techn. Appl,)'.
     Stud. Surf. Sci. Catal. 1985, <u>24</u>, 1.
4.   Chen. N.Y. and Deganan, T.F. Chem. Eng. Progr. 1988,
     32.
5.   Newsam, J.M. Science 1986, 1093.
6.   Breck, D.W. and Anderson, R.A. 'Kirk Othmer's
     Encyclopedia of Chemical Technology', 3rd edition,
     John Wiley and Sons, New York 1981, p. 638.
7.   Wells, A.F. 'Structural Inorganic Chemistry', 4th
     edition, Clarenson Press, Oxford 1975, p. 829.
8.   Loewenstein, W. Am. Mineral. 1954, <u>39</u>. 92.
9.   Meier, W.M. and Olson, D.H. 'Atlas of zeolite
     structure types', Polycrystal Book Service, Pittsburg,
     1978.
10. Marler. B. Zeolites 1987, <u>7</u>. 393.
11. Barrer, R.M. 'Inclusion Compounds Vol. 1', Eds. J.L.
     Atwood. J.E.D. Davies and D.D. MacNicol, Academic
     Press, London 1984, p. 191.
12. Jansen, J.C. and Bekkum. H. van. I^2-Procestechnologie
     1985. 15.
13. Schafheutl. Muenchner Gelehrte Anzeigen 1845, 557.
14. St. Claire Deville, H. de. Compt. Rend. 1862, <u>54</u>,
     324.
15. Barrer. R.M. 'Hydrothermal Chemistry of Zeolites',
     Academic Press. London 1982.
16. Barrer, R.M. and Denny. P.J. J. Chem. Soc. 1961, 971.

17. Lok, B.M., Cannan, T.R. and Messina, C.A. Zeolites 1983, 3, 282.
18. Wadlinger, R.L., Rosinski, E.J. and Planck. C.J. US Patent 3,308,069 (1967).
19. Tracey, N.M.J. and Newsam. J.M. Nature 1988. 332. 249.
20. Argauer, R.J. and Landolt, G.R. US Patent 3,702,886 (1972).
21. Mobil Oil Corp. Neth. Patent Appl. 7,014.807 (1971).
22. Chu, P. US Patent 3,709,979 (1973).
23. Flanigen, E.M., Bennet, J.M., Grose, R.W., Cohen, J.P., Patton, R.L., Kirchner, R.M. and Smith, J.V. Nature 1978, 271, 512.
24. Bibby, D.M., Milestone, N.B. and Aldridge, L.P. Nature 1979, 280, 664.
25. Grose, R.W. and Flanigen, E.M. US Patent 4,104,294 (1978).
26. Gies, H. and Gunawardane. R.P. Zeolites 1987. 7, 442.
27. Koningsveld. H. van, Bekkum, H. van and Jansen, J.C. Acta Cryst. 1987, B43, 127.
28. Vaughan, D.E.W. Chem. Eng. Progr. 1988, 23.
29. Maesen, Th.L.M., Bruinsma, D.S.L., Kouwenhoven, H.W. and Bekkum, H. van. J. Chem. Soc., Chem. Commun. 1987, 1284.
30. Gaag, F.J. van der, Jansen, J.C. and Bekkum, H. van. Appl. Catal. 1985, 17, 261.
31. Araya, A. and Lowe, B.M. Zeolites 1986, 6, 111.
32. Stewart, A. and Johnson. D.W. Abstract of the 'International Symposium on Innovation in Zeolite Materials Science', Nieuwpoort. Belgium, September 13–17, 1987, p. 29.
33. Febre, R.A. le, Kouwenhoven, H.W. and Bekkum, H. van. Zeolites 1988, 8, 60.
34. Way, T. and Roy, J. Agric. Soc. 1850, 11. 313.
35. Thompson and Roy, J. Agric. Soc. 1850, 11, 68.
36. Lemberg, J. Z. Deutsch. Geol. Ges. 1876, 28, 519.
37. Semmens, M.J. 'Zeo-Agriculture. Use of Natural Zeolites in Agriculture and Aquaculture', Eds. W.G. Pond and F.A. Mumpton), Westview Press Inc., Boulder 1984, p. 45.
38. Nieuwenhuizen, M.S., Ebaid, A.H.E.F., Duin, M. van, Kieboom, A.P.G. and Bekkum, H. van. Tenside Detergents 1984, 21, 221.
39. Llenado, R.A. Proc. Int. Zeolite Conf. 6th 1983 (Publ. 1984; Ed. D. Olson, A. Bisio), p. 940.
40. Breck, D.W. 'Zeolite Molecular Sieves'. John Wiley and Sons, New York 1974.
41. Rabo, J.A. 'Zeolite Chemistry and Catalysis', ACS Monograph 171, 1976.
42. McDaniel, C.V. and Maher. P.K. in ref. 34, p. 285.
43. Tamman, G. Z. Phys. Chem. 1889, 27, 323.
44. Grandjean, M. Bull. Soc. Fr. Mineral. 1910, 33, 5.
45. McBain, J.W. 'the Sorption of Gases and Vapours by Solids', Rootledge and Sons, 1932.
46. Rohrman jr., A.C., LaPierre, R.B., Schlenker, J.L., Wood, J.D., Valyocsik, E.W., Rubin, M.K., Higgins, J.B. and Rohrbauch, W.J. Zeolites 1985, 5, 352.
47. Schlenker, J.L., Rohrbauch, W.J., Chu, P., Valyocsik,

E.W. and Kokotailo, G.T. Zeolites 1985, 5, 355.

48. Davis, M.E., Falbarriaga, C., Montes, C. and Garces, J. Communication at the Symposium on Innovation in Zeolite Materials Science, Nieuwpoort, Belgium 1987; Chem. Eng. News 1988, 22.

49. Derouane, E.G., Von Ballmoos, R.N. EP 0,146,389 (1985); US 562,673 (1983).

50. Wu, P., Debebe, A. and Ma, Y.H. Zeolites 1983, 3, 118.

51. Choudbary, V.R. and Singh, A.P. Zeolites 1986, 6, 206.

52. Harrison, I.D., Leach, H.F. and Whan, D.A. Zeolites 1987, 7, 28.

53. Nambi, S., Kanai, Y., Shoji, H. and Yoshima, T. Zeolites 1984, 4, 77.

54. Bendoraitis, J.G., Chester, A.W., Dwyer, F.G. and Garwood, W.E. 'New Developments in Zeolite Science Technology'. Proc. 7th Int. Zeolite Conf., Eds. Y. Murakami, A. Iijima and J.W. Ward. Kodansha Ltd., Tokyo 1986, p. 669.

55. Wilson, S.T., Lok, B.M., Messina, C.A., Cannan, T.R. and Flanigen, E.M. 'Intrazeolite Chemistry', Eds. G.D. Stucky and F.G. Dwyer. ACS Symp. Series 1983, 218, 79.

56. Kouwenhoven, H.W. and Stork, W.H.J. US Patent 4,208,305 (1980).

57. Taramasso, M., Perego, G. and Norari, B. Proc. 5th Int. Conf. Zeolites, Heyden, London 1980, p. 40.

58. Lok, B.M., Messina, C.A., Patton, R.L., Gajek, R.T., Cannan, T.R. and Flanigen, E.M. J. Am. Chem. Soc. 1984, 6092.

59. Flanigen, E.M., Lok, B.M., Marcus, B.K., Messina, C.A. and Wilson, S.T. Eur. Patent EP 0,158,977 (1985).

60. Lok, B.M., Marcus, B.K., Messina, C.A., Patton, R.L., Wilson, S.T. and Flanigen, E.M. Eur. Patent EP 0,158,349 (1985).

61. Flanigen, E.M., Lok, B.M., Patton, R.L. and Wilson, S.T. Pure Appl. Chem. 1986, 58, 1351.

62. Meier, W.M. 'New Developments in Zeolite Science Technology'. Proc. 7th Int. Zeolite Conf., Eds. Y. Murakami, A. Iijima and J.W. Ward. Kodansha Ltd., Tokyo 1986, p. 13.

63. Csicsery, S.M. Pure Appl. Chem. 1986, 58, 841.

64. Chang, C.D., Lang, W.H. and Bell, W.K. 'Catalysis of Organic Reactions', Ed. W.R. Moser. Marcel Dekker Inc., New York 1981, p. 73.

65. Weisz, P.B. and Frilette, V.J. J. Phys. Chem. 1960, 64, 382.

66. Weisz, P.B., Frilette, V.J., Maatman, R.W. and Mower, E.B. J. Catal. 1962, 1, 307.

67. Csicsery, S.M. ACS Monograph 171, Ed. J.A. Rabo, Amer. Chem. Soc., Washington D.C. 1976, p. 680.

68. Shabtai, J. Chem. Ind. (Milan) 1979, 61, 734.

69. Satterfield, C.N. 'Heterogeneous Catalysis in Practice', McGraw-Hill, New York 1980, p. 151.

70. Chen, N.Y., Maziuk, J., Schwartz, A.B. and Weisz, P.B. Oil Gas J. 1968, 66, 154.

71. Yamaguchi, I. Joh, T. and Tekahashi, S. J. Chem. Soc., Chem. Commun. 1986, 1412.

72. Dessau, R.M. J. Catal. 1984, 89, 520.

73. Cavallaro, S., Pino, L., Tsiakaras, P. Giordano, N. and Rao, B.S. Zeolites 1987, _7_, 408.
74. Huizinga, T., Scholten, J.J.F., Wortel. Th. M. and Bekkum, H. van. Tetrahedron Letters 1980, _21_, 3809.
75. Wortel, Th.M., Oudijn, D. Vleugel, C.J., Roelofsen, D.P. and Bekkum, H. van. J. Catal. 1979, _60_, 110.
76. Chiche, B., Finiels, A., Gauthier, C., Geneste, R., Graille, J. and Pioch, D. J. Org. Chem. 1986, _51_, 2128.
77. Oudejans, J.C. and Bekkum, H. van. J. Mol. Catal. 1981, _12_, 149.
78. Flanigen, E.M. 'Zeo-Agriculture. Use of Natural Zeolites in Agriculture and Aquaculture', (Eds. W.G. Pond and F.A. Mumpton), Westview Press Inc., Boulder 1984, p. 55.
79. Planck, C.J. and Rosinski, E.J. US Patent 3,140,249 (1964).
80. Vedrine, J.C. 'Solid State Chemistry in Catalysis', Eds. R.K. Grasseli and J.F. Brazdill, ACS Symp. Ser. _279_, Amer. Chem. Soc., Washington D.C. 1985, p. 257.
81. Kouwenhoven, H.W., Van Zijll Langhout, W.C. Chem. Eng. Progr. 1971, _67_, 65.
82. Holderich, W., Hesse, M. and Naumann, F. Angew. Chem. 1988, _100_, 232.
83. Bekkum, H. van and Kouwenhoven, H.W. in 'Heterogeneous Catalysis and Fine Chemicals' (Eds. M. Guisnet et al.), Elsevier, Amsterdam 1988, p. 45.
84. Sersale, R. 'Zeolites: Synthesis, Structure, Technology and Application', Eds. B. Drzjai, S. Hocevar and S. Pejovnik. Stud. Surf. Sci. Catal. _24_, Elsevier, Amsterdam 1985, p. 503.
85. Roelofsen, D.P. Ph. D. Thesis, Delft University of Technology, Delft 1972.
86. Wortel, Th.M. Ph. D. Thesis, Delft University of Technology, Delft 1979.
87. Oudejans, J.C. Ph. D. Thesis, Delft University of Technology, Delft 1984.
88. Gaag, F.J. van der. Ph. D. Thesis, Delft University of Technology, Delft 1987.
89. Gaag, F.J. van der, Jansen, J.C. and Bekkum, H. van. Zeolites 1984, _4_, 369.
90. Gaag, F.J. van der, Louter, F., Oudejans, J.C. and Bekkum, H. van. Appl. Catal. 1986, _26_, 191.
91. Gaag, F.J. van der, Louter, F. and Bekkum, H. van. 'New Developments in Zeolite Science Technology'. Proceedings of the 7th International Zeolite Conference (Eds. Y. Murakami, A. Iijima and J.W. Ward). Kodansha Ltd., Tokyo 1986, p. 763.
92. Suzuki, T. and Komatsu, C. Eur. Pat. Appl. EP 0,154,236.
93. Hoefnagel, A.J., Peters, J.A. and Bekkum. H. van. Recl. Trav. Chim. Pays-Bas 1988, _107_, 242.

CHAPTER II

THE ~1030 CM^{-1} BAND IN IR SPECTRA OF ZEOLITE ZSM-5

ABSTRACT

Crystalline ZSM-5 materials, of different composition, morphology and particle size, were studied with infrared spectroscopy. A frequently observed but never assigned absorption in the 1060-1010 cm^{-1} region is discussed. It is concluded that the absorption indicates non-ZSM-5 framework material in the surface layer of the particles with an average particle size larger than 2 microns.

INTRODUCTION

When studying ZSM-5 synthesis, IR spectroscopy can be used as a fast initial selection on the quality of the zeolite material obtained (1). Apart from the characteristic lattice vibrations of ZSM-5 an indication about purity is found by the intensity ratio of the 550 and the 450 cm^{-1} band (2). Frequently we observed a vibration between 1060 and 1010 cm^{-1} in IR spectra of ZSM-5 particles. Several published IR spectra of ZSM-5 also show this absorption band although no assignment is given (3-7).

To examine if this vibration can be correlated to the ZSM-5 framework or to an impurity, the effects of several parameters, such as morphology and chemical composition, on the band between 1060 and 1010 cm^{-1} were studied.
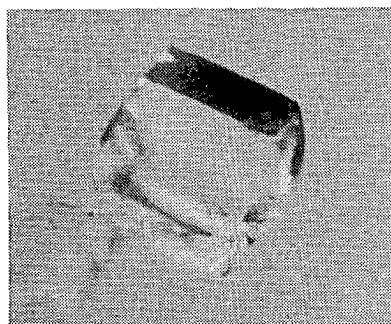
EXPERIMENTAL

Several preparation methods were used to obtain
crystalline ZSM-5 materials of different morphologies
(3,8-13). Large monocrystals (up to 400 microns in the
c-direction) were grown from systems with relatively low Si
and Al concentrations (14).

The samples were identified with rontgen diffraction (XRD)
and characterized by IR and scanning electron microscopy
(SEM). Some samples were quantitatively analyzed by X-ray
fluorescence (XRF). The chemical composition of the
monocrystals was determined by electron microprobe analysis
(EMPA). A monocrystal structure, including the template, has
been solved (15).

The mid IR spectra were recorded in the transmission mode
on a Perkin Elmer 521 Grating Infrared Spectrometer using
the KBr pellet technique, in such a way, that the sample was
mixed well with the powdered KBr whereafter a disc was
pressed. An IR spectrum of a large monocrystal (polished
down to a thickness of 6 microns along the b-axis) was
recorded on a Bruker IFS 85 Spectrometer, equipped with a
Bruker Infrared Microscope using a diaphragm of 120
microns. The crystal was directed parallel to the b-axis.
X-ray powder diffraction data were obtained with a Type II
Guinier de Wolff camera, using CuKα radiation. SEM
photographs were made on a Jeol Jxa-50A Electron
Microanalyzer. The electron microprobe analysis was
performed on a Jeol Superprobe 733. XRF analyses were
performed on a Philips PW 1400 Rontgen Spectrometer using
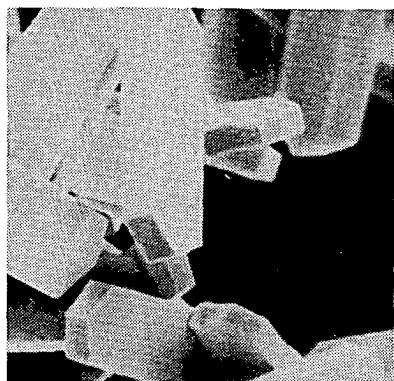lithium borate glass pellets containing the disclosed
sample.

RESULTS AND DISCUSSION

SEM photographs show five different morphologies of ZSM-5:
type IA, large monocrystals, type IB, apparently well grown
small monocrystals but internal twinning around the a-axis

Type IA   ⊢————⊣
                           100 µ
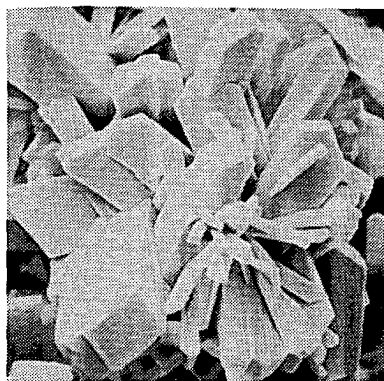
Type IB   ⊢————————⊣
                  . 5 µ
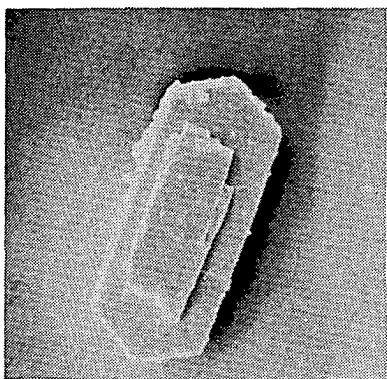
Type IIA   ⊢————————⊣
                    5 µ
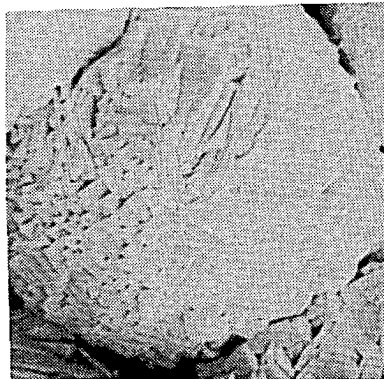
Type IIB   ⊢————⊣
                  5 µ

Type III   ⊢————⊣
                   2 µ

Figure 1. A macroscopic photograph and scanning electron
micrographs of zeolite ZSM-5 showing different types of
morphologies.   IA. monocrystal (mounted on a glass capil-
lary; IB. internally twinned monocrystals (here Silica-
lite-1); IIA. 'intergrown' crystals; IIB. 'twinned' crys-
tals; and III. spherulites.

is not excluded (16), type IIA. 'intergrown' crystals, type
IIB. 'twinned' crystals and type III. spherulites.
Characteristic examples are shown in Figure 1.

   The morphology types IA, IB and IIA are observed for
crystals with high Si/Al ratios. These materials did not
show the extra vibration in the 1060–1010 cm^{-1} region.
Crystalline products with lower Si/Al ratios, generally show
strongly intergrown and spherulitic morphologies (types IIB,
III), as reported by von Ballmoos (3). In these materials we
observed unambiguously the extra 1060–1010 cm^{-1} vibration.

   Irrespective of morphology type, no extra vibration was
found in IR spectra of ZSM-5 particles with an average ·
diameter less than 2 microns. This holds for as synthesized
particles as well as for powdered materials. It is observed
that the ease of powdering is by far the highest for type
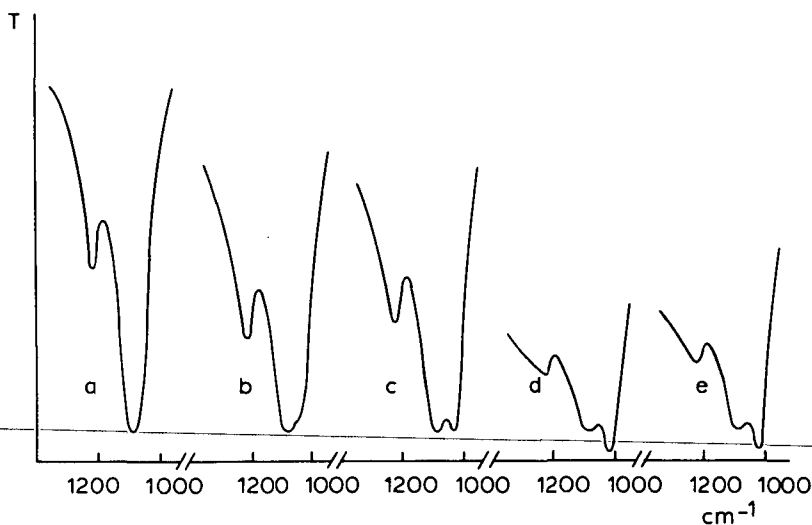III particles.

Figure 2. Effect of the synthesis temperature on the
formation of the extra IR-vibration in type III ZSM-5
particles. Reactant Si/Al = 50. Preparation according to
reference 9. a) T=118°; b) T=140°; c) T=160°; d) T=180° and
e) T=200°C. Reaction time 48 hours.

Varying the synthesis time shows that the extra peak
develops in intensity and decreases in wavenumber during a
later stage of the synthesis. A similar effect was found
when the crystallization rate was altered by temperature
variation as depicted in Figure 2.

Techniques used to etch the surface of the particles
(partly dissolving by heating in HF at 60°C or in refluxing
2M NaOH. described in Chapter III) brings about a decrease
in intensity and an increase in wavenumber of the extra
vibration, as shown in Figure 3 for the NaOH treatment,
which is in harmony with the observations made during
synthesis. XRF measurements on a ZSM-5 sample (type IIB)
show a significant increase in Si/Al ratio after 1 hour
refluxing in 2M NaOH.

Infrared spectra, recorded at room temperature. of
'twinned' crystals (type IIB), which were heated up to
1300°C still show the extra vibration while the ZSM-5
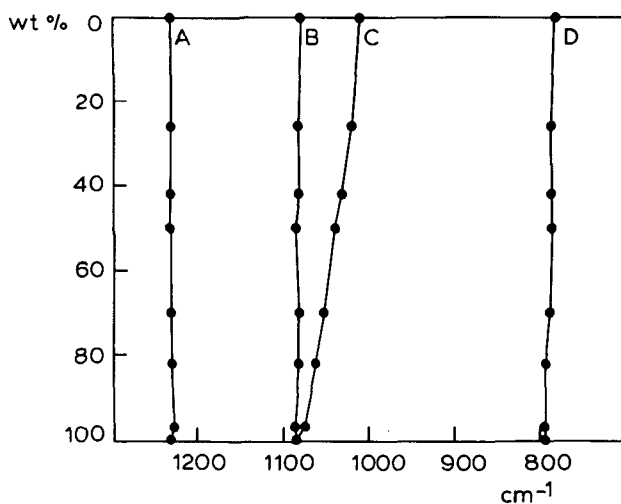
Figure 3. Effect of dissolving ZSM-5 crystallites (type IIB)
in a refluxing 2M NaOH solution (as described in Chapter
III) on the IR frequencies of the remaining solid. A
represents the transmission around 1220 cm^{-1}; B the 1080
cm^{-1} vibration: C the extra vibration and D the 890 cm^{-1}
vibration.
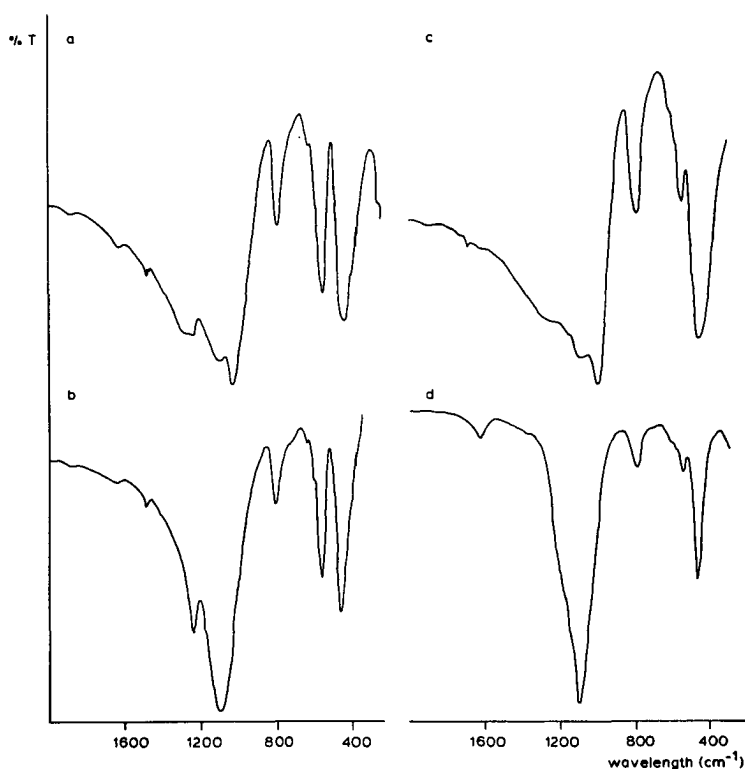
Figure 4. Infrared spectra of type IIB zeolite ZSM-5 particles. a) Original material; b) original material after powdering; c) after heating the original material to 1300°C; and d) after powdering of the heated product.

structure lattice bands at 1220 cm^{-1} and 550 cm^{-1} are no longer present. Powdering the heated or the original sample leads to the disappearence of the extra vibration. These spectra are depicted in Figure 4.

– Origin of the extra lattice vibration

A typical IR spectrum of ZSM-5 particles (type IIB, see Figure 1), containing the extra vibration, is depicted in Figure 4a. Powdering these particles (SEM shows an increase in fragments < 2 microns) leads to an intensity-increase for the asymmetric T-O-T stretch vibration at about 1090 cm^{-1} and to disappearance of the extra 1060-1010 cm^{-1} vibration.

According to Duyckaerts (17) only particles with a diameter
< 2 microns show 100% transmission. Larger particles tend
to reduce both the apparent intensity and the resolution of
the spectrum (Christiansen effect). This means there is no
correlation between particle size and absorption frequency.
Using a sample thickness of 6 microns we observed no
transmission between 1350 and 1000 cm^{-1}. Thus the IR
transmission through large particles is just partly recorded
from the core of the particles, and mainly from the boundary
layers, where the transmission pathway through the particle
is < 6 microns. It is therefore believed that the extra IR
vibration between 1060 and 1010 cm^{-1} is related to the outer
layers of the crystals. When the average particle size
becomes < 2 microns, the extra peak is overruled by the
intensity of the ~1090 cm^{-1} T-O-T asymmetric stretch
vibration. This indicates heterogeneity in the ZSM-5
particles.

   This idea is supported by IR transmission measurements
performed on large monocrystals (type IA) of ZSM-5
(Si/Al=270), with a homogeneous Al distribution (16). Here,
the extra band is not present at all (confirmed with DRIFT).

   Heterogeneities in ZSM-5 crystalline materials with
comparable morphologies, are known in literature. It is
mentioned that Al-rich aluminosilicate entities are
incorporated into the framework only at the end of the
crystallization process (18-20). In addition, ESCA studies
of the surface chemistry of zeolites (21) show that ZSM-5
exhibits an extensive surface presence of both alumina and
sodium aluminate impurities. The presence of an Al-gradient
is supported by our observations done during synthesis. The
observed decrease in wavenumber of the extra vibration might
indicate a change in Si/Al ratio of the outer rim of larger
particles, which strongly affects the T-O-T asymmetric
stretch vibration (22,23). The absence of the extra peak
after extensive powdering indicates that the total amount of
impurities present is less than 5 wt% (IR determination
range).

Experiments to investigate the cause of the extra
vibration revealed no information on defined materials.
Besides the 1060–1010 cm^{-1} absorption, there are found no
significant other extra vibrations in the ZSM-5 IR spectra.
Also the 550/450 intensity ratio reveals no information on
extra material. XRD measurements show no additional
diffraction patterns as well.

A heat treatment experiment shows a higher thermal
stability for the cause of the extra IR vibration at about
1030 cm^{-1}, with respect to the 1220 and 550 cm^{-1} ZSM-5
framework vibration bands. This would indicate that the
extra IR absorption is caused by non-ZSM-5 framework
material.

ACKNOWLEDGEMENTS

REFERENCES

1.   Jansen, J.C., Gaag. F.J. van der and Bekkum, H. van.
     Zeolites 1984, 4, 369.
2.   Coudurier, G., Naccache, C. and Vedrine, J.C. J. Chem.
     Soc., Chem. Commun. 1982, 1413.
3.   Ballmoos, R. von. Ph.D. Thesis, Zurich 1981.
4.   Jacobs. P.A., Beyer, H.K. and Valyon, J. Zeolites
     1981, 1, 161.
5.   Post, J.G. Ph.D. Thesis. Eindhoven 1984.
6.   Howden, M.G. 'The role of the tetrapropylammonium
     template in the synthesis of ZSM-5', 1982, CSIR Report
     CENG 413, CERG-CSIR PO Box 395, Pretoria 0001, South
     Africa.
7.   Chao, K., Tasi, T.C., Chen, M. and Wang, I. J.Chem.
     Soc., Faraday Trans. 1 1981, 77, 547.
8.   Flanigen. E.M. and R.L. Patton. US Patent 4.073.865.
9.   Argauer, R.J. and Landolt. G.R. US Patent 3.702.886.
10. Casci. B.L., Lowe. B.M. and Whittam. T.V. Eur Pat.

Appl. EP 0.042.225.
11. Ghanami, M. and Sand L.B. Zeolites 1983, 3, 155.
12. Mostowitz, R. and Sand, L.B. Zeolites 1983, 3, 219.
13. Gaag, F.J. van der, Jansen, J.C. and Bekkum, H. van.
    Appl. Catal. 1985, 17, 261.
14. Lermer, H., Draeger, M., Steffen, J. and Unger, K.K.
    Zeolites 1985, 5, 131.
15. Koningsveld, H. van, Jansen, J.C. and Bekkum, H. van.
    Acta Crystallogr. 1987, B43, 127.
16. Jansen, J.C., Schalkoord, B., Koningsveld, H. van and
    Bekkum, H. van. To be published.
17. Duyckaerts, G. Analyst 1959, 84, 201. Hair, M.L.,
    'Infrared Spectroscopy in Surface Chemistry', Marcel
    Dekker Inc., New York 1967, p. 59.
18. Gabelica, Z., Nagy, J.B., Bodart, P. and Nastro, A.
    Thermochim. Acta 1985, 93, 749.
19. Debras, G., Gourgue, A., Nagy, J.B. and De Clippeleir,
    G. Zeolites 1985, 5, 369.
20. Ballmoos, R. von, Gubser, R. and Meier, W.M. Proc.
    Int. Conf. Zeolites 6th (Ed. D. Olson and A. Bisio)
    1983, 803.
21. Barr, T.L. and Lishka, M.A. J. Am. Chem. Soc. 1986,
    108, 3178.
22. Breck, D.W. 'Zeolite Molecular Sieves: Structure,
    Chemistry and Use', John Wiley and Sons, New York
    1974, p. 415.
23. Wendlandt, K.P., Bremer, H., Jank, M., Weber, M.,
    Starke, P. and Mueller, D. Proc. Int. Symp. Zeolites
    Catal., Siofok (Hung.) 1985, 35.

CHAPTER III

SOME BASE AND ACID DISSOLUTION EXPERIMENTS WITH MFI-ZEOLITES

ABSTRACT

The dissolution process of ZSM-5 and Silicalite-1 in 2M
sodium hydroxide has been followed by scanning electron
microscopy (SEM) and Si/Al analysis. It is shown that the
Al gradient present in ZSM-5 influences the rate and
selectivity of the dissolution of the zeolite particles.
Experiments on ZSM-5 and Silicalite-1 with 1.0M hydrofluoric
acid reveal a more homogeneous mechanism to be effective.

INTRODUCTION

In Chapter II the presence of an extra IR vibration
between 1070 and 1010 cm^{-1} in IR spectra of zeolite ZSM-5
particles is discussed, which is assigned to non-ZSM-5
framework material (1). The existence of heterogeneities in
ZSM-5 materials is known in literature (2-5). Von Ballmoos
et al. (2) describe the presence of an Al-gradient in ZSM-5.
The presence of aluminum-contaning non-framework material on
ZSM-5 is reported by Barr et al. (5). Experiments performed
in the previous Chapter indicate that the presence of an
Al-gradient in ZSM-5 crystallites affects their solubility
in aqueous basic media. A complete description of these
experiments is given in this Chapter.

Treatment of zeolites with alkali bases is no new topic.
In 1981 von Ballmoos (6) described the removal of amorphous
silica-rich material, present after zeolite synthesis, by
refluxing the non-calcined zeolites in a 1M NaOH solution
for 1 hour. Recently Miale et al. (7) have claimed that

alkali treatment of zeolite ZSM-5 enhances the activity of
the zeolite catalyst.

EXPERIMENTAL

The preparation of the molecular sieve materials tested
was based on a procedure described by Ghanami and Sand (6).
Preparation of ZSM-5: molar reactant composition: 100 SiO_2;
1.7 Al_2O_3; 206 NH_4OH; 13.2 TPA-Br; 3500 H_2O. Reaction
conditions: teflon-lined stainless steel autoclave; no
stirring during reaction; T=180°C; t=120 hours.
Preparation of Silicalite-1: molar reactant composition: 100
SiO_2; 132 NH_4OH; 8.5 TPA-Br; 2076 H_2O. Reaction conditions:
teflon-lined stainless steel autoclave; no stirring during
reaction; T=180°C; t=48 hours.

Dissolution experiments with alkali base were performed as
follows: As-synthesized, tetrapropylammonium containing,
Silicalite-1 and ZSM-5 samples were refluxed in 2M NaOH (100
ml/0.5 g zeolite). In view of the blocking of the channels
by the template molecules, mainly surface interactions are
assumed to occur. The dissolution reaction was stopped by
directly filtering off the hot suspension over a Buchner
funnel and washing the residue with cold demineralized
water. The residue was dried overnight at 100°C whereafter
the weight of the sample was measured.
For comparison some experiments were performed in acidic
medium (aquous hydrogen fluoride). The procedure was:
As-synthesized ZSM-5 or Silicalite-1 material was suspended
in 1.0M HF (1.0 g/100 ml) which was sufficient to dissolve
50 wt% of the zeolite material. The suspensions were kept
at 60°C for 6 hours in closed polypropylene flasks. After
cooling the flasks in ice the remaining solids were filtered
off over a Buchner funnel and washed several times with
demineralized water. Subsequently the samples were dried
overnight at 100°C.

The samples obtained were subjected to SEM, IR and
elemental analysis. SEM photographs were made on a Jeol Jxa
50A Electron Microanalyzer. The description of the IR

measurements was given in Chapter II. Of some samples the
Si/Al ratio was determined by AAS using a Perkin Elmer 460
Atomic Absorption Spectrophotometer.

RESULTS AND DISCUSSION

As described in Chapter II, Figures 2 and 3, an increase
in wavenumber and a decrease in intensity of the extra IR
lattice vibration was observed upon dissolution of ZSM-5
crystallites in NaOH, which is opposite to the observations
made during synthesis. This IR-effect was also observed for
aqueous HF as dissolving agent.

The solubility of silica(-alumina) depends on the amount
of impurities present (9-11). For instance, aluminum(III),
when present in minute amounts, not only reduces the rate of
dissolution of silica, but by chemisorption on the surface
of silica, also reduces the solubility of silica at
equilibrium. This means that exposed intracrystalline
material, having a higher Si/Al ratio, can dissolve faster
than at surfaces with a lower Si/Al ratio. The influence of
aluminum on the dissolution rate becomes apparent when
non-calcined Silicalite-1 is treated with 2M NaOH. This
(almost) Al-free ZSM-5 type molecular sieve dissolves at a
rate about five times higher than the ZSM-5 particles
(Si/Al=35.8) described below.

SEM photographs of ZSM-5 particles, treated with 2M NaOH
(Figure 1) show an attack on the (amorphous) surface of the
particles, especially where the twins cross (Figure 1,
pictures 1 and 2). When the Al-rich surface partly has been
dissolved the silica-rich inner part of the zeolite can be
attacked. Because of its higher Si/Al ratio this inner part
dissolves faster than the outer surface (Figure 1, pictures
3, 4 and 5). When all Si-rich parts have been dissolved, a
part of the Al-rich crust remains, which finally slowly
dissolves (Figure 1, pictures 6 and 7). It may be noted that
the final material still exhibits an IR-spectrum which is
characteristic for ZSM-5.
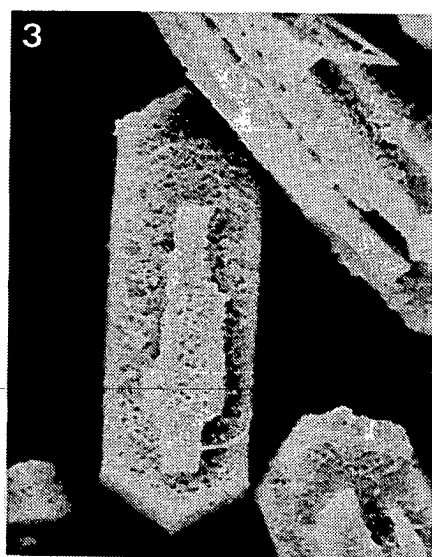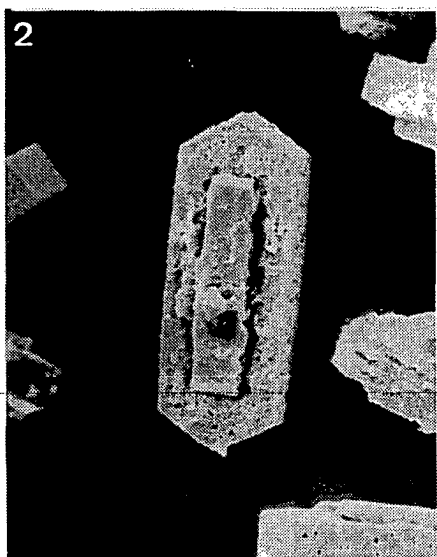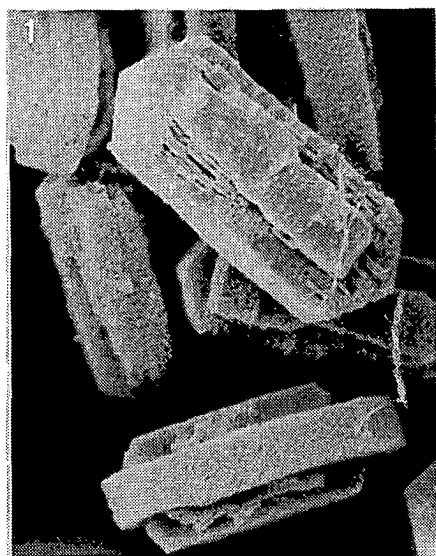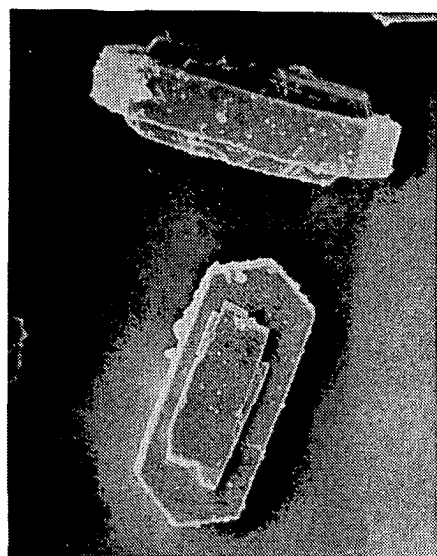
Figure 1. SEM photographs of ZSM-5 particles during reflux-
ing in aqueous 2M NaOH. The numbers on the pictures indicate
the reflux time in hours.
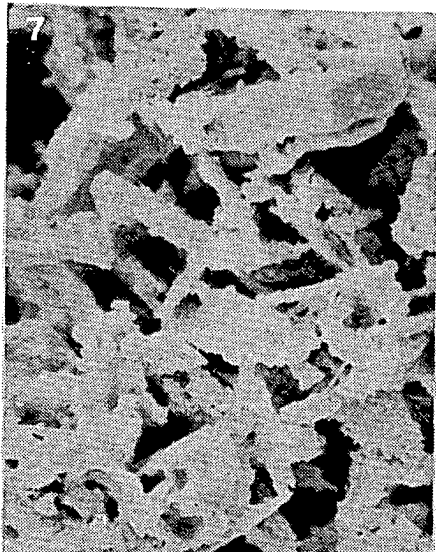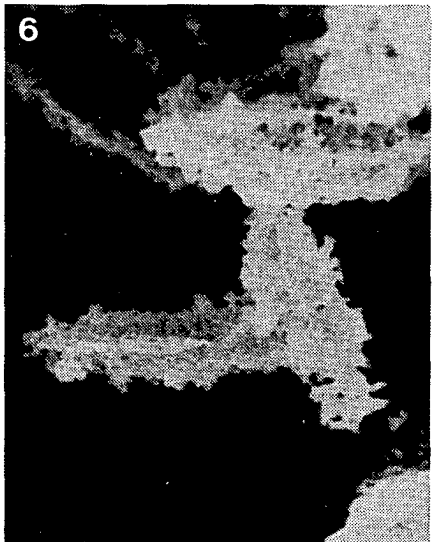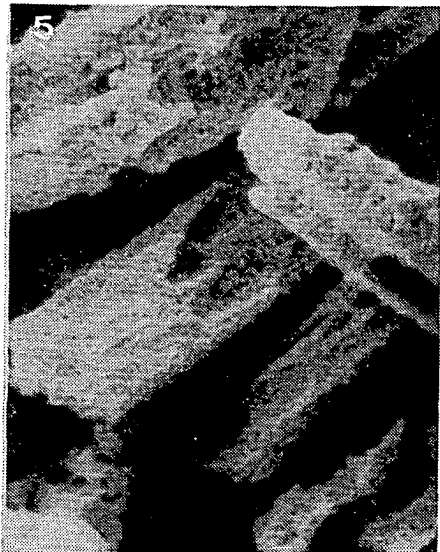
Figure 1 (continued).
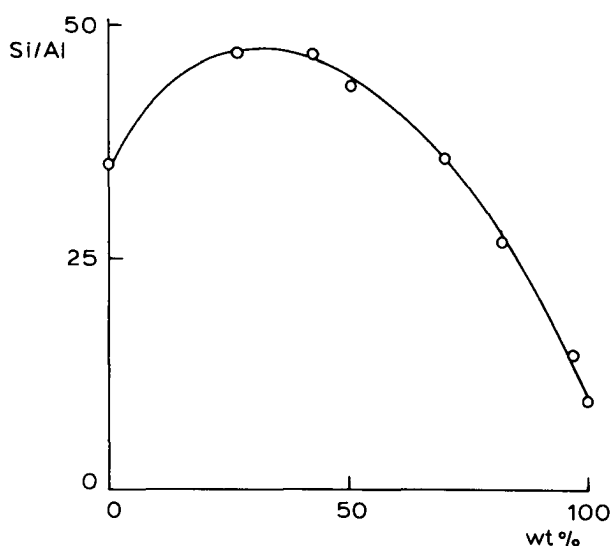
Figure 2. A plot of the Si/Al ratio of the remaining ZSM-5
solids versus the amount of material dissolved in 2M NaOH.
The measuring points represent the samples of Figure 1.

The dissolution sequence as monitored with SEM is
supported by measurements of the Si/Al ratio of the
remaining solid. As can be seen in Figure 2, first the
Al-rich part of the zeolite is attacked resulting in an
increase in Si/Al ratio. When the surface layer is
sufficiently perforated the extraction of Si-rich material
accounts for the decrease in Si/Al ratio.

The observed shift of the extra IR vibration towards 1100
cm^{-1} together with a decrease in intensity (Chapter II) not
only indicates a continuous dissolution at the surface (at a
lower rate than for the Si-rich inner parts of the
crystallites) but also a decrease in 'surface' Si/Al ratio
due to preferential Si-dissolution.

The difference in dissolving behaviour between ZSM-5 and
Silicalite-1 not only expresses itself in dissolution rate
but can also be observed with SEM (Figures 1 and 3a,b). As
mentioned above. ZSM-5 seems to be hollowed out. This in
contrast to Silicalite-1 which shows a fast dissolution at
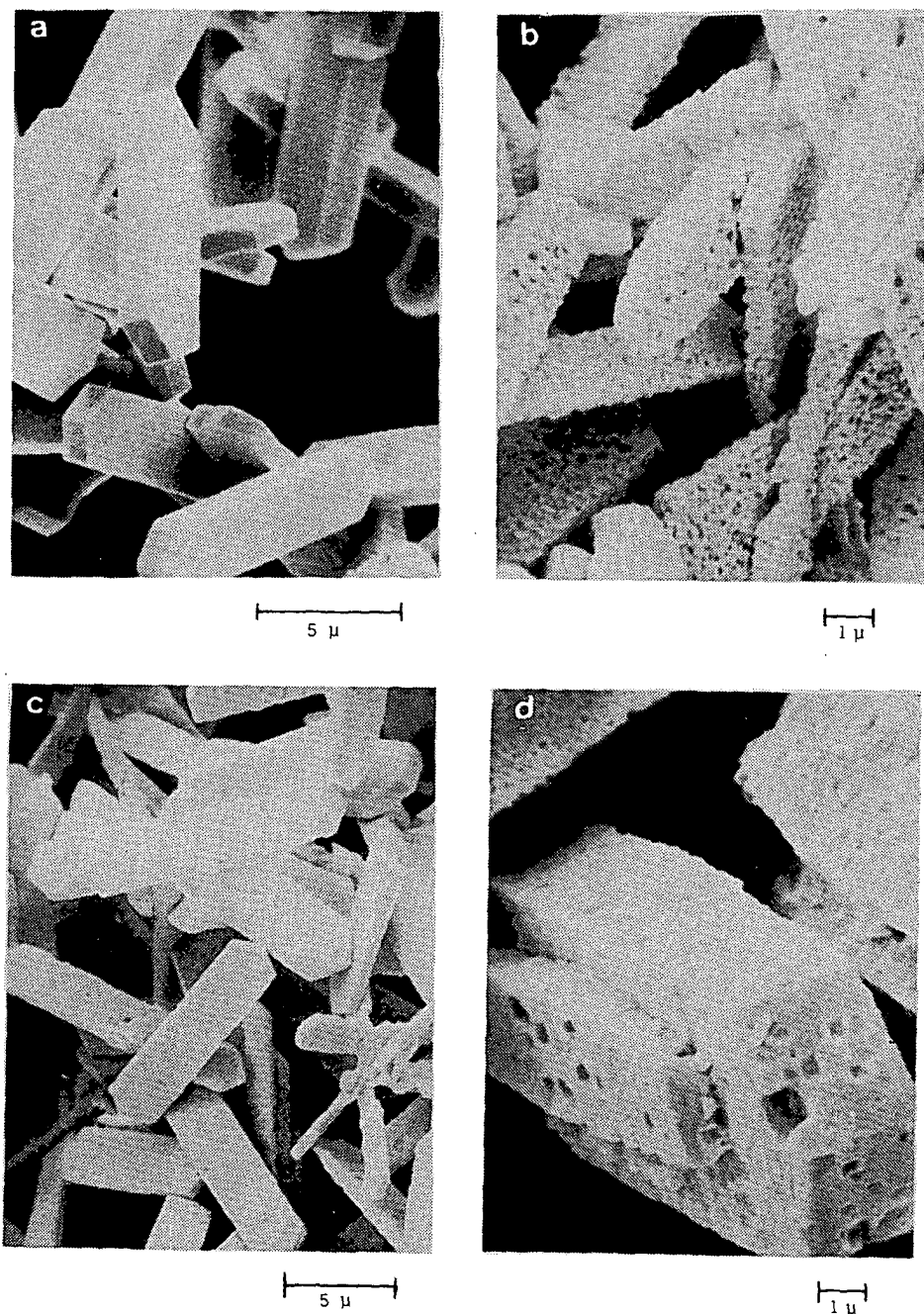
Figure 3. SEM photographs of Silicalite-1 and ZSM-5. a)
Silicalite-1, starting material; b) Silicalite-1, treated
with 2M NaOH for 45 minutes: c) Silicalite-1. treated with
1.0M HF and d) ZSM-5. treated with 0.1M HF.

the surface of the crystallite, giving it the appearance of Swiss cheese.

As shown in Figure 3c,d experiments using aqueous hydrofluoric acid show a more homogeneous dissolution behaviour for ZSM-5 as well as for Silicalite-1 which operates at or close to the crystal surface. This in contrast to the dissolution experiments with NaOH in which deeper reagent penetration and crystal decay is observed. A more close examination of the SEM photographs for HF-treated ZSM-5 (Figure 3d) and Silicalite-1 (Figure 3a,b,c), shows that different disslution patterns are involved as well, emphasizing the role of the Al-rich crust.

ACKNOWLEDGEMENTS

REFERENCES

1. Febre, R.A. le, Jansen. J.C. and Bekkum, H. van. Zeolites 1987. $\underline{7}$, 471; This Thesis, Chapter II.
2. Ballmoos, R von., Gubser, R. and Meier. W.M. Proc. Int. Conf. Zeolites 6th (Ed. D. Olson and A. Bisio) 1983, 803; Ballmoos, R. von and Meier. W.M. Nature 1981, $\underline{289}$, 782.
3. Hughes, A.E., Wilshier. K.G., Sexton. B.A. and Smart. P. J. Catal. 1983, $\underline{80}$, 221.
4. Geurts. F.M.M., Kentgens. A.P.M. and Veeman, W.S. Chem. Phys. Lett. 1985. $\underline{120}$, 206.
5. Barr, T.L. and Lishka. M.A. J. Am. Chem. Soc. 1986. $\underline{108}$, 3178.
6. Ballmoos. R. von. Ph.D. Thesis. Zurich 1981.
7. Miale. J.N. and Chang. C.D. AU 567,686.
8. Ghanami. M. and Sand. L.B. Zeolites 1983. $\underline{3}$, 155.
9. Iler, R.M. 'The Chemistry of Silica'. John Wiley and Sons, New York 1979, p. 56.
10. Guth. J.L., Caullet, P. and Wey. R. Proc. Int. Conf. Zeolites 5th (Ed. W.V.C. Rees) 1980, 30.
11. Wendlandt, K.P., Bremer, H., Jank, M., Weber, M., Starke, P. and Mueller. D. Proc. Int. Symp. Zeolite Catal. Siofok (Hung.) 1985, 35.

CHAPTER IV

FACTORS AFFECTING THE SYNTHESIS OF ZEOLITE THETA-1/Nu-10

ABSTRACT

The crystallization of Theta-1/Nu-10 has been investigated.
Among the templates studied oligo-iminoethylenes are the
most suitable. The alkaline cation determines the Si/Al
ratio at which crystalline material is formed. In the
presence of Na$^+$, essentially pure Nu-10 is obtained at Si/Al
ratios between 34 and 52, whereas K$^+$ allows a Si/Al ratio
between 9 and 17. The effects of variation of template
concentration. OH$^-$/SiO$_2$ ratio and synthesis time on the
formation of pure Theta-1/Nu-10 are reported.

INTRODUCTION

In the years 1981-82 a series of high silica zeolites (see
Table 1) were reported showing an essentially identical
XRD-pattern. One of them, Nu-10, is reported to show a
relatively high selectivity to p-xylene in the methylation
and disproportionation of toluene and a predominant
formation of olefins in methanol conversion (6,7).

The structures of Theta-1 (8-10) and of ZSM-22 (11), based
on XRD-data (12), have been published. The zeolite has a

Table 1. Theta-1 type zeolites.

Zeolite name	Reference
1. Theta-1	1
2. Nu-10	2
3. ZSM-22	3
4. KZ-2	4
5. ISI-1	5

a   b
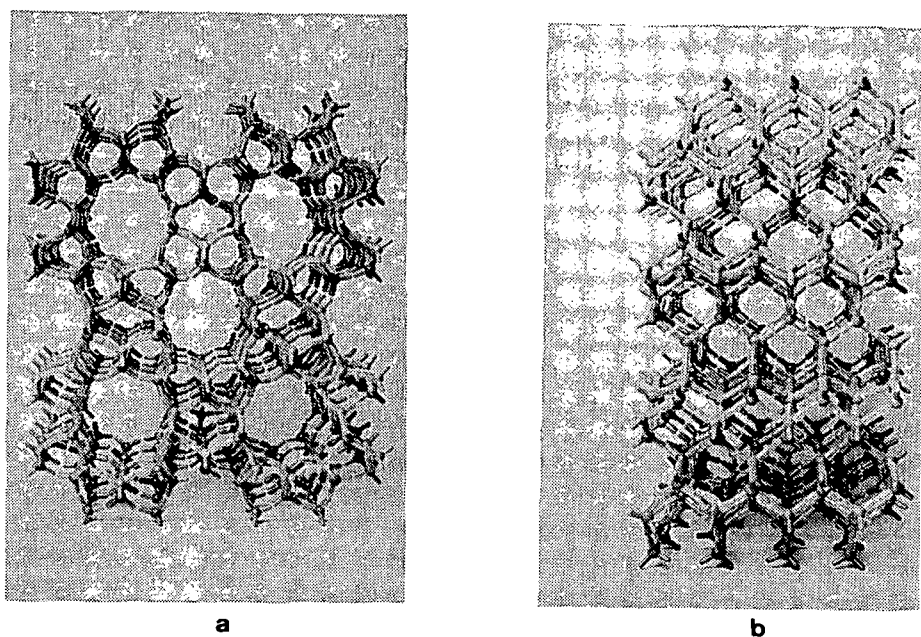
Figure 1. Framework structure of Nu-10. a) view down the
c-axis; b) view down the a-axis.
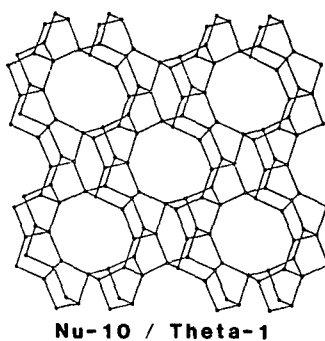
Nu-10 / Theta-1
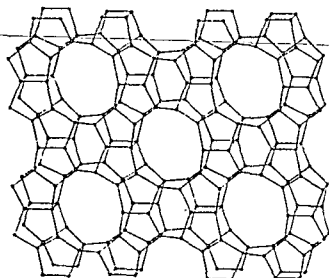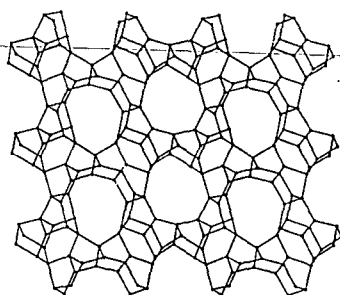
ZSM-48   **ZSM-23**

Figure 2. Structure of ZSM-48. ZSM-22 and ZSM-23. Drawings
according to references 11. 13 and 14.

medium pore size. The framework is shown in Figure 1 and
can be constructed from 5-1 secondary building units which
places the zeolite in the pentasil group of zeolite
structures. The system is one-dimensional with channels
running parallel to the c-axis. The channel is formed by an
elliptical 10-T-ring system (diameters 0.45x0.55 nm).

   Several other zeolites have a related structure. For
example, the proposed structure of ZSM-48 ((13) similar to
EU-2, EU-11 and ZBM-30) consists of ferrierite sheets
analogous to ZSM-22 with non interpenetrating linear
channels of 0.53x0.56 nm. ZSM-23 ((14, 15)
rontgenisomorphous with ISI-4 and KZ-1) is also closely
related to ZSM-22, although subtle differences exist in the
shapes of the pore openings. ZSM-22 and ZSM-23 contain 5-3
secondary building units. The resulting structure only

Table 2. Templates reported in literature to obtain the zeolites named
in Table 1.

Template		References	Results according to literature
1. $H_2N(C_2H_4NH)_3C_2H_4NH_2$	TEPA	2,6,17,18	Nu-10
2. $H_2N(C_2H_4NH)_2C_2H_4NH_2$	TETA	2,6	Nu-10
3. $H_2NC_2H_4NHC_2H_4NH_2$	DETA	4,6	Nu-10, KZ-2
4. $C_2H_5NHC_2H_4NHC_2H_5$		2,6	Nu-10
5. $(C_2H_5)_2NC_2H_4NH_2$		2,6	Nu-4[1]
6. $C_2H_5NHC_2H_5$		3,4	ZSM-22, KZ-2
7. $HOC_2H_4NHC_2H_4OH$	DEA	1,9	Theta-1
8. $H_2NC_2H_4NH_2$	EDA	16,9	Nu-10
9. $H_2NC_3H_4NH_2$		6	Nu-10
10. $(H_2N)_2CHC_2H_5$		6	Nu-10 + ferrierite
11. $H_2NC_4H_8NH_2$		16	Nu-10 + α-cristobalite
12. $H_2NC_4H_9$		4	KZ-2
13. $H_2NC_5H_{10}NH_2$		20	ZSM-22
14. $H_2NC_3H_6CH(NH_2)C_2H_5$		4	KZ-2
15. $H_2NC_6H_{12}NH_2$	HXDM	3,16,19,20	ZSM-22, Nu-10
16. $H_2NC_7H_{14}NH_2$		20	ZSM-22
17. $H_2NC_8H_{16}NH_2$		16,20	ZSM-22, Nu-10
18. $H_2NC_{10}H_{20}NH_2$		16	Nu-10
19. $H_2NC_{12}H_{24}NH_2$		16	Nu-10 + α-cristobalite
20. $HOC_2H_4NHC_2H_4NH_2$		9	Theta-1 + α-cristobalite
21. $HOC_2H_4OC_2H_4NH_2$		9	Theta-1
22. $HOC_2H_4OC_2H_4OH$		9	Theta-1 (+ α-cristobalite)
23. CH_3OH		5	ISI-1
24. $NH_2C_3H_7 + (CH_3)_4NCl$		13	ZSM-48[1]
25. $Br(CH_3)_3NC_7H_{14}N(CH_3)_3Br$		21	ZSM-23[1]

[1] Added for comparison.

Table 3. Results from syntheses following directives and
molar compositions from literature.

Experiments according to	Template	Expected result	Results[1]
Ref. 1 exp. 1	DEA	Theta-1	ZSM-5
Ref. 1 exp. 2	DEA	Theta-1	amorphous + t ZSM-5 + t α-quartz
Ref. 1 exp. 2[2]	DEA	Theta-1	Theta-1 + t α-cristobalite + t ZSM-5
Ref. 9	DEA	Theta-1	ZSM-5
Ref. 2 exp. 5	TEPA	Nu-10	Nu-10 + ? [3]
Ref. 2 exp. 12	TETA	Nu-10	ZSM-5
Ref. 6	TETA	Nu-10	Nu-10 + t ZSM-5
Ref. 19 exp. A	HXDM	ZSM-22	ZSM-5

[1] t=trace. [2] Example modified. See text. [3] 3 additional
non-assigned lines in XRD.

Table 4. Chemicals used in the experiments.

SiO$_2$ sources:	Ludox AS 40 (Dupont, 40 wt% SiO$_2$)
	Aerosil 200 (Degussa Al$_2$O$_3$; 7000 SiO$_2$; 490 H$_2$O)
Al$_2$O$_3$ sources:	Sodium aluminate (BDH Chemicals, technical grade, 44.2 wt% Al$_2$O$_3$; 27.8 wt% Na$_2$O; 28.0 wt% H$_2$O)
	Sodium aluminate (Riedel de Haen, 54 wt% Al$_2$O$_3$; 41 wt% Na$_2$O; 0.02 wt% Fe$_2$O$_3$)
	Aeroal (Degussa, δ-Al$_2$O$_3$, BET 100 m^2/g)
	Al(OH)$_3$ (Baker, analytical grade)
	AlCl$_3\cdot$9H$_2$O
Templates:	Tetraethylenepentamine (TEPA, Janssen Chimica, >98%)
	Triethylenetetramine (TETA, Janssen Chimica, >98%)
	Diethylenetriamine (DETA, Merck, >98%)
	Ethylenediamine (EDA, Merck, >99%)
	Polyethyleneimine (PEI, 30% solution in water, Janssen Chimica, average MW 50000-100000)
	Tetraethylene glycol (TEGA, Janssen Chimica, 98%)
	Triethylene glycol (TRIGO, Janssen Chimica, 99%)
	Diethanolamine (DEA, Baker, analytical grade)
	Triethanolamine (TEA, Fluka AG, pure)
	Triethylamine (TELA, Janssen Chimica, >99%)
	1,6 hexanediamine (HXDM, Janssen Chimica, >99.5%)
	1,4 dimethylpiperazine (DMP, Merck, 98%)
Others:	NaOH (EKA Kimi, >98%)
	KOH (pro analysis, >99%)
	NaCl (technical grade)
	KCl (analytical grade)
	HCl (technical grade)
	FeSO$_4\cdot$7H$_2$O (>98%)

contains 5. 6 and 10-rings of T-atoms. On the other hand
ZSM-48 contains a 5-5 secondary building unit (analogous to
ZSM-5) which allows the occurrence of 4-rings in the
structure. Structural differences between ZSM-22. ZSM-23
and ZSM-48 are illustrated in Figure 2.

  Methods for the preparation of the zeolites mentioned in
Table 1 show a large variety in synthesis conditions and
templates (see Table 2). Some exploratory experiments
following directions given in literature were not conclusive
(Table 3) and from discussions with other research workers
we learned that they were facing similar problems.
Accordingly we decided to investigate the synthesis
conditions more in detail in order to determine the
synthesis limits and to find the compositions where maximum
crystallinity is reached.

EXPERIMENTAL

  Materials used in the syntheses are described in Table 4.
Three types of autoclaves were used:

  - A stainless-steel autoclave (capacity 1000 ml) equipped
    with a vertical stirrer (experiments in Table 3).
  - A stainless-steel autoclave (capacity 120 ml). with
    teflon insert. rotating along its cylindrical axis in
    an oven (experiments in Table 3).
  - Small stainless-steel autoclaves (capacity 30 ml).
    placed in a caroussel. as described by van der Gaag et
    al. (22). were used to study the crystallization
    behaviour.

The reaction mixtures were prepared according to the
following method:

  - The Al source and the OH^--source are dissolved. as well
    as possible, in H_2O (suspension A).
  - The template is dissolved in suspension A (suspension
    B).
  - The silica source is dispersed in H_2O (suspension C).
  - Suspension B is added directly to suspension C. and the
    mixture is stirred thoroughly (suspension D).
  - Then the required amount of salt is mixed well with
    suspension D.
  - Directly thereafter. the gel formed is transferred into

the reaction autoclave.

- The autoclave is heated at the temperature chosen, for the appropriate time, while stirring the synthesis gel with a teflon-coated magnetic stirrer.

- The reactions are quenched by rapid cooling of the autoclaves, and the solid products are filtered off and washed several times with hot water on a Buchner funnel.

- The products are dried overnight at 100°C.

The samples were identified with X-ray diffraction (XRD) and characterized by infrared (IR) spectroscopy. X-Ray powder diffraction data were obtained with a Type II Guinier de Wolff camera, using CuKα radiation. The mid IR spectra were recorded in the transmission mode on a Perkin Elmer 521 Grating Infrared Spectrometer using the KBr pellet technique. Figure 3 shows the IR spectrum of Nu-10.
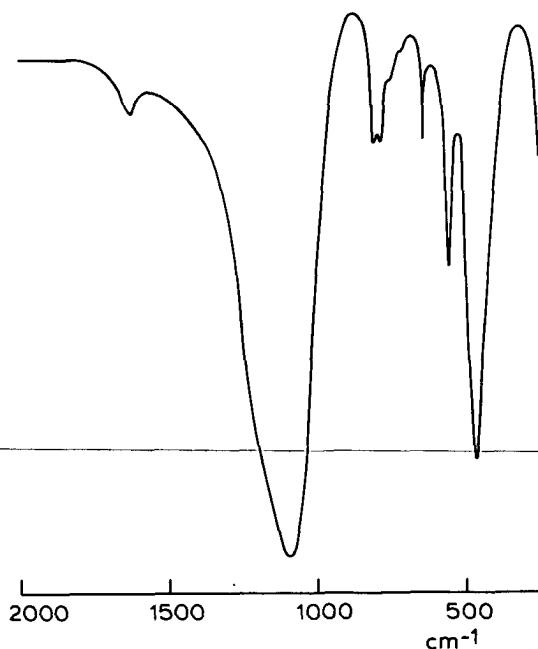
Figure 3. KBr IR-spectrum of Nu-10.

RESULTS AND DISCUSSION

Introductory experiments following the literature produced
the results presented in Table 3. Only in the experiments
performed according to references 2 (example 5) and 15
satisfactory results were obtained. Experiments performed
according to reference 1 (example 2) showed variable
results. When using, as described, a stainless-steel
autoclave (rotating in an oven) only amorphous material was
obtained. However, using a modified experimental procedure
(teflon insert, longer reaction time) the main product was
Theta-1. This was in contrast to the experiments resulting
in Nu-10 where no direct influence of the reaction vessel
was found. This might indicate, for diethanolamine as the
template, that the nature and/or texture of the vessel's
walls play a role in the nucleation phenomena of the
synthesis reaction.

As the best results in the exploratory experiments were
obtained using a molar composition described by Hogan et al.
(6) this formulation was used as a starting point for
further experiments.

For convenience we will refer to the zeolites from Table 1
by using the name Nu-10. The crystallinity of the Nu-10
formed is relative and is based on IR and XRD measurements.
The accuracy of the measurements is ~10%.

- template variation

Several compounds were tested for Nu-10 synthesis
efficiency. The results are recorded in Table 5. Under the
conditions given, also considering the results of Table 3,
the oligo-iminoethylenes are satisfactory as templates and
triethylenetetramine (TETA) seems to represent the optimum
chain length. The fact that polyethyleneimine (PEI) does
not work as a template may be related to the flocculation
properties of cationic linear polymers (23); PEI is
irreversibly absorbed onto the silica particles (at pH
5-10). It is also clear from Table 5 that the amino groups
play an important role; when completely replaced by oxygen

Table 5. Synthesis of zeolite Nu-10 using different tem-
plates and various conditions[1].

x	template	T(°C)	t(h)	Results[2]
26.67	TEPA[3]	180	40	Nu-10. s ZSM-5. t α-cristobalite
26.67	TEPA	160	71	ZSM-5 + Nu-10 (ca. 60:40)
28.70	TETA	180	40	Nu-10. t ZSM-5. mt α-cristobalite
28.70	TETA	160	71	Nu-10. t ZSM-5. mt α-cristobalite
28.73	DETA	180	40	Nu-10. s ZSM-5. mt α-cristobalite
28.73	DETA	160	71	Nu-10. s amorphous. s ZSM-5. mt α-cristobalite
32.45	EDA	180	40	Nu-10 (60%). amorphous. t ZSM-5
32.45	EDA	160	71	Nu-10 (60%). amorphous. t ZSM-5. t α-cristobalite
0.32	PEI	180	40	amorphous. t ZSM-5
0.32	PEI	160	71	amorphous
27.54	TEGO	160	71	amorphous
30.42	TRIGO	160	71	amorphous
32.38	DEA	160	71	amorphous
42.89	TEA	160	71	amorphous
31.04	TELA	160	71	ZSM-5
32.90	DMP	160	71	amorphous

[1] 1.09 Al_2O_3; 100 SiO_2; 2.55 Na_2O; x template; 4172 H_2O;
58.34 NaCl. [2] s=some; t=trace; mt=minute trace. [3] See Table
4 for explanation.

groups (TEGO or TRIGO) no crystalline material was
detected. On the basis of these results TETA was chosen as
the template for further experiments. Several variables in
the molar composition were studied except for the NaCl
concentration. Aiello et al. (17) have shown that
crystallization of Nu-10 is favoured by salt addition.

– synthesis time

   The synthesis time was varied in order to study the
crystallization behaviour of Nu-10 and to check the
stability of the formed product in the reaction mixture.
Batches were made with three molar compositions:

   I. 1.11 Al_2O_3; 100 SiO_2; 2.47 Na_2O; 28.64 TETA; 4206 H_2O;
      59.90 NaCl

  II. 0.36 Fe_2O_3; 1.11 Al_2O_3; 100 SiO_2; 2.47 Na_2O; 28.64
      TETA; 4757 H_2O; 59.90 NaCl

 III. 1.12 Al_2O_3; 100 SiO_2; 2.54 Na_2O; 33.78 EDA; 4223 H_2O;
      61.01 NaCl

   The results of a series of synthesis experiments at 180°C

are summarized in Figure 4 and Table 6. An induction period
of about 10 hours is observed while the reaction in the case
of TETA is completed after 25 hours yielding essentially
pure and stable Nu-10 containing just a trace of
α-cristobalite. However, in the presence of ethylenediamine
(EDA). α-cristobalite is found as soon as Nu-10 is present
in the reaction mixture. After 30 hours cocrystallization
of another product is observed which is rontgenisomorphous

Table 6. Synthesis of Nu-10. Effect of crystallization time
for various molar compositions at 180°C.[1,2,3]

	No.[4]	t(h)	% Nu-10	Results[5]
TETA	1.	16	20	amorphous, s Nu-10
	2.	23	98	Nu-10, t α-cristobalite
	3.	40	95	Nu-10, t α-cristobalite(>2)[4]
	4.	47	97	Nu-10, t α-cristobalite(<3)
	5.	64.25	97	Nu-10, t α-cristobalite(<3)
	6.	72	96	Nu-10, t α-cristobalite(<3)
TETA	7.	41	98	Nu-10, mt α-cristobalite
	8.	64.25	98	Nu-10, t α-cristobalite(>7)
	9.	72	99	Nu-10, t α-cristobalite(~8)
EDA	10.	1	0	amorphous
	11.	2	0	amorphous
	12.	4.25	0	amorphous
	13.	7	0	amorphous
	14.	23	45	amorphous, s Nu-10, t α-cristobalite
	15.	31.5	58	amorphous, s Nu-10, t α-cristobalite (>14), mt D
	16.	47	30	amorphous. Nu-10, s α-cristobalite, t D
	17.	71	27	α-cristobalite, Nu-10(~16),s D(>16). s amorphous
	18.	143.25	5	α-cristobalite(>17), s amorphous. s D(>17), t Nu-10(<17)

[1] 1.11 Al_2O_3; 100 SiO_2; 2.47 Na_2O; 28.64 TETA; 4206 H_2O;
59.90 NaCl. [2] 0.36 Fe_2O_3; 1.11 Al_2O_3; 100 SiO_2; 2.47 Na_2O;
28.64 TETA; 4757 H_2O; 59.90 NaCl. [3] 1.12 Al_2O_3; 100 SiO_2;
2.54 Na_2O; 33.78 EDA; 4220 H_2O; 61.01 NaCl. [4] In this table
and the following tables numbers between brackets refer to
an experiment number indicating the relative amount of a
component in a product compared to that in the experiment
no. specified. [5] s=some. t=trace. mt=minute trace.
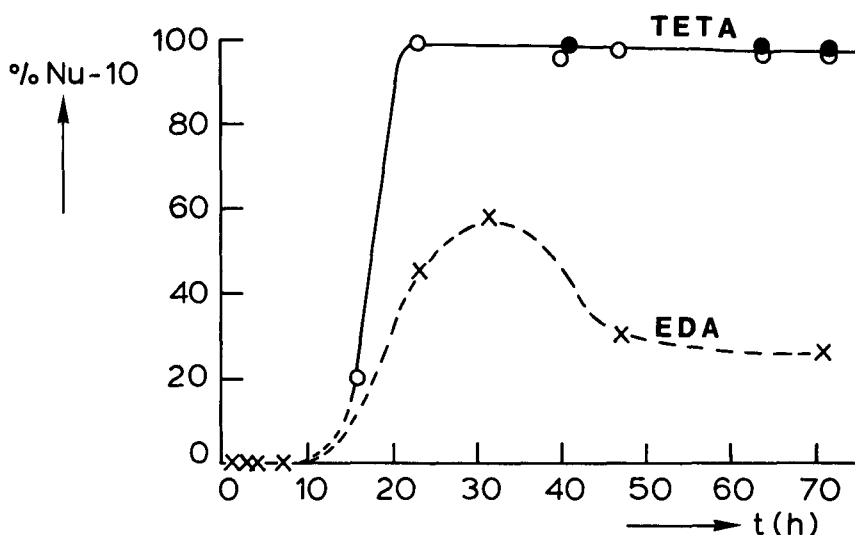
Figure 4. Synthesis of Nu-10. Crystallization curves ob-
tained at 180°C for batch compositions containing EDA (x)
and TETA (●,o). with (●) and without (o) addition of Fe_2O_3.

with SrD, a ferrierite type zeolite. This zeolitic product
will be referred to as D. These results demonstrate that the
stability of the products formed depends on the templates
used. The presence of Fe_2O_3 in the reaction mixture seems
not to influence the crystallization of Nu-10 (cf. Figure
4).

– OH^- concentration

The effect of the OH^-/SiO_2 ratio was studied using the
following crystallization formulation;

IV. 1.08 Al_2O_3; x Na_2O; 100 SiO_2; 28.69 TETA; 2097 H_2O;
     57.85 NaCl

The molar amount of Na_2O varied from 1.35 to 8.88. resulting
in a OH^-/SiO_2 ratio of 0.027 to 0.176. The results for
T=180°C and t=68 h are presented in Figure 5 and Table 7. It
is clear that relatively pure Nu-10 can be made in the
narrow range OH^-/SiO_2 = 0.04-0.08. At low OH^-/SiO_2 ratios
(<0.027) mainly ZSM-5 together with some α-cristobalite is
formed. Also, at higher OH^-/SiO_2 ratios cocrystallization

of ZSM-5 and α-cristobalite is observed which is in
agreement with the observations of Hogan et al. (6).   At a
OH^-/SiO_2 ratio of 0.178 the product is mainly α-cristobalite
(no Nu-10 detectable with XRD) together with ZSM-5.
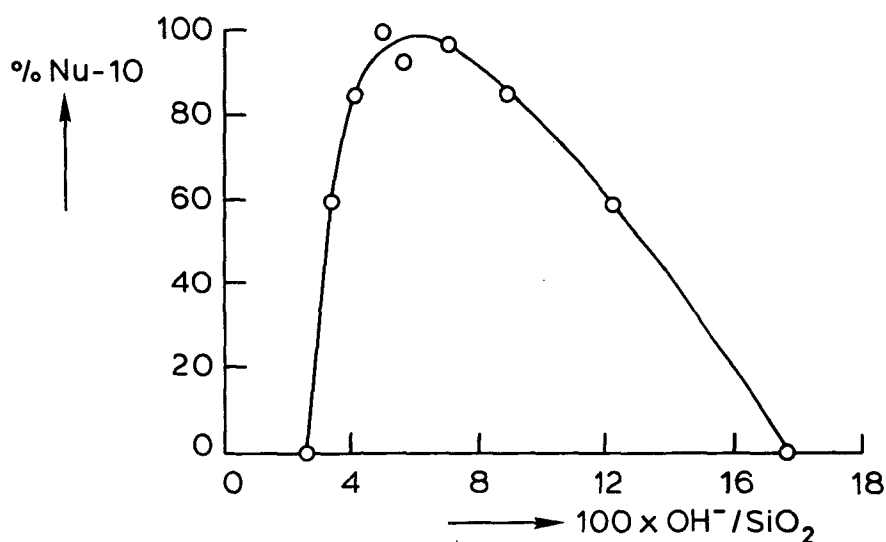
Figure 5. Synthesis of Nu-10. Effect of the OH^-/SiO_2 ratio
on the amount of Nu-10 present in the reaction products.

Table 7. Synthesis of Nu-10. Effect of OH^-/SiO_2 ratio.[1]

No.	OH-/SiO2 x100	% Nu-10	Results[2]
1.	2.67	0	ZSM-5, t α-cristobalite
2.	3.46	59	Nu-10, t α-cristobalite, mt ZSM-5
3.	4.14	84	Nu-10, t α-cristobalite, mt ZSM-5
4.	4.93	99	Nu-10, t α-cristobalite, mt ZSM-5
5.	5.60	93	Nu-10, t α-cristobalite, mt ZSM-5
6.	7.06	96	Nu-10, t α-cristobalite, mt ZSM-5
7.	8.80	85	Nu-10, s ZSM-5(>6), t α-cristobalite
8.	12.25	59	Nu-10, s ZSM-5(>7), t α-cristobalite
9.	17.73	0	s ZSM-5(~8), s α-cristobalite

[1] 1.08 Al_2O_3; 100 SiO_2; x Na_2O; 28.69 TETA; 2097 H_2O; 57.85
NaCl. [2] s=some, t=trace, mt=minute trace.

- template concentration

   The effect of the TETA-concentration in the gel was
studied using a molar composition of
    V. 1.08 Al_2O_3: 2.48 Na_2O; 100 SiO_2; y TETA; 4081 H_2O;
      57.67 NaCl
The results at T=180°C. t=67 h and varying y from 4.79 to
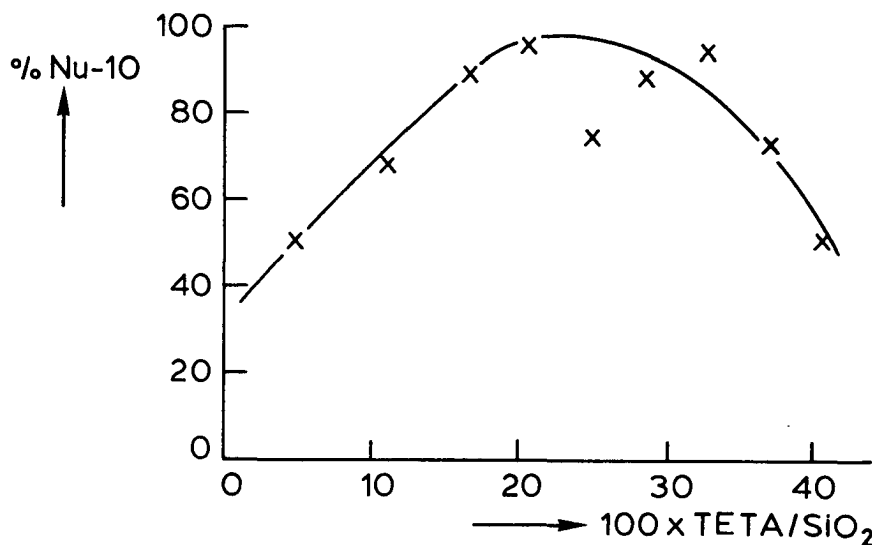
Figure 6. Synthesis of Nu-10. Effect of the $TETA/SiO_2$ ratio
on the amount of Nu-10 present in the reaction products.

Table 8. Synthesis of Nu-10. Effect of template concen-
tration.[1]

No.	y	% Nu-10	Results[2]
1.	4.79	50	Nu-10. t α-cristobalite, mt ZSM-5
2.	11.01	68	Nu-10. t α-cristobalite. mt ZSM-5
3.	16.54	89	Nu-10. t α-cristobalite, mt ZSM-5
4.	20.70	96	Nu-10. t α-cristobalite, mt ZSM-5
5.	24.83	75	Nu-10. t α-cristobalite, mt ZSM-5
6.	28.61	89	Nu-10. t α-cristobalite, mt ZSM-5
7.	32.80	95	Nu-10, t α-cristobalite. mt ZSM-5
8.	37.19	73	Nu-10, s amorphous, t α-cristobalite (<7), mt ZSM-5
9.	40.64	50	Nu-10, s amorphous. t α-cristobalite (~8), mt ZSM-5

[1] 1.08 Al_2O_3; 100 SiO_2; 2.48 Na_2O; y TETA; 4081 H_2O; 57.67
NaCl. [2] s=some, t=trace, mt=minute trace.

40.64 are shown in Figure 6 and Table 8. The optimum
TETA/SiO$_2$ ratio seems to range from 0.15-0.33. The amount of
α-cristobalite increases when the amount of amorphous
material decreases (TETA/SiO$_2$<0.18) and when the amount of
TETA increases (TETA/SiO$_2$>0.32). A small trace of ZSM-5 is
noticeable but no relation was found with the amount of
TETA.

– Al$_2$O$_3$-concentration and cation variation

   In order to study the effect of the SiO$_2$/Al$_2$O$_3$ ratio on
Nu-10 crystallization the following starting compositions,
involving three different cations, were chosen:
   VI. a Al$_2$O$_3$; 2.45 Na$_2$O; 100 SiO$_2$; 28.75 TETA; 4084 H$_2$O;
       57.79 NaCl
   VII. b Al$_2$O$_3$; 1.61 K$_2$O; 100 SiO$_2$; 29.03 TETA; 4092 H$_2$O;
       57.50 KCl
   VIII. c Al$_2$O$_3$; 4.25 (NH$_4$)$_2$O; 100 SiO$_2$; 29.02 TETA; 4097
       H$_2$O; 57.54 NH$_4$Cl
a varied from 0 to 3.30, b and c from 0 to 11.7, T=180°C,
t=67 h. For formulations VI and VII the results are given
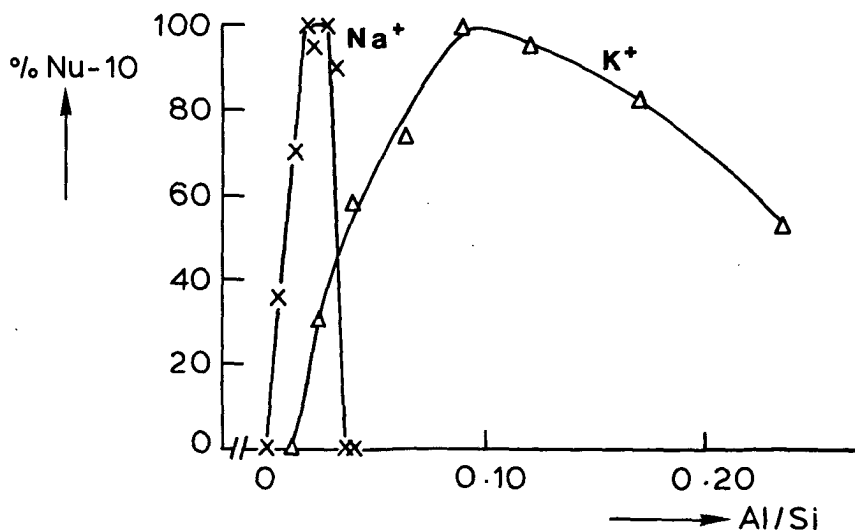
Figure 7. Synthesis of Nu-10. Effect of the Si/Al ratio
using Na$^+$ (×) as cation and K$^+$ (Δ) as cation.

Table 9. Synthesis of Nu-10 in a Na^+ system. Effect of Si/Al ratio.[1]

No.	a	% Nu-10	Results[2]
1.	1.96	0	ZSM-5
2.	1.87	0	ZSM-5
3.	1.55	90	Nu-10, t ZSM-5, mt α-cristobalite
4.	1.40	98	Nu-10, t ZSM-5, mt α-cristobalite(>3)
5.	1.08	95	Nu-10, t α-cristobalite(>4)
6.	0.93	98	Nu-10, t ZSM-5, t α-cristobalite(>5)
7.	0.70	70	Nu-10, t α-cristobalite(>6), mt ZSM-5
8.	0.32	36	Nu-10, t α-cristobalite(>6), mt ZSM-5
9.	0	0	α-quartz, mt Nu-10

[1] a Al_2O_3; 100 SiO_2; 2.45 Na_2O; 28.75 TETA; 4084 H_2O; 57.79 NaCl. [2] s=some, t=trace, mt=minute trace.

Table 10. Synthesis of Nu-10 in a K^+ system. Effect of Si/Al ratio.[1]

No.	b	% Nu-10	Results[2]
1.	11.78	53	Nu-10, s amorphous
2.	8.62	82	Nu-10, s amorphous, t D
3.	6.02	95	Nu-10
4.	4.44	99	Nu-10
5.	3.16	74	Nu-10, t α-cristobalite, t ZSM-48
6.	2.02	58	Nu-10, t α-cristobalite, t ZSM-48(>5)
7.	1.14	30	Nu-10, s ZSM-48(>6), t α-cristobalite
8.	0.58	0	α-cristobalite
9.	0	0	α-quartz

[1] b Al_2O_3; 100 SiO_2; 1.61 K_2O; 29.03 TETA; 4092 H_2O; 57.50 KCl. [2] s=some, t=trace, mt=minute trace.

in Figure 7 and Tables 9 and 10. The formulations with NH_4^+ as a cation invariably yielded amorphous products (only without Al_2O_3 (c=0) a trace of α-cristobalite was found). Sodium and potassium cations show some remarkable differences in Nu-10 crystallization. With both cations, highly crystalline Nu-10 materials can be obtained. For Na^+, a maximum is found for Si/Al=34-52. With K^+, pure Nu-10 can be synthesized with Si/Al=8-11.5, which can be compared with the values 28-85 (Na^+) and 12.5-250 (K^+, Cs^+, Rb^+) reported by Hogan et al. (6). This difference in maxima is not OH^-/SiO_2 dependent as will be shown later. Sodium and

potassium show the tendency to yield α-cristobalite as a
sideproduct at increasing Si/Al ratio (a<0.70, b<2.92).
With K^+ also the formation of ZSM-48 (1.11<b<3.16) was
observed. Decreasing the Si/Al ratio shows different
tendencies for both cations. For Na^+, the ZSM-5 content is
rapidly increasing when Si/Al<35 and pure ZSM-5 is obtained
at Si/Al<26.8. With K^+ as cation cocrystallization of D
occurs when Si/Al=~5.8. Below Si/Al=6.5 Nu-10 is still
present but the amount of amorphous material increases.

   The present experiments show that the crystallization of
pure Nu-10, with Na^+ as cation and TETA as template, is
possible over a narrow range in the molar composition of the
synthesis mixture. When K^+ is used Nu-10 can be synthesized
over a wider Al-concentration range. The conditions for
Nu-10 synthesis, using K^+ as the cation, have not been
described in literature. Accordingly we have investigated
this type of formulation in more detail. The Si/Al ratio
and the OH^-/SiO_2 ratio, having the largest effect upon the
synthesis results, were varied. The following molar
composition was used:
   IX. x Al_2O_3; y K_2O; 100 SiO_2; 29.04 TETA: 4094 H_2O;
       57.31 KCl
T=180°C and t=67 h; x=0-12 and y=-1.11-3.51. To obtain a
negative value of y 37% HCl was used instead of KOH. The
results are presented in Figures 8 and 9. Both Figures show
clearly that pure materials according to IR and XRD can be
obtained when the Si/Al ratio is between 8.6 and 17.1 and
the OH^-/SiO_2 ratio is between 0.03 and 0.06 (24). At higher
Si/Al values cocrystallization of ZSM-48 occurs, with the
purity of the latter increasing with decreasing OH^-/SiO_2
ratio. This is in agreement with the results of Araya and
Lowe (25) who state that ZSM-48 can be prepared at high
Si/Al ratios and low OH^- concentrations. At high OH^-/SiO_2
ratios ZSM-5 cocrystallizes as expected from the previous
results. It is also clear that, under these conditions, it
is not possible to prepare an aluminum-free zeolite. As
soon as Al_2O_3 was absent in the synthesis mixture
α-cristobalite or α-quartz was formed.
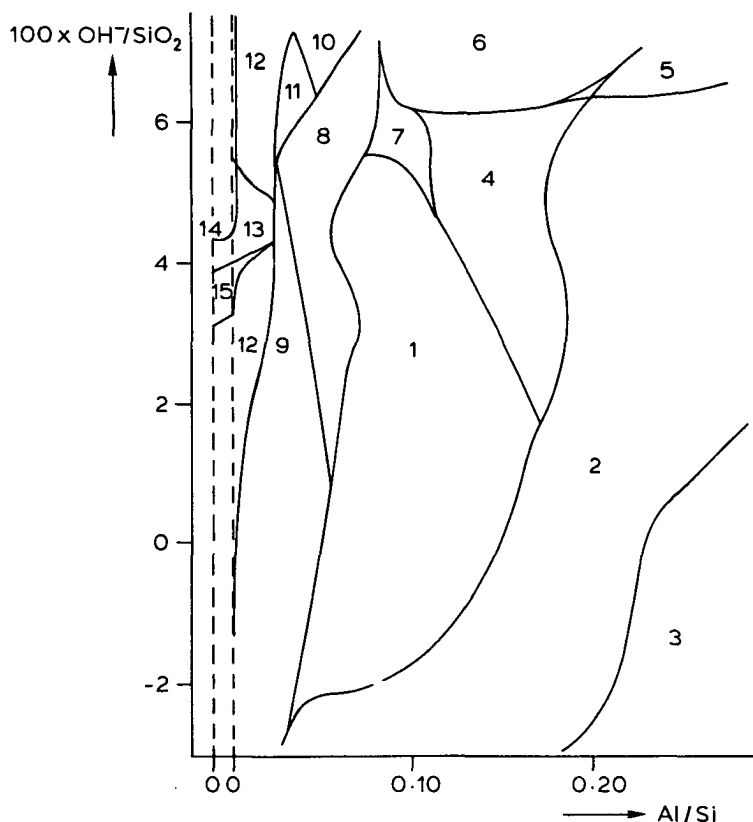
Figure 8. Synthesis of Nu–10 in a system containing K^+ as a cation. The effect of the OH^-/SiO_2 ratio and the Si/Al ratio on the product distribution. (1) Nu–10; (2) Nu–10 + amorphous; (3) amorphous; (4) Nu–10 + trace D; (5) Nu–10 + amorphous + trace ZSM–5; (6) Nu–10 + trace D + trace ZSM–5; (7) Nu–10 + trace α–cristobalite; (8) Nu–10 + trace α–cristobalite + trace ZSM–5; (9) ZSM=48 + trace Nu–10 + trace α–cristobalite; (10) α–cristobalite + trace Nu–10; (11) α–cristobalite + trace ZSM–5; (12) α–cristobalite; (13) α–cristobalite + trace α–quartz; (14) α–quartz + trace α–cristobalite; (15) α–quartz.
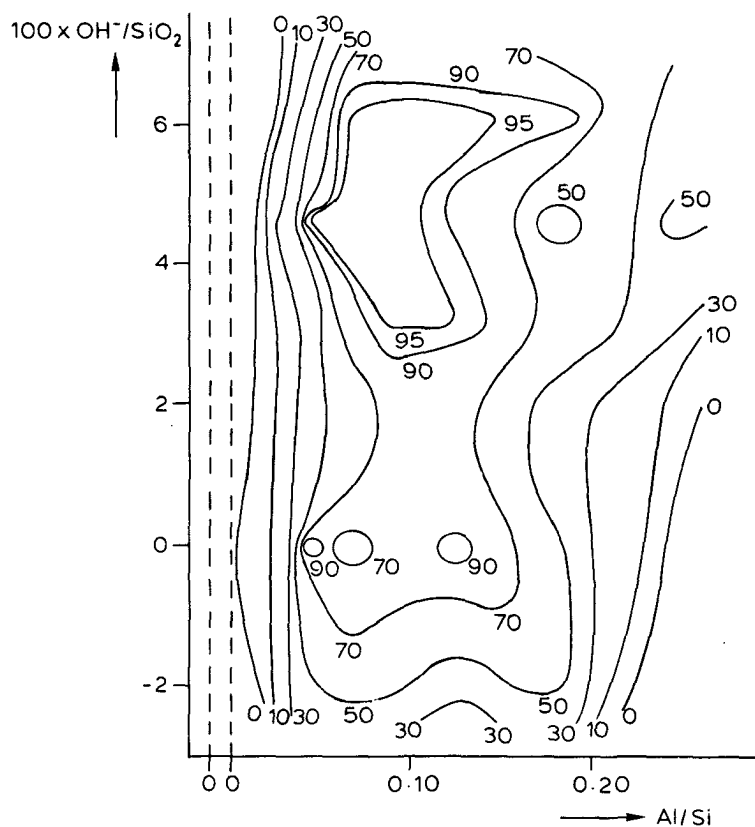
Figure 9. Synthesis of Nu-10 in a system containing K^+ as a cation.   The contour lines give the % Nu-10.

CONCLUSIONS

   Crystallization of zeolites with the Nu-10/Theta-1/ZSM-22 framework asks for carefully chosen synthesis formulations. The cation has a pronounced effect on both the Si/Al ratio, at which crystallization occurs and on the nature of the byproducts formed.

ACKNOWLEDGEMENT

   The author would like to thank Mr. J.F. van Lent (Laboratory of Metallurgy) for the XRD analyses.

REFERENCES

1. Barri. S.A.I.. Howard. P. and Telford. C.D. EP 0,057,049.
2. Hogan, P.J., Stewart. A. and Whittam. T.V. EP 0,065,400.
3. US Patent Appl. 4,556,477.
4. Parker, L.M. and Bibby, D.M. Zeolites 1983, 3, 8.
5. Takatsu, K. and Kaweta, N. EP 0,087,017; JP 16395/82.
6. Hogan, P.J., Whittam, T.V., Birtill, J.J. and Stewart, A. Zeolites 1984, 4, 275.
7. Harrison. I.D., Leach. H.F. and Whan. D.A. Zeolites 1987, 7, 28.
8. Barri, S.A.I.. Smith, G.W.. White. D. and Young, D. Nature 1984, 312, 533.
9. Ashton, A.G., Barri. S.A.I. and Dwyer, J. a) Acta Phys. Chem. 1985, 31, 25. b) 'Proc. Int. Symp. Zeolite Catal.' Siofok (Hungary), May 13-16, 1985, p. 25.
10. Highcock. R.M., Smith, G.W. and Wood. D. Acta Cryst. 1985, C41, 1391.
11. Kokotailo, G.T., Schlenker, J.L., Dwyer, F.G. and Valyocsik, E.W. Zeolites 1985, 5, 349.
12. Conventional X-ray structural methods are not appropriate because no large single crystals have been synthesized. Crystals mentioned in literature were varying in length from 100 to 2000 nm. However, prior to the publication of this Chapter a single crystal structure refinement of silica-ZSM-22 was described: Marler, B. Zeolites 1987, 7, 393. Crystal data; orthorhombic, $Cmc2_1$, a=1.3836(3), b=1.7415(4), c=0.5042(1) nm.
13. Schlenker, J.L., Rohrbauch. W.J., Chu. P., Valyocsik, E.W. and Kokotailo, G.T. Zeolites 1985, 5, 355.
14. Rohrman Jr., A.C., LaPierre, R.B., Schlenker, J.L., Wood, J.D., Valyocsik, E.W., Rubin, M.K., Higgins, J.B. and Rohrbauch, W.J. Zeolites 1985, 5, 352.
15. Wright, P.A., Thomas, J.M., Millward, G.R., Ramdas, S. and Barri, S.A.I. J. Chem. Soc. Chem. Commun. 1985. 1117.
16. Araya, A. and Lowe, B.M. Zeolites 1984. 4, 280; EP 0,077,624.
17. Aiello, R., Nastro, A. and Pellegrino, C. 'Proc. 7th Int. Zeolite Conf.' (Ed. Murakami, Y., Iijima, A. and Ward, J.W.). Japan, 1986, 255.
18. Dewing, J., Spencer. M.S. and Whittam, T.V. Catal. Rev. Sci. Eng. 1985. 27(3). 461.
19. Olson, D.H., Calvert. R.B. and Valyocsik. E.W. EP 0,102,716.
20. Valyocsik. E.W. CA 1.202.941.
21. Valyocsik. E.W. EP 0,178,846.
22. Gaag, F.J. van der, Jansen, J.C. and Bekkum, H. van. Appl. Catal. 1985, 17, 261.
23. Iler. R.M. 'The Chemistry of Silica'. John Wiley and Sons, New York 1979, p. 384.
24. The Nu-10 samples described in this Chapter show the existence of differences between NaNu-10 and KNu-10

with respect to morphology and surface area and
therefore in catalytic behaviour. In Chapter V a more
detailed description is presented. A possible cause
for this difference might be the Al—source used,
although the presence of the cation can not be
underestimated. Thus, results obtained for potassium
(with AeroAl as aluminum source, Figure 7,
experimental Al/Si=0.09) can not be duplicated with
sodium as cation. By contrast, Hogan et al. (6)
report just small differences between Na and K by
using an aluminate as Al—source.
Additional experiments with $AlCl_3$ as the Al—source
show that a maximum Nu—10 purity of 63% can be
obtained at Al/Si=0.033 using potassium as the
cation. When sodium is used as the cation no Nu—10 is
observed.
25. Araya, A. and Lowe, B.M. J. Catal. 1984. <u>85</u>, 135.

This Chapter has been published:

Febre, R.A. le, Kouwenhoven, H.W. and Bekkum, H. van.
Zeolites 1988, <u>8</u>, 60.

CHAPTER V

THE REACTION OF AMMONIA AND ETHANOL OR RELATED COMPOUNDS

TOWARDS PYRIDINES OVER ZEOLITE Nu-10

ABSTRACT

Pyridine bases are formed by the reaction of ethanol and
ammonia over zeolite Nu-10 in the presence of oxygen, which
is shown to play an essential role. Different
proton-introduction procedures of the catalyst result in
different catalytic activities and selectivities. Several
other small amines and oxygenates are tested in the
presence/absence of oxygen with respect to their selectivity
towards pyridines. A combination of ethanol, methylamine
and air and Nu-10 or ZSM-5 as the catalyst gives high
selectivities towards pyridine and 4-methyl-pyridine. A high
selectivity towards acetonitrile is found for Nu-10
catalysts containing iron besides aluminum.

INTRODUCTION

   Compared to other heterocyclic systems, pyridine is
relatively important for the chemical industry. This is
reflected amongst others in the number of references and
patents devoted to it. The chemical properties of the
pyridine system can be divided into three categories (1): i.
properties roughly parallel to those of the benzene system,
modified in some degree by the presence of the ring
nitrogen; ii. properties unusual for the benzene system;
iii. properties associated with the unshared electron pair
on the ring nitrogen.
Nowadays a demand is present for pyridines as intermediates
in the synthesis of medicines, dietary supplements,

herbicides and other pesticides and desinfectants.

Two commercially important sources for pyridine bases are coal carbonisation by-products and synthetic cyclization reactions. Pyridine bases obtained from either of the two sources have their own fields of application. For instance, pharmaceutical industries need pyridine and methylpyridines (picolines) of a purity which can not be achieved by coal carbonisation.

The present large demand for pyridine bases has resulted in an appreciable increase in the world-production of synthetic pyridines from ca. 36000 tonnes for 1972 to 50000 tonnes in 1978 (2). At present, the total capacity for pyridines is estimated at 60000 tonnes per year (3).

Several synthetic routes towards pyridines have been described in literature (1-5) including aliphatic carbonyl compounds, pyrans and carbohydrates together with ammonia as starting compounds. Reactions of ketones and/or aldehydes with ammonia using metal-oxides such as silica-alumina as catalyst at temperatures between 300 and 500°C are usually applied commercially. The high costs of several aldehydes and their reactivity (instability) towards not-wanted byproducts induces several industries to investigate new reaction pathways. For example; alkenes, as aldehyde precursor, have been studied by Halasz et al. (6) as feedstock for the formation of pyridines. As early as the 1930's methods were described to obtain pyridine bases by reacting alcohols (except methanol) with ammonia over mixed metal-oxide catalysts (i.e. Zn:Al:Si or Cd:Al:Si) (7). Chang and Lang (8) were the first investigators to describe a successful application of zeolite ZSM-5 as a catalyst for the manufacture of pyridine bases out of aldehydes and ammonia. They claim a commercially attractive system showing almost no catalyst deactivation during operation. By combining the dehydrogenation, oligomerization and aromatization properties of the zeolite van der Gaag et al. (9,10,11) found that ethanol and ammonia, in the presence of oxygen, react towards pyridines when using the zeolite HZSM-5 as a catalyst. An optimal selectivity to pyridine

was obtained by using a HZSM-5 catalyst with Si/Al around 55
at temperatures between 325 and 375°C. Similarly the
formation of 2,6-lutidine from acetone, methanol and ammonia
over HZSM-5 was observed (12).

Recently in this laboratory the synthesis of the zeolite
Nu-10/Theta-1/ZSM-22 was studied (13). This zeolite is a
one-dimensional system with channels running parallel to the
c-axis. The channels are formed by elliptical 10-T-ring
systems (diameter 0.47x0.55 nm (14)) giving it a medium pore
size. Like ZSM-5 (diameter 0.53x0.55 and 0.54x0.56 nm), the
zeolite is placed in the pentasil group of zeolite
structures because its framework can be constructed from 5-1
secondary building units. Essentially pure NaNu-10 was
obtained at Si/Al ratios between 34 and 52 which is close to
the optimal Si/Al ratio of HZSM-5 for the conversion of
ethanol and ammonia towards pyridines. Zeolite HNu-10 is
known to exhibit a relatively high selectivity towards
p-xylene in the disproportion of toluene and a predominant
formation of olefins in MeOH conversion similar to ZSM-5
(15,16). A major difference between p-xylene in ZSM-5 and
Nu-10 is that in the former zeolite intersections are
present which allow substantially larger reaction transition
states than in Nu-10. On these grounds we decided to
investigate the reaction of ethanol and ammonia over Nu-10
as the catalyst to compare its catalytic properties to those
of ZSM-5.

Besides Nu-10 and ZSM-5 the present study includes
mordenite as well for comparison. Mordenite was chosen
because it belongs to the ferrierite type of materials to
which Nu-10 is closely related.

Besides ethanol and ammonia as reactants several other
oxygenates and small amines were tested for their
pyridines-forming ability over zeolite Nu-10 and ZSM-5 at
several reaction temperatures.

EXPERIMENTAL

Materials

The Nu-10 zeolites used in this article were prepared as
described earlier (13). The NH_4-ZSM-5 zeolite used was
prepared according to Ghanami and Sand (17). The zeolite
NH_4-Mordenite was supplied by Union Carbide.

The activation of the zeolite samples used in this study
is described in Table 1. As an example the activation
treatment of sample D is given here: A 1M HNO_3 solution. 15
ml/g, was added to sample C. The suspension obtained was
stirred for 3 hours, using a teflon coated magnetic stirrer.
under reflux conditions. Thereafter the zeolite was
filtered off over a Buchner filter and washed several times
with water of 60°C. The zeolite was then dried at 100°C for
one hour and subsequently calcined at 550°C during 16 hours.
yielding sample D.

The zeolites were characterized using IR. XRD. AAS and
TPD. BET surface areas were obtained using a single point
method. Some Nu-10 samples underwent additional SEM and TEM
characterizations.

All catalytsts were dry pressed, crushed and sieved to
obtain particles of 1.4-2.0 mm.

Procedure

The apparatus used in the catalytic experiments is
essentially the same as described by Oudejans (18).

The catalyst (1 g) was placed in a fixed-bed continuous
flow glass reactor of 8 mm internal diameter. The reactor
was placed in an electronically controlled fluid bed oven.
The carrier gas. either air or nitrogen, was passed through
two thermostatted saturators containing the organic
oxygen-reactant (OR) and a 0.5M aqueous solution of the
N-reactant (NR). respectively. The desired flows of the
reactants were obtained by adjusting and controlling the
temperature of the saturators and the flow of carrier gas
through the saturators.

The saturated gas streams were mixed and fed to the reactor at WHSV (OR) = $0.5/X$ h^{-1} (X=number of C-atoms in OR). The molar composition $NR:OR:H_2O:N_2:O_2$ of the reaction mixture was 1:3:6:73:17 and 1:3:6:90:0 for air or nitrogen as the carrier gas, respectively.

The reaction was carried out at a reaction temperature of 350°C and monitored every hour over a period of 18 hours by automatic sampling. The samples were analyzed on a Hewlett Packard 429 gas chromatograph equipped with a 3m 10% PEG on Chromosorb with FID for organic components and on a Perkin Elmer gas chromatograph equipped with a 1m PORAPAK Q column with TCD for inorganic components (i.e. CO and CO_2) respectively. Peak integration was performed on a SpectraPhysics SP4270 integrator which was connected to the gas chromatographs.

After 18 hours the reactor temperature was raised to 450°C in steps of 25°C. After each temperature increase the catalyst remained on that temperature for 55 minutes to reach a steady state before analysis was performed.

RESULTS AND DISCUSSION

Materials

The zeolite Nu-10 samples were found to have two different morphologies as shown in Figure 1. The samples B, C and D (see Table 1) consist of small needles, length ~1 μm whereas the samples F, G and H are needles of ~20 μm in length.

The treatment of H-Mordenite with HNO_3 (sample M) leads to partial dealumination of the zeolite (cf. Table 1). XRD and IR show no structural damage. The occurence of extra hydroxyl nests, as indicated by the absorption at 940 cm^{-1} (19) in the IR spectrum of sample M shows that recrystallisation just partly occurs during calcination.

The low value of S of sample J (Table 1) compared to samples B, C and D might be caused by small deposits of Fe_2O_3 present in the zeolite channels. Because of its

a	b
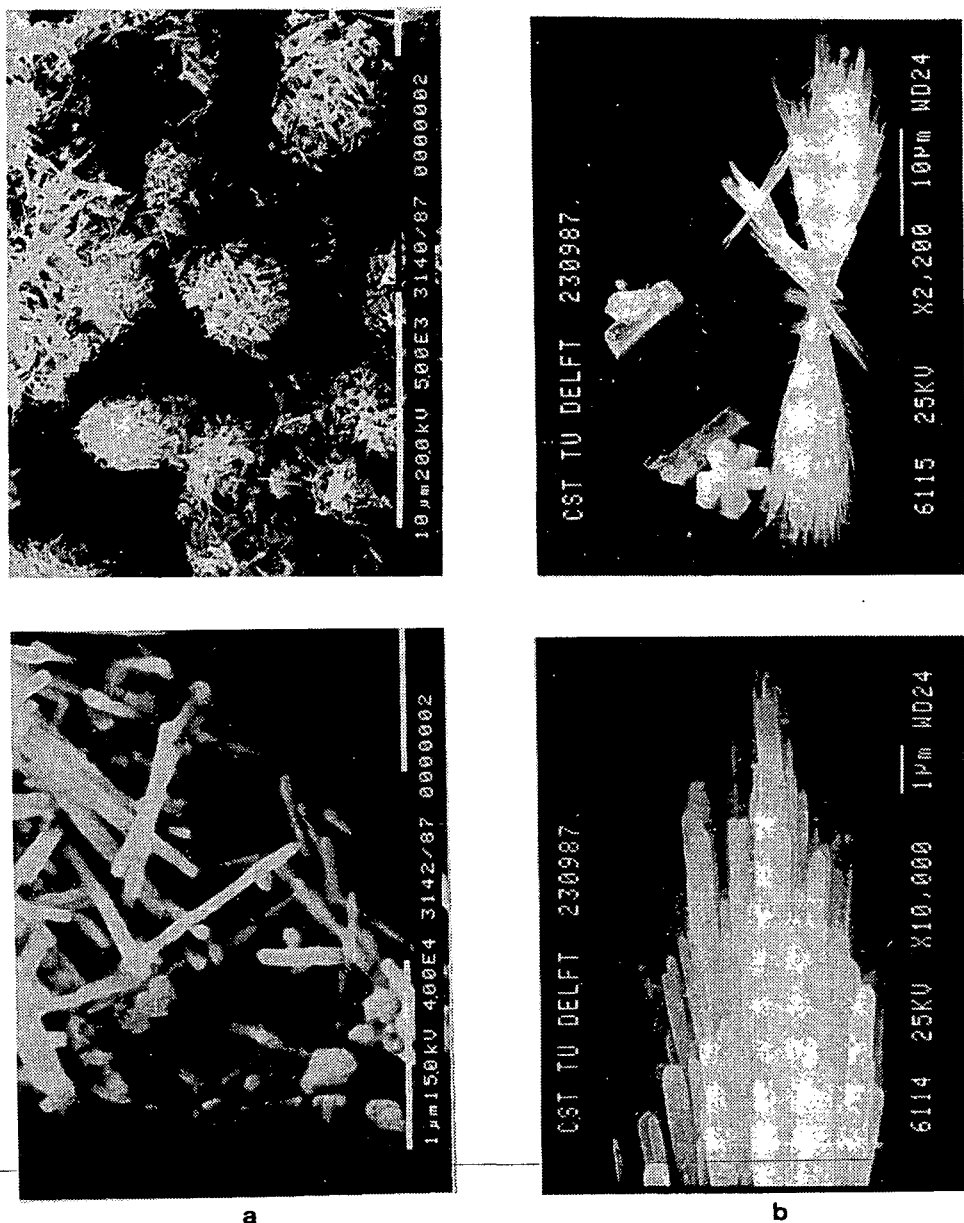
Figure 1. SEM-photographs of a) NaNu-10 and b) KNu-10 samples. The presence of a small amount of ZSM-5 in the KNu-10 sample (indicated by XRD) is supported by SEM.

one-dimensional structure the sorption capacities of Nu-10 can be strongly influenced by small deposits of materials leading to differences in rate and capacity of adsorption (20).

Table 1. Preparation of the samples plus some characteristics.

Sample	Zeolite	Preparation[1]	Si/Al	S(m²/g)
A	NaNu-10	according to reference 13, calc. 550°C, 72h	44.9	107
B	HNu-10	sample A exchanged with 0.3M NH₄Cl, 33 ml/g, T=RT, t=24h, calc. 550°C, 16h	44.5	127
C	HNu-10	sample A exchanged with 0.3M HCl, 33 ml/g, T=RT, t=24h, calc. 550°C, 16h	46.5	149
D	HNu-10	sample C treated with 1M HNO₃, 15 ml/g, T=reflux, t=3h, calc. 550°C, 16h	45.6	190
E	KNu-10	according to reference 13, calc. 650°C, 72h	10.1[2]	38
F	HNu-10	sample E exchanged with 0.3M NH₄Cl, 33 ml/g, T=RT, t=24h, calc. 550°C, 16h	11.7[2]	49
G	HNu-10	sample F treated with 1M HNO₃, 15 ml/g, T=reflux, t=3h, calc. 550°C, 16h	13.0[2]	95
H	HNu-10	sample G treated with 2M HCl, 47 ml/g, T=reflux, t=3h, calc. 550°C, 72h	14.3[2]	109
I	NaNu-10(Fe)	according to reference 13, Fe added to synthesis gel. calc. 550°C, 72h	–	–
J	HNu-10(Fe)	sample I exchanged with 0.3M NH₄Cl, 33 ml/g, T=reflux, t=3h, calc. 550°C, 72h	41.1 100.5[3]	102
K	HZSM-5	according to reference 17, calc. 550°C, 16h	35.8	276
L	HMordenite	NH₄-Mordenite, calc. 550°C, 3h	8.8	296
M	HMordenite	sample L treated with 1M HNO₃, 10 ml/g, T=reflux, t=3h, calc. 550°C, 16h	36.6	324

[1] See text. RT = Room Temperature, calc = calcination temperature.
[2] Despite the low bulk Si/Al ratio, TEM measurements show that the needles (see Figure 1b) are pure Nu-10 with a Si/Al ratio between 40 and 50. Apart from this amorphous Al-rich material (neither XRD nor IR-detectable and not visible in Figure 1b) is present. [3] Si/Fe ratio.

Reactions

   The results of reactions of ethanol and ammonia over several Nu-10 catalysts (samples B-J) at 350°C are presented in Table 2. All NaNu-10 derived HNu-10 samples turned out to be active catalysts for the formation of pyridine. The data for samples B, C and D show that different ion exchange procedures can lead to different results. Sample C differs from samples B and D in giving a lower conversion and pyridine selectivity. Probably treatment with HCl at room temperature (sample C) gives some aluminum extraction from the T-sites in the zeolite. Because of the low ion exchange

Table 2. Results of the reaction of ethanol and ammonia over several Nu-10 catalysts at 350°C; $WHSV_{EtOH}=0.25\ h^{-1}$. Time on stream is averaged between 5 and 18 hours.

Sample[1)	B	C	D	F	G
Carrier gas	Air	Air	Air	Air	Air
Conv. EtOH (%)	7.9	4.9	9.1	2.5	2.8
Select. (mol%)					
Ethene	9.3	6.6	15.5	19.4	22.2
Diethyl ether	12.5	8.7	16.5	30.9	39.4
Ethanal	13.4	16.0	7.9	10.6	7.5
Ethylamine	–	26.3	–	13.6	8.2
Ethyl acetate	1.8	1.5	2.2	–	–
Acetonitrile	2.7	<1.2	<2.1	–	–
Pyridine	11.7	5.8	15.2	–	–
2-Picoline	1.5	<1.0	<0.5	–	–
CO_2	47.1	32.8	42.4	25.4	22.7
Sample[1)	H	J	B	F	J
Carrier gas	Air	Air	N2	N2	N2
Conv. EtOH (%)	2.5	10.9	7.4	2.7	9.6
Select. (mol%)					
Ethene	22.8	4.3	22.5	9.5	15.7
Diethyl ether	37.2	7.3	71.0	83.5	82.9
Ethanal	9.2	25.9	3.3	0.3	–
Ethylamine	0.4	12.7	3.2	6.2	3.3
Ethyl acetate	1.9	1.7	–	0.4	–
Acetonitrile	–	10.9	–	–	–
Pyridine	7.1	<1.4	–	–	–
2-Picoline	3.7	–	–	–	–
CO_2	14.8	35.8	–	–	–

[1) See Table 1.

temperature almost no Al is extracted from the pore system, leaving some alumina type species in the channels. A difference in catalytic sites (γ-peak) is also shown in the TPD spectra of samples B and C (Figure 2). Acidic exchange under reflux conditions (preparation sample D) removes eventually formed dealumination products from the zeolite, leaving the channels open, resulting in a catalytic activity slightly exceeding that of sample B, and a TPD spectrum similar to sample B.
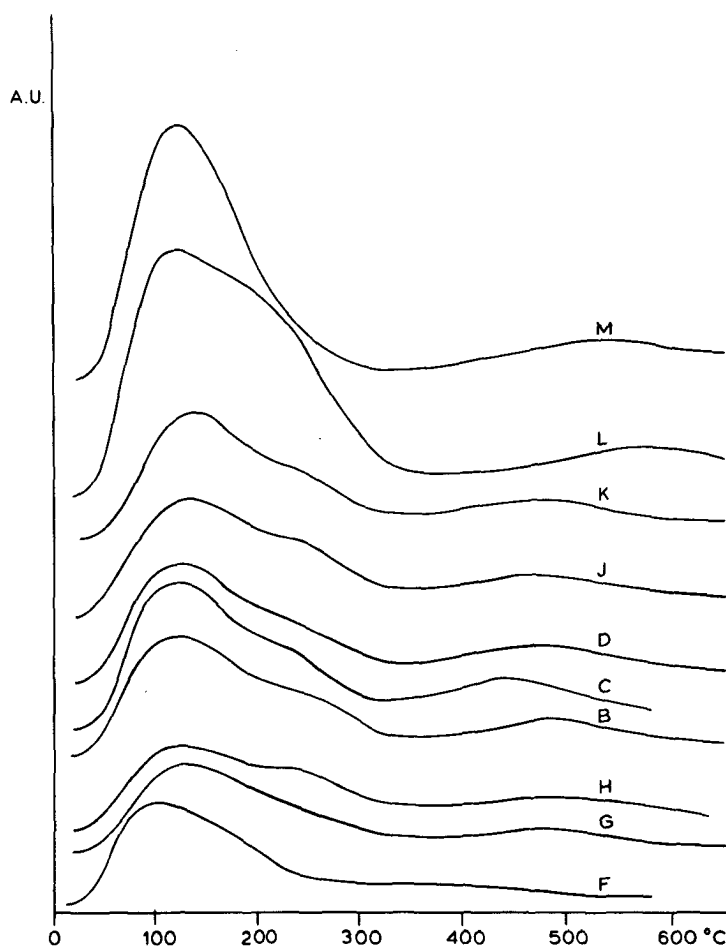
Figure 2. TPD spectra of the samples B, C, D, F, G, H, J, K, L and M.

The product mixture obtained with sample J (lower pyridin. higher ethanal selectivity) is comparable with sample C. Again small particles (Fe_2O_3) present in the channels might prevent pyridine-formation. The relatively high selectivity to acetonitrile might be due to the oxidative properties of iron oxide.

Oxygen plays an important role in the formation of ethanal, ethylamine, acetonitrile and pyridine as can be seen from the experiments with nitrogen as a carrier gas (on

samples B, F and J). Although no appreciable changes in
conversion were found, a large change in selectivity is
observed. Mainly diethyl ether and ethene are formed.

In all the KNu-10 derived HNu-10 samples (F-H) quite a low
pyridine-forming ability was found in the reactions
studied. Although not as good as samples B and D, just
sample H is capable of making pyridines. A major difference
between the samples F,G and H is the low value of S (Table
1) for samples F and G compared to sample H. Stirring during
the ion-exchange procedures results in some cracking of the
original needles (sample E, Figure 1b) giving an improvement
in channel-accessibility. A comparison of samples F, G and
H indicates that aromatic nitrogen-containing compounds are
formed intrazeolitic while species as ethene, diethyl ether
and ethylamine might be formed on the outer surface of the
catalyst.

Table 3. The reaction of ethanol and ammonia, using air as
carrier gas, over the zeolites ZSM-5 (sample K) and morde-
nite (samples L and M) at 350°C: $WHSV_{EtOH} = 0.25 \ h^{-1}$. Time
on stream is averaged between 5 and 18 hours.

Sample[1]	L	M	K
Conv. EtOH (%)	20.6	14.5	9.2
Select. (mol%)			
Ethene	64.6	73.2	10.9
??-1[2]	—	—	0.3
Diethyl ether	1.8	3.4	10.2
Ethanal	5.0	2.0	3.7
Ethylamine	4.5	2.0	1.7
Ethyl acetate	0.3	0.3	1.1
Acetonitrile	1.2	6.4	4.0
Pyridine	0.9	0.8	18.6
2-Picoline	0.1	—	4.8
CO_2	21.6	12.0	44.7

[1] See Table 1. [2] ??-1 = not-identified compound.

The results of the reaction of ethanol + ammonia over some other zeolites are presented in Table 3. Zeolite HZSM-5 (sample K) shows a higher conversion towards pyridines than HNu-10 (Table 2. sample B). This because of its 2-dimensional framework resulting in a much lower "outer surface/inner pores" ratio.

Mordenite (samples L and M) not only shows a very low pyridine selectivity, but dealumination also shows almost no effect on catalytic activity. Because its Bronsted acid sites are somewhat stronger than those of HZSM-5 and HNu-10 (see Figure 1) the reaction is directed more towards the dehydration of ethanol. Despite the increase in S (table 1) combined with the almost identical catalytic behavior of the samples L and M. we must conclude that the NH_4-mordenite used. contains intrazeolitic aluminumoxide deposits which have probably no catalytic activity.

Some other oxygen compounds. i.e. diethyl ether and some other amines as methylamine and ethylamine were tested over HNu-10 in an effort to increase conversion and selectivities towards pyridine and to contribute to the understanding of the pyridine-formation reactions. The results of these experiments are given in Table 4.

A mixture of tetrahydrofuran (THF) and NH_3 does not produce any pyridines. It is known in literature (1) however that THF can react with hydrogen cyanide in the vapor phase to produce pyridine. though good yields are not reported. Another possibility is the formation of pyrrole out of THF and NH_3 (3). However Table 4 shows that with THF as reactant much deep oxidation products together with heavy aromatic compounds are found. caused by cracking -. oxidation - and isomerization reactions in the zeolite.

Diethyl ether (EtOEt) shows a very reactive behaviour when fed together with NH_3 over Nu-10 in the presence of oxygen. Noticable is the selectivity towards 4-piccline. During the first hours on stream a good selectivity towards pyridines is found which rapidly decreases. probably caused by coke

Table 4. Testing of several organic compounds on their sele
$WHSV_{OR}$ = 0.5/X h^{-1} (See text). Time on stream is averaged b

Sample[1]	B	B[4]	B[4]	B	B[4]
Carrier gas	Air	Air	Air	N_2	Air
OR[2]	THF	EtOEt	EtOAc	EtOAc	EtOEt
NR[2]	NH_3	NH_3	NH_3	NH_3	$MeNH_2$
Conv. on OR(%)	14.1	73/76	38/31	40.3	79/77
Select. mol%					
Ethene	3.2	4.1	4.3/5.4	4.7	1.3/2.3
??-1[3]	1.7	–	–	–	–
Diethyl ether	–	–	16/4.5	1.0	–
Ethanal	1.7	3.5/6.8	0.6/0.9	0.1	–[5]
Ethylamine	1.6	–	–	–	–
??-2[3]	8.5	–	–	–	1.4
Ethyl acetate	–	15/8.3	–	–	16/30
Ethanol	2.4	–	58/66	76.8	–
Acetonitrile	1.2	0.7/0.4	12.6	17.4	0.2
Tolu/p–Xylene	–	–	–	–	0.3/1.0
Pyridine	–	11/2.5	1.9	–	8.3/0.9
2–Picoline	–	–	–	–	1.1/0.4
2,6–Lutidine	–	–	–·	–	–
4–Picoline	–	1.4/0.1	–	–	1.5/0.2
M.E.P[6]	–	–	–	–	–
C_{10}/C_{11} arom.	17.1	–	–	–	–
CO_2	63.7	65/68	7.6/8.2	–	69/62

[1] See Table 1. [2] OR = O–containing reactant: NR = N–contain
reaction was not stable after 5 hours on stream. The '/' re
[5] Measurements influenced by $MeNH_2$. Products probably prese
possible. [6] 2–methyl–5–ethyl pyridine.

formation or intrazeolitic polymerization, although the
ether conversion stays high. The oxidation of EtOEt over
Nu–10 is so pronounced that most EtOEt is converted to CO_2.
Also oxidation towards ethyl acetate (EtOAc) is found. When
methylamine is used as N–containing reactant together with
diethyl ether the increase in selectivity towards EtOAc
suggests that deactivation of the active sites enhances the
activity of oxidation sites. The role of oxygen is
emphasized once more when N_2 is used as carrier gas.
Although not presented in Table 4 no reaction of diethyl
ether with ammonia is observed (Conversion EtOEt 1.6%.
selectivity towards EtOH 82 mol% and towards ethene 18
mol%).

ctivity towards pyridine at 350°C over Nu-10 and ZSM-5.
etween 5 and 18 hours.

Sample[1]	B	B	B[4]	K[4]	K[4]
Carrier gas	Air	N_2	Air	Air	Air
OR[2]	EtOH	EtOH	EtOH	EtOH	EtOH
NR[2]	$MeNH_2$	$MeNH_2$	$EtNH_2$	$MeNH_2$	$EtNH_2$
Conv. on OR(%)	6.3	0.4	22/17	30/22	30/22
Select. mol%					
Ethene	4.3	100	4.2/3.0	2.3/3.4	4.6
??-1[3]	0.5	–	–	0.1	0.3/0.2
Diethyl ether	–[5]	–[5]	0.1	–[5]	0.1
Ethanal	–[5]	–[5]	–	–[5]	0.1
Ethylamine	–	–	–	–	–
??-2[3]	–	–	–	0.3/0.1	4.6/2.1
Ethyl acetate	3.8	–	0.2	0.7	3.9/1.4
Ethanol	–	–	–	–	–
Acetonitrile	–	–	1.2	–	2.4/1.3
Tolu/p-Xylene	2.0	–	5.3/2.7	0.5	–
Pyridine	41.6	–	11/6.1	46.7	21/17
2-Picoline	1.4	–	4.8/1.8	1.1/0.6	3.2/2.3
2.6-Lutidine	–	–	–	–	0.7/0.4
4-Picoline	7.3	–	1.6/0.0	24.9	12/9.1
M.E.P[6]	–	–	–	–	0.8/0.5
C_{10}/C_{11} arom.	–	–	0.8	0.9/1.5	1.8/0.5
CO_2	39.4	–	70/84	23/20	45/62

ing reactant. [3] ??-1 ; ??-2 not-identified compounds. [4] The
presents the situation at t=5 h and t=18 h respectively.
nt in small amounts, quantitative determination not

As can be seen in Table 4 EtOAc or acetic acid is the
precursor for acetonitrile, through acetamide or ammonium
actetate, and not for pyridine. It is also shown that the
step from acetic acid towards acetonitrile is not oxygen
dependent. With EtOAc the conversion to pyridine seems to
be caused by reaction of the EtOH formed (by hydrolysis)
with NH_3.

Ethanol with methylamine as N-reactant over Nu-10 shows a
good conversion towards pyridine and is competitive towards
the ethanol/ammonia/ZSM-5 system in selectivity. Remarkable
is the formation of 4-substituted pyridines in the reactions
where alkylamines are used as N-containing reactant. More
than methylamine, ethylamine has a tendency towards
intrazeolitic polymerisation, at least more on Nu-10 than on

ZSM-5, judged by the catalyst deactivation. Also noteworthy
is the formation of numerous byproducts with ethanol and
ethylamine over ZSM-5. The formation of these byproducts and
the lower amount of intrazeolitic polymerisation must be due
to the presence of cavities in ZSM-5 with a diameter larger
than the channels of Nu-10, allowing not only the formation
of heavier products but also keeping the reaction
intermediates more separated from each other.

The higher conversion towards pyridines for alkylamines is
presumably due to their basicity. The gas-phase basicities
for ammonia, methylamine and ethylamine are reported to be
198, 209.8 and 212.5 kcal/mol respectively (21). This means
that even at high temperatures, alkylamines more easily form
a positive ammonium ion than ammonia and therefore react
more easily with the acid sites of the zeolite resulting in
a higher intrazeolitic N-concentration. Another important
factor is the competitive intrazeolitic chemisorption
between amines and pyridines. An experiment by Camia et al.
(22) regarding ammonia and pyridine on HZSM-5 shows a nearly
equivalent affinity to the protons of HZSM-5 with values of
207 and 222 kcal/mole for ammonia and pyridine respectively.

Figures 3 to 7 give data over the temperature range from
350 to 450°C. In Figure 3 the NaNu-10 based samples B, C, D
and J are compared. The presence of Fe_2O_3 in sample J is
visible as a much steeper increase in EtOH-conversion, as
can be seen in Figure 3a. The difference in change of
EtOH-conversion for sample C compared to samples B and D
affirms the idea that sample C posesses intrazeolitic
barriers, probably some form of aluminum oxide. The best
performer in making pyridine is sample D at 350°C.
Remarkable however is that sample C, having a not so good
conversion at 350°C, shows the best performance at 450°C.

When using K-originated Nu-10 (Figure 4) it can be seen
that, for samples F and G, at higher temperatures some
pyridine appears as if it has to be squeezed out of the
zeolites channels, again indicating blocked channels.
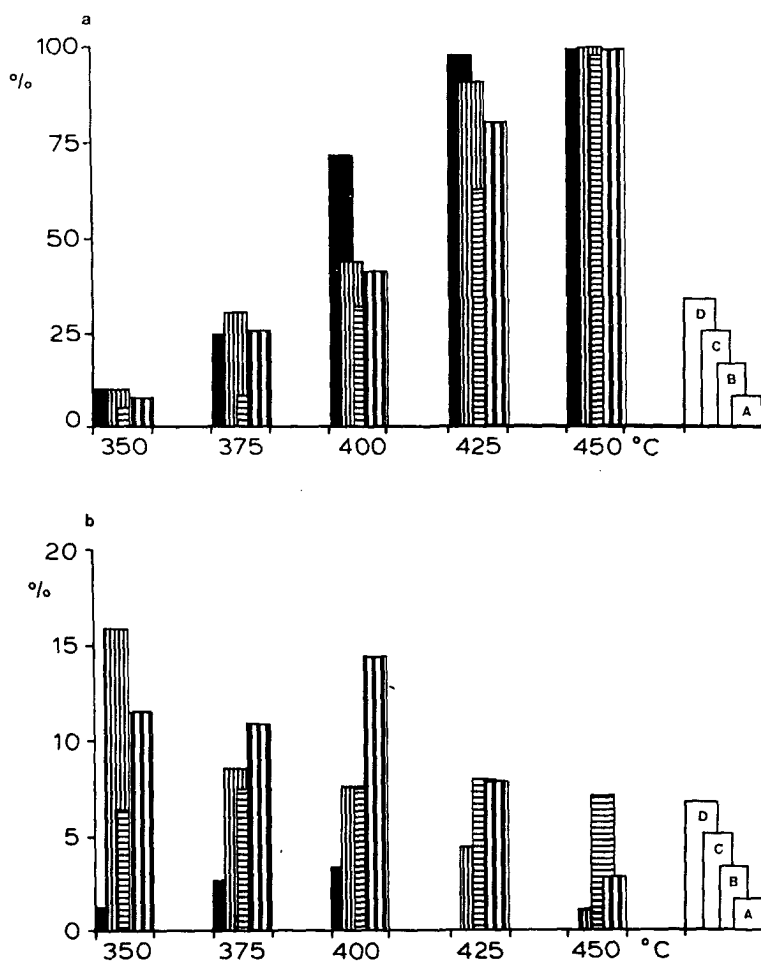
Figure 3. Effect of the reaction temperature on the reac-
tion of ethanol. ammonia and air towards pyridines using the
Nu-10-catalyst samples B, C, D and J. a) conversion of EtOH;
b) selectivity towards pyridines.   Legends: A=sample B;
B=sample C; C=sample D; D=sample J.

However for the more accessible sample H. a higher con-
version towards pyridines is found at lower temperatures.
This can also be seen by the conversion-behavior; when more
channel-openings are present there is more conversion.
There is however no visible effect in the conversion-change
upon heating.
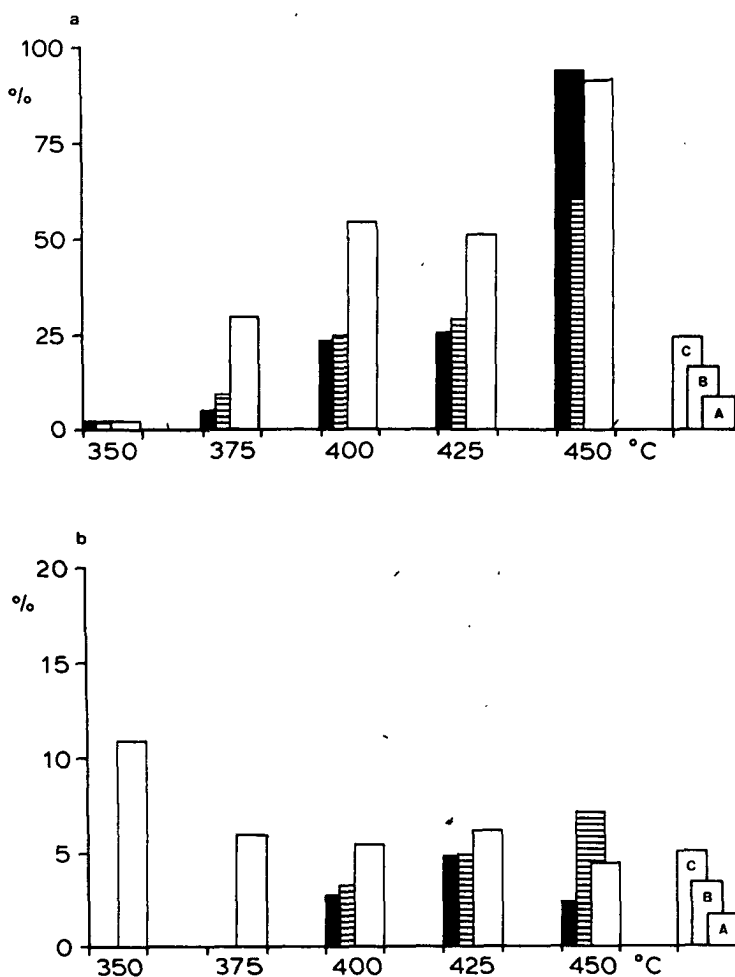
Figure 4. Effect of the reaction temperature on the reaction of ethanol. ammonia and air towards pyridines using Nu-10 (samples F, G and H) as the catalyst. a) conversion of EtOH; b) selectivity towards pyridines. Legends: A=sample H;. B=sample G; C=sample F.

Mordenite (Figure 5). producing small amounts of pyridine at 350°C. does not improve its selectivity towards pyridine at higher temperatures. It shows however a very good selectivity towards ethene. A 90% selectivity for ethene at 425 and 450°C for sample M compared to 81% for sample L. The conversion of ethanol to pyridine catalyzed by ZSM-5 looks
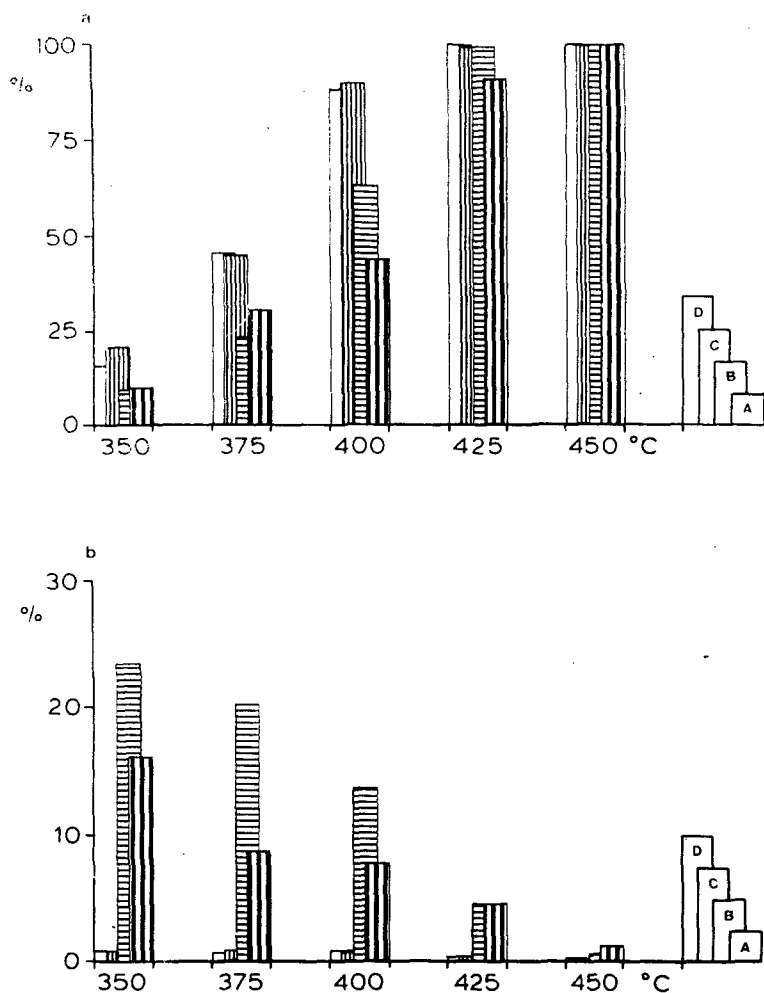
Figure 5. Effect of the reaction temperature on the reac-
tion of ethanol and ammonia over zeolites Nu-10 (sample D),
ZSM-5 (sample K) and mordenite (samples L and M) using air
as carrier gas.   a) conversion of EtOH; b) selectivity to-
wards pyridines.   Legends: A=Nu-10; B=ZSM-5; C=mordenite
(L); D=mordenite (M).

similar to those of Nu-10 in line with the fact that both
catalysts have the same type of catalytically active sites.
The difference in conversion in favour to ZSM-5 can be
explained by the more open structure of ZSM-5. Only at 450°C
diffusion rates are so fast that almost no difference in
catalytic behaviour between Nu-10 and ZSM-5 is observed.
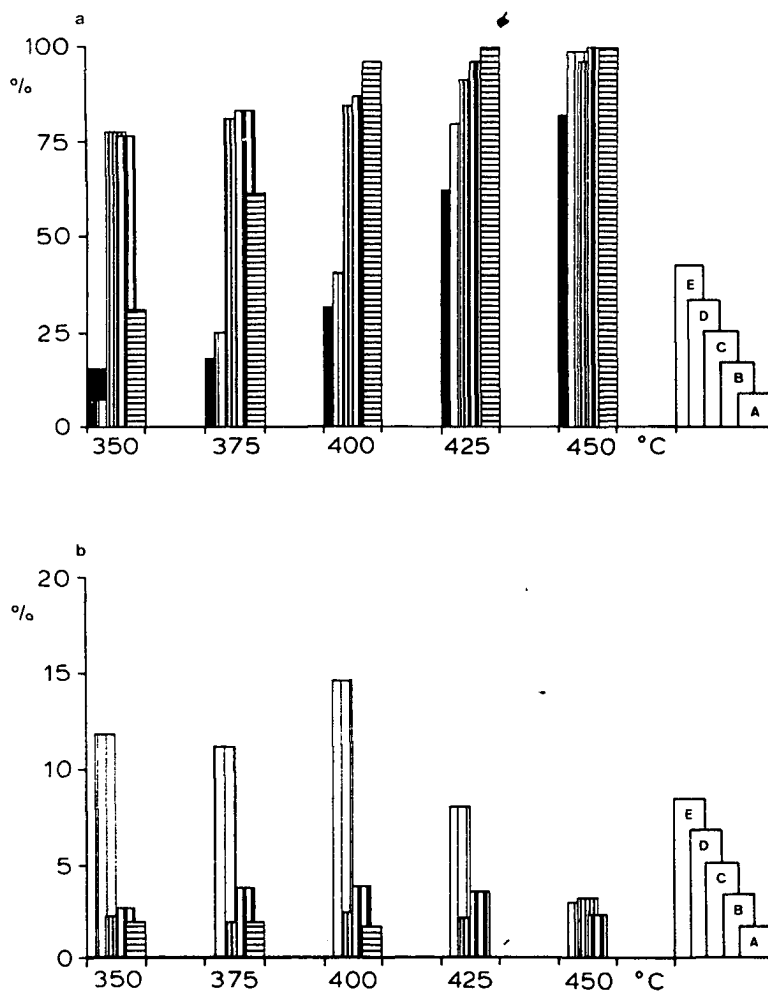
Figure 6. Effect of the reaction temperature on the conver-
sion and selectivity for Nu-10 (sample B) using ethyl ace-
tate (legend A), diethyl ether (legends B, C), ethanol (le-
gend D), THF (legend E), ammonia (legends A,B,D,E), methyl-
amine (legend C) and air. a) conversion of O-containing
reactants; b) selectivity towards pyridines.

From Figure 6 it becomes clear that an ethanol/ammonia
mixture gives the best selectivity towards pyridines
compared to ethyl acetate, diethyl ether and tetra-
hydrofuran. The high conversion rate of EtOEt, even at
350°C, shows the reactivity of this compound in the presence
of zeolites. Alas it does not lead to a high selectivity
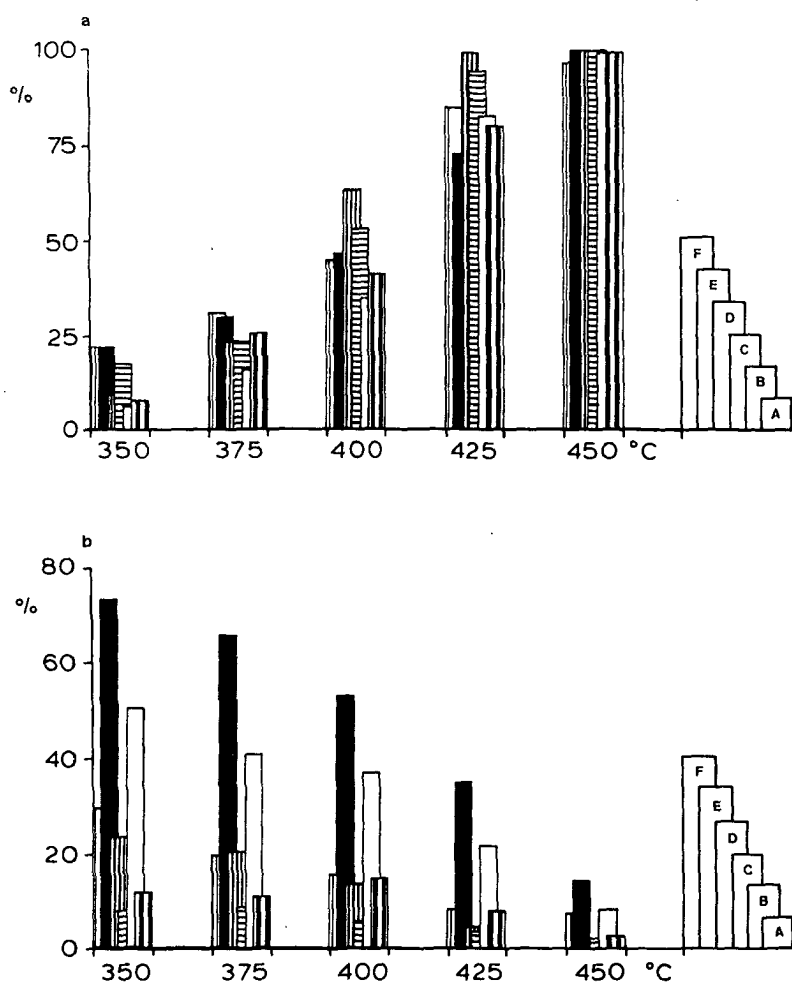
Figure 7. Effect of the reaction temperature on the conver-
sion and selectivity towards pyridines for the catalysts
Nu-10 (sample B. legends A,B,C) and ZSM-5 (sample K, le-
gends D,E,F) using EtOH as O-reactant and ammonia (legends
A,D), methylamine (legends B,E) or ethylamine (legends C,F)
as N-reactant with air as carrier gas. a) conversion of
EtOH; b)selectivity towards pyridines.

towards pyridines even when methylamine is used as

N-reactant. Although not depicted, noticable however is the

increase in CO_2-formation at temperatures above 400°C, for

ethyl acetate as organic compound (even when N_2 is used as

carrier gas) indicating a decarboxylation of the ethyl

acetate or subsequently producing acetic acid. the latter
indicated by an increase in acetonitrile selectivity.

In Figure 7 it is shown that methylamine causes a
substantial increase in the selectivity towards pyridines.
At low temperatures conversion is better on ZSM-5 than on
Nu-10 but at temperatures above 400°C no large differences
are observed.   The large difference between $MeNH_2$ and
$EtNH_2/NH_3$ cannot be explained just by gas-phase basicity.   A
possible explanation is that methylamine is an intermediate
in the reaction of ethanol and ammonia towards pyridines or
a more efficient building block.   A more detailed discussion
on this subject will be given in the subsequent Chapter.

CONCLUSIONS

1.   Just as ZSM-5, Nu-10 is a catalyst suitable for the
     preparation of pyridines out of ethanol and ammonia.
2.   Ion-exchange methods used to prepare the Nu-10
     catalyst partly determine its catalytic behaviour.
3.   Preferable reaction-temperatures are between 350 and
     400°C giving moderate conversions and selectivities.
4.   The use of methylamine as N-containing reactant
     creates a system having a high selectivity for
     pyridines on Nu-10 as well as on ZSM-5.
5.   The presence of iron in zeolite HNu-10 gives a
     catalyst suitable for the manufacture acetonitrile out
     of ethanol and ammonia.

REFERENCES

1. "The chemistry of heterocyclic compounds, vol. 14:
    Pyridine and its derivatives, part one". Ed. A.
    Weissberger. Interscience Publishers Inc. New York,
    1960.
2. "Ullmanns Enzyklopedie der technischen Chemie", Band
    19, 45 Aufl., Verlag Chemie, Weinheim 1980, 591.
3. "Pyridines: Bereiding. Markt en Toepassingen. Een
    literatuurstudie". P. Hollestelle, Technical
    University Delft, 1986.
4. Golunski, S.E. and Jackson. D. Appl. Catal. (1986),
    23, 1.
5. "Kirk Othmer's Encyclopedia of Chemical Technology",
    Vol. 19, John Wiley & Sons,New York, 1982, 453.
6. Halasz, J., Varga, K., Fejes, P., Laszlo. J. and
    Hernadi. K. Appl. Catal. 1987, 34, 135.
7. German Patent 565798 (1932); German Patent 569630
    (1933).
8. Chang, C.D. and Lang, W.H. US Appl. 4.220.783 (1980).
9. 'Nederlandse Organisatie voor Zuiver Wetenschappelijk
    Onderzoek te 's Gravenhage' and 'Technical University
    Delft', Dutch Patent 8202884 (1984).
10. Gaag, F.J. van der, Louter, F., Oudejans, J.C., and
    Bekkum, H. van. Appl. Catal. 1986, 26, 191.
11. Gaag, F.J. van der, Louter, F. and Bekkum, H. van.
    "New Developments in Zeolite Science Technology".
    Proceedings of the 7th International Zeolite
    Conference. (Ed. Y. Murakami, A. Iijima and J.W. Ward)
    Kodansha Ltd. Tokyo, Japan 1986, p. 763.
12. Gaag, F.J. van der, Ph. D. Thesis, Delft University of
    Technology 1987.
13. Febre, R.A. le, Kouwenhoven, H.W., and Bekkum, H.
    van. Zeolites 1988, 8, 60; this Thesis, Chapter IV.
14. Marler. B. Zeolites 1987, 7, 393.
15. Hogan, P.J., Whittam, T.V., Birtill, J.J., and
    Stewart, A. Zeolites 1984, 4, 275.
16. Harrison, I.D., Leach, H.F., and Whan, D.A. Zeolites
    1987, 7, 28.
17. Ghanami, M., and Sand, L.B. Zeolites 1983, 3, 155.
18. Oudejans, J.C. Ph. D. Thesis, Delft University of
    Technology 1984.
19. Boccuzzi. F., Coluccia, S., Ghiotti, G., Morterra, C.
    and Zecchina, A. J. Phys. Chem. 1978, 82, 1298.
20. Dewing, D., Spencer, M.S. and Whittam, T.V. Catal.
    Rev. Sci. Eng. 1985, 27, 461.
21. Aue. D.H., Webb, H.M. and Bowers, M.T. J. Am. Chem.
    Soc. 1972, 94, 4726.
22. Camia. M., Gherardi. P., Gubitosa, G., Petrera. M. and
    Pernicone. N. Proc. 8th Int. Cong. on Catal. 1984
    (publ 1985), 4, Vol. IV. p. 747.

CHAPTER VI

PYRIDINE FORMATION FROM ETHANOL AND AMMONIA OVER

HIGH-SILICA ZEOLITES. MECHANISTIC CONSIDERATIONS

ABSTRACT

A general discussion is given on acidic and radical sites
present in high-silica zeolites as HNu-10 and HZSM-5, with
relevance to pyridine-forming reactions. Zeolitic acid
sites are shown to catalyze the dehydrogenation of ethanol
together with condensation, cyclisation and aromatisation,
while structural defects probably produce oxidation products
as ethanal and formaldehyde which are thought to play an
important role in the reaction. A C_1/C_2-reactant system is
presented, showing a selectivity towards pyridines of 80%.

INTRODUCTION

Although numerous methods have been claimed for the
preparation of pyridine bases from acyclic molecules (such
as carbonyl and dicarbonyl compounds, dicyanoalkanes,
alkenes and alkynes), only a limited number of these
procedures (notably the condensation of aldehydes with
ammonia) are commercially applied. The use of crystalline
aluminosilicates as catalysts in the reaction of aldehydes
and ammonia towards pyridines has been reviewed by Golunski
and Jackson (1). Halasz et al. (2) describe a bifunctional
catalyst, based on oxides of tin, antimony and tellurium and
containing acidic as well as selective oxidation surface
centers for the preparation of pyridines out of propene and
ammonia. Aluminosilicate catalysts, capable of converting
aliphatic alcohols and ammonia into pyridines were found in
this laboratory and include HZSM-5 and HNu-10 (3-6), both

belonging to the pentasil group of zeolite materials. Their
catalytic activity and selectivity was found to depend
amongst others on their Si/Al ratio which governs the number
and strength of Bronsted acid sites.

Much research has been devoted to the conversion of
carbonyl compounds towards pyridine bases (1), here
relatively simple straightforward reaction schemes are
believed to apply. However, this is not the case when
ethanol and ammonia are reacted over high-silica zeolites to
obtain pyridines. A description of possible reaction
mechanisms with regard to the formation of 2.6-lutidine from
a mixture of acetone, methanol and ammonia over HZSM-5 was
given by van der Gaag (5).

In this Chapter some catalytic experiments are reported,
which were carried out in order to unravel the reaction
mechanism of the formation of pyridines out of ethanol and
ammonia in the presence of oxygen over high-silica
zeolites. The experiments include variations in the organic
N-compounds as well as in their relative concentration in
the reactant mixture. Also experiments reported in Chapter
V will be taken into consideration.

A general discussion on the occurrence of acidic and
radical sites in zeolites preceeds the discussion of
pyridine formation from ethanol over HNu-10 and HZSM-5.

EXPERIMENTAL

The preparative and catalytic testing procedures were
described in Chapters IV (7) and V. For convenience, the
coding of the preceding chapter is maintained. For full
details on sample B as well as on the reaction conditions,
see Chapter V.

RESULTS AND DISCUSSION

General considerations

The catalytic activity of zeolites is often mainly related
to their acidity, which arises from the bridging hydroxyl
groups, associated with Bronsted acid sites. In contrast to
Bronsted acid sites the characterisation of Lewis acid sites
in zeolites is as yet difficult (8). For some time a
tricoordinated aluminum species was held responsible for the
formation of Lewis acid sites (9). However, X-ray studies
showed no evidence for such sites (10). Upon dehydroxylation
(of faujasite) an increase in the number of hexacoordinated
Al atoms was found, using NMR techniques, with the remaining
lattice aluminum atoms being tetracoordinated. ^{27}Al MAS NMR
studies also provide evidence that the Lewis acid sites are
not the assumed trivalent lattice species but Al-species
whose precise nature has not been identified (10).

Acidic sites

For ZSM-5 zeolites, Kulkarni et al. (11) showed the
presence of three types of acid sites; weak, medium and
strong, by temperature programmed desorption of ammonia.
The strong acid sites originate from lattice aluminum atoms,
while the weak and medium strength acid sites are due to
terminal silanol groups and occluded extra lattice species
of aluminum, respectively. The influence of these terminal
silanol groups may not be underestimated. For instance, for
silica-rich ZSM-5 a concentration of 4.9 silanol groups per
unit cell, i.e. per 96 T-atoms, was observed by Dessau et
al. (12). The concentration of internal silanols is shown to
increase as the aluminum content decreases (13) and might be
correlated, at least partly, with the charge compensation of
the template molecules. A discussion concerning the
presence of isolated or clustered silanol groups in ZSM-5 is
going on at this moment between Dessau et al. (14) and van
Hooff et al. (15). High temperature steaming however brings
about structural rearrangements and a decrease in the number
of silanol groups with assumed repair of the lattice (12).

Using IR-techniques, Brunner (16) however, was able to show
that a bond breaking reaction in HZSM-5 by water molecules
is operative, even at ambient temperatures. This reaction
is not associated with Al and can be reversed at higher
temperatures under evacuation. The presence of the
structural defects mentioned in this paragraph is confirmed
by the fact that the cation exchange capacity of ZSM-5
exceeds that calculated from the aluminum content of the
tetrahedral framework (17).

Zeolite ZSM-5 is best known for its (super) strong acid
sites (8,11,18). Strong Bronsted acid sites in HZSM-5 are
situated at channel intersections and are associated with
lattice aluminum atoms. At low aluminum content, AlO_4^-
tetrahedra are far from each other, and maximum proton
acidity is reached. As described by Barthomeuf (19) the
acid strength of the strong acid sites is dependant on the
number of Al-atoms on the next nearest neighbour (NNN)
sites, the acidity being maximal when this number is zero.
At higher intrazeolitic aluminum concentrations the extra
aluminum atoms are to be included in the form of additional
lattice aluminum species lowering the average -but enhancing
the total- Bronsted acidity, or should occupy a
non-framework position, corresponding to strong acid sites
and Lewis acid sites, respectively.

Lago et al. (20) describe the formation of highly active
catalytic sites by mild steaming of ZSM-5 with a specific
activity 45-75 times greater than that of the normal sites.
These authors suggest the formation of Al species with just
a loose binding to the framework, so on its way to become
extra lattice Al. Zoned aluminum distribution as observed in
ZSM-5 (21,22) makes the co-existence of strong acid sites
and somewhat weaker acid sites acceptable.

Radical sites

Steinike et al. (23) recently showed that upon mechanical
treatment of quartz radical structures, by Si-O-Si bond
breaking are formed and assumed these to be $\equiv Si\cdot$ and $\equiv SiO\cdot$
of which the former actually was detected. Under oxygen

pressure the primarily created radicals react to
oxygen-containing radicals according to

$$-Si\cdot + \cdot O{:}O\cdot \longrightarrow -Si-OO\cdot \rightleftharpoons -Si^+O_2^-$$

$$2\ -Si\cdot + \cdot O{:}O\cdot \longrightarrow 2\ -Si-OO\cdot$$
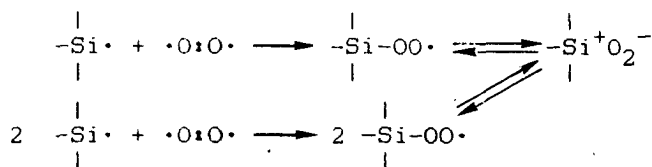
Hydrogen also reacts with the radicals initially created by
bond fracture to form $\equiv Si-H$ and $\equiv Si-OH$ structures,
respectively.

Krylov (24) also describes the formation of such radical
centers upon grinding of SiO_2, GeO_2 and SnO_2. Furthermore
this author postulates a number of reactions concerning
these radical sites, such as

$$\equiv SiOO\cdot + CO \longrightarrow \equiv SiO\cdot + CO_2$$

$$\equiv SiO\cdot + RH \longrightarrow \equiv SiOH + R\cdot$$

$$\equiv SiOO\cdot + C_2H_4 \longrightarrow \equiv SiO\cdot + H_2C\overset{O}{\overbrace{\diagup\diagdown}}CH_2$$

$$\equiv SiO\cdot + C_2H_4 \longrightarrow \equiv SiOCH_2\dot{C}H_2 \longrightarrow \equiv Si\dot{C}H_2 + H_2CO$$
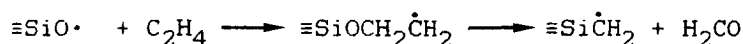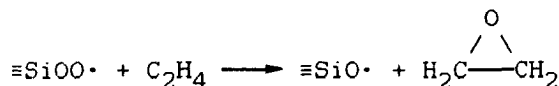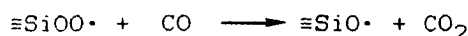
It is known that O_2^- species are active species in
heterogeneous catalysis. With regard to zeolites the effect
of oxygen on the formation of radicals is not new. Already
in 1967 Dollis and Hall (25) showed that the concentration
of radicals in decationated faujasites was dependant on both
the amount of oxygen available and the presence of
dehydroxylated sites. Removal of O_2 by evacuation overnight
at 550°C was not possible showing oxygen to be strongly
chemisorbed. Similarly Wierzchowski et al. (26) reported
that adsorption of benzene on HZSM-5 gave rise to the
formation of the monomeric benzene cation radical $C_6H_6^+\cdot$ and
that the presence of oxygen enhanced the ionizing properties
of this zeolite acting as a strong oxidizer. The presence
of intrazeolitic radicals in Silicalite-1 and HZSM-5 is
further supported by results of Huizinga et al. (27) on the
gas phase chlorination of benzene giving mainly rise to
addition products, requiring radical intermediates.

Table 1. Testing of several compounds at 350°C over Nu-10 (
towards pyridines. $WHSV_{OR}$=0.5/X h^{-1} (see Chapter V, experim
between 5 and 18 hours.

Column nr.	1	2[3)]	3[4)]	4	5
Sample	B	B[3)]	_[4)]	B	B
OR[1)]	EtOH	EtOH	EtOH	EtOH	EtOH
NR[1)]	–	–	NH_3	NH_3	NH_3
ratio NR:OR	0:3	0:3	1:3[5)]	1:3[5)]	2:3[5)]
Conv. on OR %	99.5	89.3	14.4	7.9	6.8
Select. mol%					
Ethene	90.0	55.7	10.9	9.3	6.8
??-1[2)]	–	0.6	–	–	0.3
Diethyl ether	–	0.5	0.4	12.5	6.7
Ethanal	3.8	12.8	25.8	13.4	8.7
Ethylamine	–	–	3.3	–	–
??-2[2)]	–	0.9	–	–	1.7
Ethyl acetate	–	0.8	–	1.8	1.9
Acetonitrile	–	–	3.2	2.7	2.8
Benzene	–	–	–	–	–
Toluene/p-Xylene	–	–	6.5	–	–
Pyridine	–	–	4.4	11.7	17.8
2-Picoline	–	–	<0.5	1.5	7.7
4-Picoline	–	–	–	–	3.3
C_{10}/C_{11} arom.	–	–	–	–	0.5
CO_2	6.3	28.4	45.3	47.1	41.2

[1)] OR = O-containing reactant; NR = N-containing reactant.
poisoned with pyridine prior to the reaction. [4)] experiment
$WHSV$=0.17 h^{-1}. [5)] an EtOH:MeOH mixture, molar ratio 2:1, was
$MeNH_2$. Products present in small amounts, quantitative dete

Recently the formation of radicals in pentasil type
zeolite-catalyzed reactions of olefins, aromatic compounds
and dimethyl ether have been reported by Slinkin (28),
Kucherov (29) and Rooney (30), respectively.

Regarding the structure of radical-forming sites no
uniform descriptions are found. Kucherov and Slinkin
(28,29,31) suggest a combination of a Bronsted acid site and
a SiO· group to be formed as a result of the cleavage of the
Si-O-Al lattice link. According to these authors the nature
of the radical-forming site is in principle the same for all
pentasil-type zeolites.

sample B) as catalyst amongst others on their selectivity
ental). Carrier gas is air. Time on stream is averaged

Column nr.	6[5)]	7	8	9
Sample	B	B	B	B
OR[1)]	EtOH/MeOH	EtOH	EtOH	EtOH
NR[1)]	NH_3	$MeNH_2$	$MeNH_2$	$MeNH_2$
ratio NR:OR	1:3	1:3	2:3	3:3
Conv. on OR %	18.1	6.3	24.6	29.5
Select. mol%				
Ethene	10.4	4.3	0.7	0.5
??-1[2)]	6.3	0.5	–	–
Diethyl ether	4.2	–[6)]	–[6)]	–[6)]
Ethanal	24.8	–[6)]	–[6)]	–[6)]
Ethylamine	–	–	–	–
??-2[2)]	2.5	–	–	–
Ethyl acetate	–	3.8	0.5	–
Acetonitrile	1.9	–	–	–
Benzene	–	–	–	0.1
Toluene/p–Xylene	–	2.0	0.4	0.3
Pyridine	14.7	41.6	47.7	51.0
2–Picoline	1.3	1.4	4.8	1.8
4–Picoline	1.9	7.3	26.9	27.0
C_{10}/C_{11} arom.	–	–	1.5	2.2
CO_2	32.1	39.4	17.6	17.1

[2)] ??-1 and ??-2 non-identified compounds. [3)] catalyst
taken from Reference 3. sample=Silicalite-1, T=365°C;
used. $WHSV_{EtOH}$=0.25 h^{-1}. [6)] Measurements influenced by
rmination not possible.

According to Shih (32) during calcination of ZSM-5 in
either air or diluted oxygen atmosphere at 500°C or higher
temperatures positive holes occur on oxygen atoms of the
zeolitic silica-alumina surface. The author suggests
interactions of the unpaired electrons with adsorbed
ionizable organic molecules with an ionization energy less
than 12.6 eV resulting in organic radical cations.

Rooney et al. (30) prove that the paramagnetic centres,
described by Shih (32) and present in the zeolite ZSM-5 in
tiny amounts as solid state defects, are the source of the
free radicals formed.

Summarizing, 4 active sites can be present on zeolites:
  I. Strong Bronsted acid sites.
 II. Lewis acid sites.
III. Weak acid sites / silanol groups.
 IV. Radical sites.

Pyridine-forming reactions in the presence of oxygen

The results of a series of experiments, performed in order
to clarify the mechanism of the reaction of ethanol and
ammonia towards pyridines using high-silica zeolites, are
presented in Table 1. It is shown that in the absence of
ammonia an ethanol/water/air gas mixture undergoes a fast
reaction on HNu-10 at 350°C (Table 1, columns 1,2), with a
high conversion towards ethene. Adsorption of pyridine on
the catalyst prior to the reaction masks most of the strong
acid sites resulting in a decrease in conversion towards
ethene and an increase in ethanal (and CO_2) formation. This
shows that dehydration of ethanol towards ethene is
performed on strong acid sites which mainly remain occupied
by pyridine at 350≡C. The increase in ethanal and CO_2
selectivity indicates the presence of oxidative sites
reacting with either ethanol and/or with ethene.
Silicalite-1 (Table 1, column 3), just having traces of
Bronsted acid sites due to Al or Fe impurities, shows not
only a lower EtOH conversion but a higher selectivity
towards ethanal as well, when compared to Nu-10 or ZSM-5
(Chapter V), emphasizing the role of acidic sites in
dehydration on the other hand. The low conversion towards
pyridine over Silicalite-1 indicates that pyridine formation
requires Bronsted sites. The relatively high selectivity of
Silicalite-1 towards oxidation products as ethanal and CO_2
shows the presence of oxidative (radical) sites to be
independent of aluminum as reported earlier (28, 29, 31, 32)
and supports the oxygen radical sites idea as described for
quartz (23,24). Dehydrogenation of alcohols towards their
respective aldehydes over Silicalite-1 and dehydrated silica
is described by Matsumura et al. (33,34). The authors not

only conclude that acid-base sites in silica do not exist,
they also suggest that the catalytic activity may be
correlated with the surface silanol concentration which
again refers to the results reported by Dessau et al.
(12,13).

Regarding the experiments described in Chapter V and Table
1, columns 1-3 the following reaction scheme can be
presented:

$$EtOH \xrightarrow[\text{sites}]{\text{acid}} \text{Ethene and/or Diethyl ether}$$

$$EtOH \xrightarrow[\text{sites}]{\text{radical}} \text{Ethanal} \xrightarrow{[O]} \text{Acetic acid} \rightleftharpoons \text{Ethyl acetate}$$

with branches: Ethene → (via [O]) Ethanal, Acetic acid, Ethyl acetate;
Ethanal $\xrightarrow{NH_3}$ Pyridines; Ethanal $\xrightarrow{[O]}$ CO$_2$; Acetic acid $\xrightarrow{NH_3}$ Acetonitrile; Ethyl acetate $\xrightarrow{NH_3}$ Acetonitrile

$$EtOH + NH_3 \longrightarrow \text{Ethylamine}$$
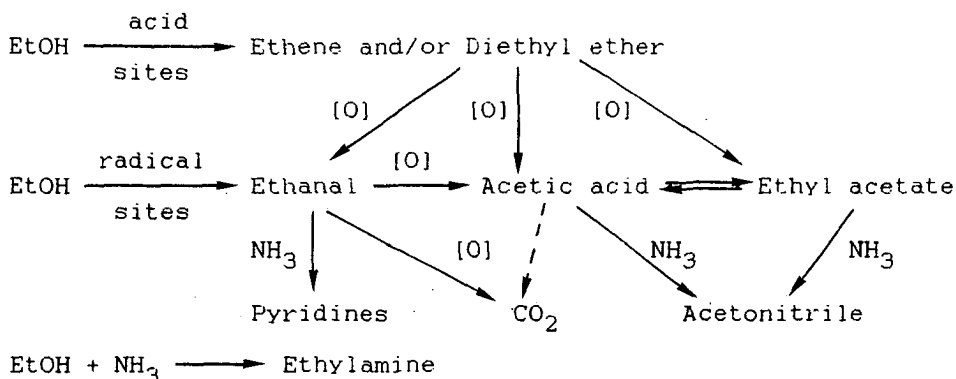
Ethene and diethyl ether are formed by acid catalysis. As
to the formation of ethanal several mechanistic pathways can
be taken into consideration. For instance, the terminal
O-atom in the $\equiv$Si-OO$\cdot$ radical might lead to partial
oxidation products, as ethylene oxide (24). The oxirane ring
system of the ethylene oxide is highly strained and opens
readily, especially in the presence of acids.

$$\underset{H_2C-CH_2}{\overset{O}{\diagup \diagdown}} \xrightarrow{H^+} \underset{H_2C-CH_2}{\overset{OH^+}{\diagup \diagdown}} \xrightarrow{H_2O} \underset{H_2C-CH_2}{\overset{HO \; OH_2+}{| \quad |}}$$

$$\underset{H_2C-CH_2}{\overset{HO \; OH}{| \quad |}} \quad \xleftarrow{-H^+} \quad \underset{H_3C-C=O}{\overset{H}{|}} \; (\Delta T)$$
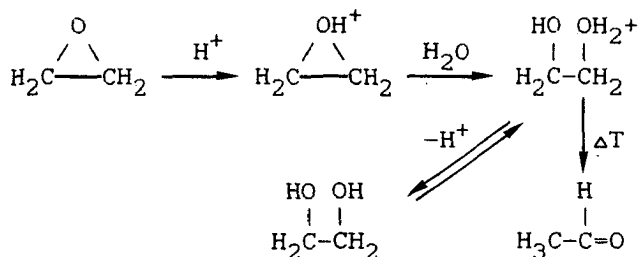
A proton catalyzed pinacol dehydration/rearrangement then
may lead to ethanal. A similar reaction, from ethylene
glycol towards ethanal over mordenite has been described by
Chang and Curthays (35). Furthermore, oxidation of ethene

over metal oxides towards acetic acid has been reported
(36a). However, these reactions are not likely to occur on
Nu-10 or ZSM-5 while during our experiments no relation was
found between an increase in ethene concentration and an
increase in oxidation products.

Perhaps more likely is the oxidation of ethanol towards
ethanal as described by Golodets and Ross (36b) and Rooney
(30), initiated by the attack of surface radicals onto a
secondary C-H yielding ethanal:

$$\equiv SiOO\cdot \qquad\qquad\qquad \equiv SiOOH$$
$$\text{or} \quad + H_3C-CH_2-OH \longrightarrow \quad \text{or} \quad + H_3C-\overset{\cdot}{C}-OH \xrightarrow{+X\cdot} H_3C-C\overset{H}{=}O + XH$$
$$\equiv SiO\cdot \qquad\qquad\qquad \equiv SiOH$$
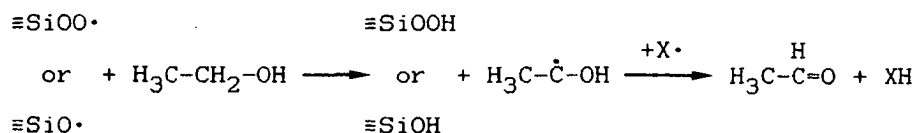
The observed fast oxidation in the reaction of diethyl
ether and ammonia (Chapter V) supports the presence of
surface-peroxy radicals in Nu-10 and ZSM-5, as ether
structures are known to be oxidized rather easily by
peroxides.

The catalytic formation of ethyl acetate from ethanol and
acetic acid, in our experiments formed by the oxidation of
ethanol, diethyl ether or ethanal, is described by Wang et
al. (37) using metal oxides such as Bi_2O_3, MoO_3 and Sb_2O_4.

Almost all products formed from ethanol including ethanol
itself are able to react with ammonia, at high temperatures
using zeolite catalysis, resulting in the products presented
in the above reaction overview. As shown in Chapter V
acetic acid is a precursor for acetonitrile and not for
pyridine.

According to literature data regarding pyridine syntheses
(1-5, 38-41) aldehydes are good starting materials. Surface
reactions of ethanal and ammonia on various heterogeneous
catalysts are known to lead to 2- and 4-methylpyridine,
roughly in a 1:1 ratio (1).

It should be noted however, that in our work on ethanol
conversion mainly unsubstituted pyridine is observed whereas
2- and 4-methylpyridine are expected on the basis of a C_2

building unit. Oxidation of the methyl group attached to the pyridine ring followed by decarboxylation is possible but experiments using 2-methyl-pyridine as the reactant were not convincing in this respect, showing just a very low conversion.

Results obtained using methylamine as N-containing reactant (Chapter V + this Chapter), using HNu-10 or HZSM-5 as the catalyst, suggest the participation of a C_1 (or C_3) building block. Addition of methanol to the EtOH/NH_3 reaction mixture (Table 1, column 6) shows an increase in pyridine selectivity, which also supports the presence of C_1-species in the zeolite during ethanol conversion.

The formation of C_1 fragments from ethanol might involve zeolite radicals converting ethanol into a radical cation followed by fragmentation. In mass spectroscopy the cleavage of the C-C bond next to the oxygen or nitrogen atom in alcohols or amines is a major fragmentation as shown by a dominant peak due to $CH_2=OH^+$ (m/e=31) or $H_2C=NH_2^+$ (m/e=30), respectively. According to McLafferty et al. (42) the following reactions might take place:

$$CH_3CH_2OH \xrightarrow[\text{site}]{\text{radical}} CH_3CH_2\overset{\bullet}{O}H^+ \longleftrightarrow \bullet CH_2CH_2OH_2^+$$

$$\cdot CH_3 + H_2C=OH^+ \qquad H\cdot + H_3CCH=OH^+$$

$$CH_3CH_2NH_2 \xrightarrow[\text{site}]{\text{radical}} CH_3CH_2\overset{\bullet}{N}H_2^+ \longleftrightarrow \bullet CH_2CH_2NH_3^+$$

$$\cdot CH_3 + H_2C=NH_2^+ \qquad H\cdot + H_3CCH=NH_2^+$$
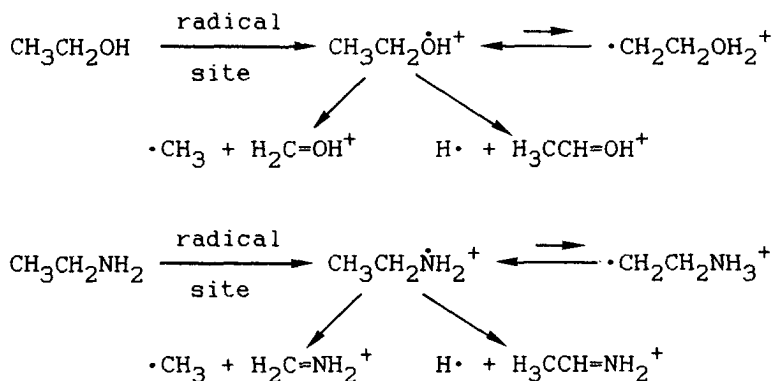
Relative abundances for $H_2C=OH^+$, $H_3CHC=OH^+$, $H_2C=NH_2^+$, $H_3CHC=NH_2^+$ are 15, 100, 100, 10 for collision activated composition (CAD) and 100, 35, 100, 20 for electron impact mass spectroscopy (EI), respectively. These values show the relatively high stability for the $H_2C=NH_2^+$ fragment compared
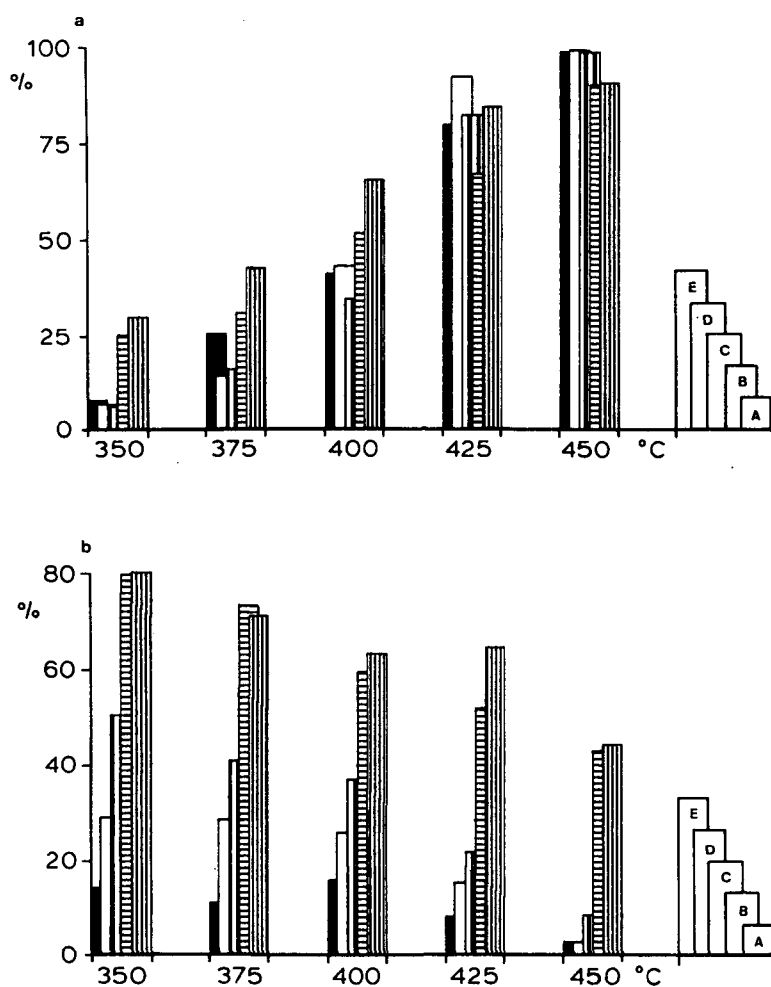
Figure 1. Effect of the reaction temperature on the conver-
sion of EtOH and selectivity towards pyridines for Nu-10
(sample B) at several N-reactant:Ethanol ratios. a) conver-
sion of EtOH; b) selectivity towards pyridines. Legends:
A=3:3 MeNH$_2$:EtOH; B=2:3 MeNH$_2$:EtOH; C=1:3 MeNH$_2$:EtOH; D=2:3
NH$_3$:EtOH; E=1:3 NH$_3$:EtOH.
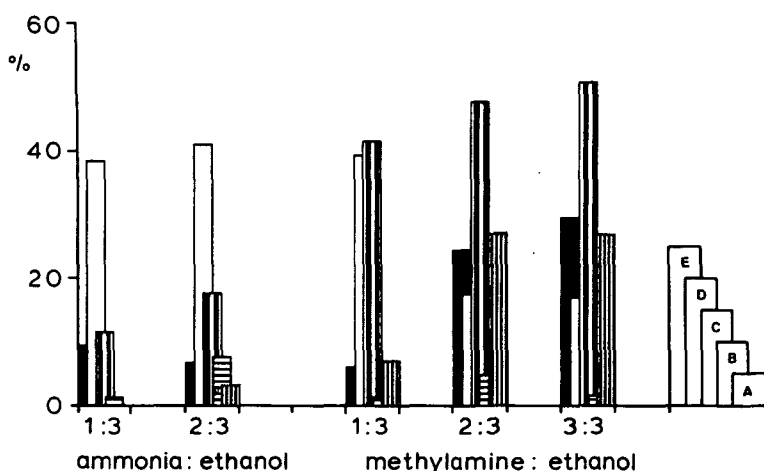
Figure 2. Effect of the N-reactant:Ethanol ratio on the conversion of EtOH and selectivity towards pyridines and CO_2 at 350°C. Legends; A=selectivity in mol% towards 4-methyl-pyridine; B=towards 2-methyl-pyridine; C=towards pyridine; D=towards CO_2; E=EtOH conversion.

to the C_2 fragments. C-C scission by very strong acid sites as described by Barthomeuf (19) is not likely to occur because of the large occupation of acidic sites by ammonia and pyridines.

When investigating higher reaction temperatures, several observations can be made (Figure 1). High methylamine concentrations prevent a 100% conversion of ethanol at 450°C when compared to ammonia (Figure 1a), indicating a higher basicity of methylamine and therefore a larger occupation of acidic sites at these temperatures. Comparing the $MeNH_2$:EtOH ratios of 2:3 and 3:3 (Figure 1b, Figure 2) almost no difference in selectivity towards pyridines and conversion is found, indicating a maximal conversion towards pyridines at these ratios, for the Nu-10 used in our experiments.

Taking this all into account it is likely that in the reaction of ethanol and ammonia towards pyridines the following intrazeolitic reactions might occur (see Figure
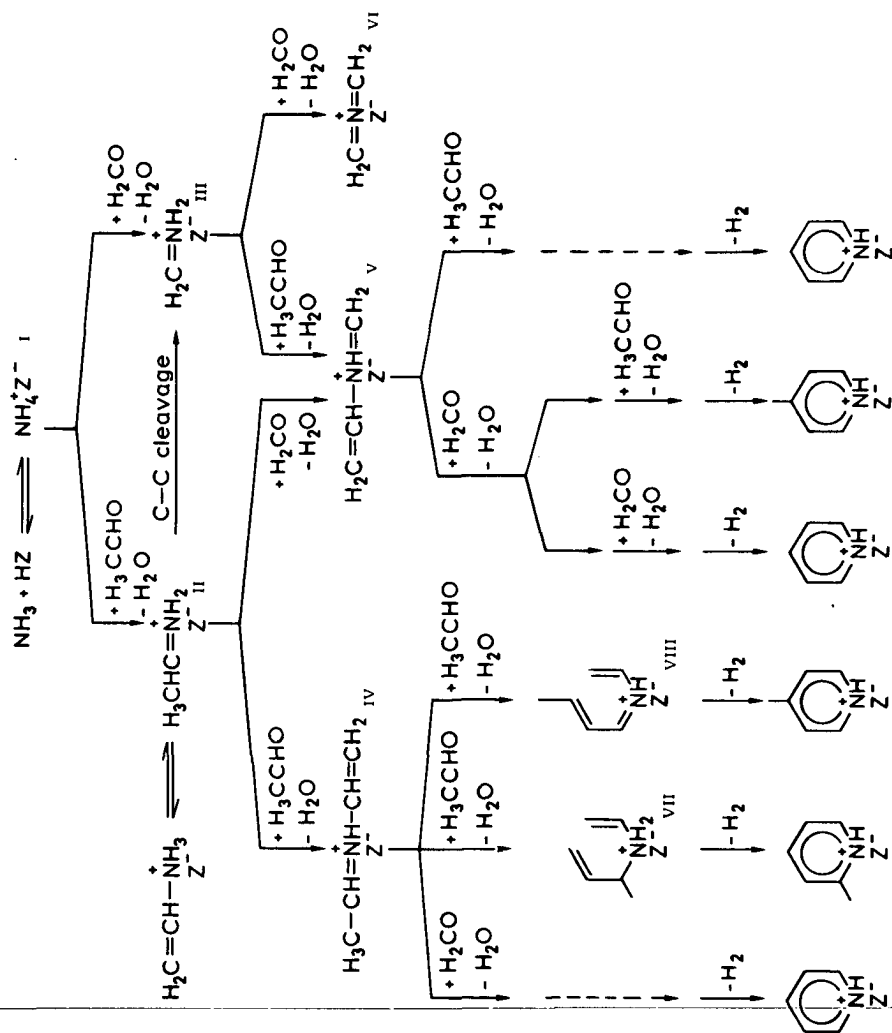
Figure 3. The pyridine forming reactions which are likely to occur during the reaction of ethanol and ammonia in the presence of air, using zeolite HNu-10 or HZSM-5 as the catalyst.

3). Ammonia which is in equilibrium with acidic sites (I) reacts with ethanal (II) whereafter a C-C cleavage, forming methylimine out of ethylimine is possible (III). In another route formaldehyde is formed by fragmentation of ionized ethanol and reacts with the zeolite-ammonium system (III).

Generally imines are fairly unstable and polymerize easily. Interactions with the Bronsted acid sites of the zeolite might prevent these polymerizations by keeping the adsorbed imines separated. The addition of a molcule of ethene to these imines is possible. Howver, this type of propagation will not be discussed.

In a second step another C_1 or C_2 aldehyde may add to the deprotonated imine, followed by dehydration (IV-VI). The bismethyleneimine formed in VI is unlikely to occur under these reaction conditions and shall not be discussed. The intermediate IV is very reactive and is able to react with an aldehyde on the C of its C=N group (43) as well as on the C of its C=C group (VII, VIII, respectively). Ring closure and aromatization then leads to 2- and 4-methyl-pyridine, respectively. Similarly intermediate V can react with another C_2 or C_1 aldehyde.

When methylamine is used instead of NH_3 the results bear mechanistically a resemblance to those obtained with the EtOH/NH_3 system. However the C_1-fragment is already present from the beginning of the reaction, intermediate V might be involved, explaining the high selectivity towards pyridine and 4-methylpyridine, especially at larger $MeNH_2$:EtOH ratios.

For a mixture of ethylamine and EtOH with Nu-10 as the catalyst reaction products, similar to those observed using NH_3, are obtained as expected (confirm Chapter V). The presence of products as 2-methyl-5-ethylpyridine and 2.6-dimethylpyridine, when ZSM-5 is used, not only supports alkylation via the C=N group (intermediate VII) but also supports the existence of a very fast C-C scission for ethylamine resulting in a high pyridine selectivity. The absence of these products in Nu-10 catalysis can be

explained by the fact that Nu-10. with its parallel channel lattice, lacks the presence of channel crossings, restricting the size of the intermediates (transition state selectivity).

The pyridine-forming reactions result in pyridines adsorbed in the zeolite. An experiment by Camia et al. (43) regarding competitive chemisorption of NH_3 and pyridine on ZSM-5 shows the heat of adsorption of ammonia and pyridine onto the Bronsted sites of the ZSM-5-catalyst to be 207 and 222 kcal/mole, respectively.

$$PyH-Zeolite + NH_3 \rightleftharpoons NH_4-Zeolite + Py$$
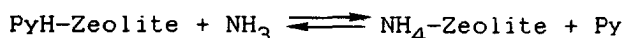
Increasing the ammonia or methylamine concentration in the feed shifts the equilibrium to the right leading to higher conversions towards pyridines as depicted in Table 1, columns 4,5,7-9 and Figure 2. Especially the increase in 4-picoline selectivity and the decrease in CO_2 formation are noticeable. As can be seen in Figure 2, at 350°C the zeolite reaches maximum selectivity of almost 80% towards pyridines at a methylamine:ethanol ratio of 3:3.

The high conversions gained using alkylamines might at least partly be due to their basicity (45). Alkylamines more easily remove a pyridine from the zeolite's acid sites than ammonia, shifting reaction presented above further to the right.

The existence of such an ammonia/pyridine equilibrium in HNu-10 is shown in Figure 4 which gives NH_3-TPD curves of various samples. In Figure 4a a 'standard' NH_3-TPD spectrum is depicted (code ABCDEF) showing the well known peaks for physisorption, medium and strong acid sites.
When heating a HNu-10 sample, used for a EtOH + NH_3 reaction, without any further modifications (code F) two desorption peaks are found. A small one around 120°C and a larger one around 600°C. The latter can be attributed to pyridines (46). Upon passing ammonia over the 'used' catalyst (code DEF), at room temperature, an increase in the area of the physisorption peak is observed together with a
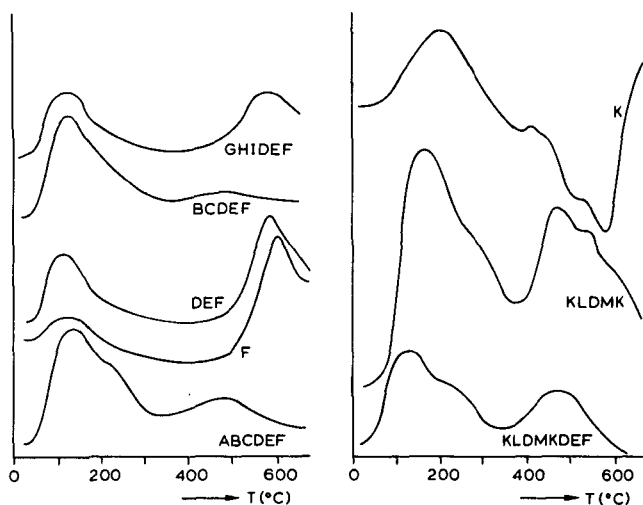
Figure 4. Several TPD spectra of zeolite HNu-10 (sample B)
used for a reaction of EtOH + NH$_3$ towards pyridines. The
lettercodes provided show the order of treatment for the
relevant sample. Explanation of the letters: A=calcination
under air; 550°C; 1 night. B=heating to 700°C; 20°/min;
under N$_2$. C=cooling down to room temp.; under N$_2$. D=NH$_3$-
adsorption at room temp; 30 min. E=desorption excess NH$_3$ at
room temp; under N$_2$. F=heating to 640°C; 10°/min; under N$_2$.
G=heating to 360°C; 20°/min; under N$_2$. H=NH$_3$-adsorption at
360°C; 20 min. I=cooling down to room temp; under NH$_3$. K, L
and M are similar to F, C and E but air is used instead of
N$_2$.

minor change in the peak around 600°C, indicating almost no
exchange of pyridine for NH$_3$ at the acid sites. However
upon passing ammonia over the 'used' catalyst at 360°C (code
GHIDEF) a substantial decrease in the area of the
high-temperature peak together with a broadening of this
peak is found, indicating the existence of an
ammonia/pyridine equilibrium on HNu-10 under these
conditions.

   The NH$_3$-TPD spectrum of a 'used' HNu-10 catalyst (Figure
4a, code BCDEF) shows a decrease in desorption peaks

corresponding to the coverage of Lewis as well as Bronsted
acid sites indicating 'coke' products, when compared to the
NH_3-TPD spectrum of a calcined HNu-10 sample (code ABCDEF).
Using air instead of nitrogen as a carrier gas the
intrazeolitic role of oxygen is emphasized once more; the
spectrum of a 'used' catalyst heated in air (Figure 4b, code
K) shows the consumption of oxygen between 300 and 600°C
causing negative TPD peaks. Passing ammonia over this
'calcined' catalyst (codes KLDMK and KLDMKDEF) shows the
regeneration of both Lewis and Bronsted acid sites. No
explanation was found for the occurrence of the shoulders
around 530°C for the spectra coded K and KLDMK.

CONCLUSIONS

The reaction mechanism for the reaction of ethanol and
ammonia towards pyridines over the high silica zeolites
HZSM-5 and HNu-10, proposed in this Chapter, is supported by
the experimental results, although further investigations
are necessary. The strong acid sites on zeolites like
mordenite, X or Y prevent the release of pyridines resulting
in almost no catalytic activity towards these compounds
(3,6).

The role of oxygen, in the reaction of EtOH and NH_3
towards pyridines, is not only the production of aldehydes,
necessary to complete the reaction, but also to restore the
radical sites and to 'de-coke' the zeolite, in order to keep
the reactive sites accessible.

REFERENCES

1. Golunski, S.E. and Jackson, D. Appl. Catal. 1986, 23,
    1 and references cited herein.
2. Halasz, J., Varga, K., Fejes, P., Laszlo, J. and
    Hernadi, K. Appl. Catal. 1987, 34, 135.
3. Gaag, F.J. van der, Louter, F., Oudejans, J.C. and
    Bekkum, H. van. Appl. Catal. 1986, 26, 191.
4. Gaag, F.J. van der, Louter, F. and Bekkum, H. van.
    "New Developments in Zeolite Science Technology".
    Proc. 7th Int. Zeolite Conf. (Eds. Y. Murakami, A.
    Iijima and J.W. Ward), Kodansha Ltd., Tokyo 1986, p.
    763.

5. Gaag, F.J. van der. Ph. D. Thesis, Delft University
    of Technology 1987.
6. This Thesis, Chapter V.
7. Febre, R.A. le, Kouwenhoven, H.W. and Bekkum, H. van.
    Zeolites 1988, 8, 60; this Thesis, Chapter IV.
8. Ashton, A.G., Batmanian, S., Clark, D.M., Dwyer, J.
    Fitch, F.R., Hinchcliffe, A. and Machado, F.J.
    "Catalysis by acids and bases" (Eds. B. Imelik, C.
    Naccache, G. Coudurier, Y. Ben Taarit and J.C.
    Vedrine). Stud. Surf. Sci. Catal. 20, Elsevier,
    Amsterdam 1985, p. 101.
9. Loktev, M.I. and Slinkin, A.A. Russian Chem. Rev.
    1976, 45, 807.
10. Lau, G.C. and Maier, W.F. Langmuir 1987, 3, 164.
11. Meshram, N.R. Hegde, S.G. and Kulkarni, S.B. Zeolites
    1986, 6, 434.
12. Dessau, R.M., Schmitt, K.D., Kerr, G.T., Woolery, G.L.
    and Alemany, L.B. J. Catal. 1987, 104, 484.
13. Woolery, G.L., Alemany, L.B., Dessau, R.M. and
    Chester, A.W. Zeolites 1986, 6, 14.
14. Dessau, R.M., Schmitt, K.D., Kerr, G.T., Woolery, G.L.
    and Alemany, L.B. J. Catal. 1988, 109, 472.
15. Kraushaar, B., Haan, J.W. de and Hooff, J.H.C. van.
    J. Catal. 1988, 109, 470.
16. Brunner, G.O. Zeolites 1987, 7, 9.
17. Chester, A.W., Chu, Y.F., Dessau, R.M., Kerr, G.T. and
    Kresge, C.T. J. Chem. Soc., Chem. Commun. 1985, 289.
18. Aukett, P.N., Cartlidge, S. and Poplett, I.J.F.
    Zeolites 1986, 6, 169.
19. Barthomeuf, D. Materials Chemistry and Physics 1987,
    17, 49.
20. Lago, R.W., Haag, W.O., Wikovsky, R.J., Olson, D.H.,
    Hellring, S.D., Schmitt, K.D. and Kerr, G.T. "New
    Developments in Zeolite Science Technology". Proc. 7th
    Int. Zeolite Conf. (Eds. Y. Murakami, A. Iijima and
    J.W. Ward), Kodansha Ltd., Tokyo 1986, p. 677.
21. Ballmoos, R. von and Meier, W.M. Nature 1981, 289,
    782; Ballmoos, R. von, Gubser, R. and Meier, W.M.
    Proc. 6th Int. Zeolite Conf. (Eds. D. Olson and
    A.Bisio) Butterworths 1983, p. 803; Chao, K. and
    Chern, J. Zeolites 1988, 8, 82.
22. Febre, R.A. le, Jansen, J.C. and Bekkum, H. van.
    Zeolites 1987, 7, 471; This Thesis, Chapters II and
    III.
23. Steinike, U. Kretzschmar, U., Ebert, I., Hennig, H.P.,
    Barsova, L.I. and Jurik, T.K. Reactivity of Solids
    1987, 4, 1.
24. Krylov, O.V. React. Kinet. Catal. Lett. 1987, 35, 315.
25. Dollish, F.R. and Hall, W.K. J. Phys. Chem. 1967, 71,
    1005.
26. Wierzchowski, P., Garbowski, E.D. and Vedrine, J.C. J.
    Chim. Phys. 1981, 78, 41.
27. Huizinga, T., Scholten, J.J.F, Wortel, Th.M. and
    Bekkum, H. van. Tetrahedron Letters 1980, 21, 3809.
28. Slinkin, A.A., Kucherov, A.V., Kondratyev, D.A.,
    Bondarenko, T.N., Rubinstein, A.M. and Minachev, Kh.M.
    J. Mol. Catal. 1986, 35, 97.

29. Kucherov, A.V., Slinkin, A.A., Kondratyev, D.A., Bondarenko, T.N., Rubinstein, A.M. and Minachev, Kh.M. J. Mol. Catal. 1986, 35, 107.

30. Clarke, J.K.A., Darcy, R., Hegarty, B.F., O'Donoghue, E., Amir-Ebrahimi, V. and Rooney, J.J. J. Chem. Soc., Chem. Commun. 1986, 425.

31. Slinkin, A.A. and Kucherov, A.V. Transl. (ENG) Kinetics and Catalysis 1983, 811.

32. Shih, S. J. Catal. 1983, 79, 390.

33. Matsumura, Y., Hashimoto, K. and Yoshida, S. J. Chem. Soc., Chem. Commun. 1984, 1447.

34. Matsumura, Y., Hashimoto, K. and Yoshida, S. J. Chem. Soc., Chem. Commun. 1987, 1599.

35. Chang, P.J. and Curthays, G. Zeolites 1981, 1, 41.

36. "Heterogeneous catalytic reactions involving molecular oxygen". Stud. Surf. Sci. Catal., 13 (Eds. G.I. Golodets and J.R.H. Ross), Elsevier Amsterdam 1983, a) p. 500; b) p. 470.

37. Wang, L., Eguchi, K., Arai, H. and Seiyama, T. Appl. Catal. 1987, 33, 107.

38. "The chemistry of heterocyclic compounds, vol. 14. Pyridine and its derivatives, part one". (Ed. A. Weissberger), Interscience Publishers Inc., London 1960.

39. Weissermehl, K. and Arpe, H.J. "Industrielle Organische Chemie, Bedeutende Vor- und Zwischenprodukte". Verlag Chemie, Weinheim 1976, p. 157.

40. "Ullmann's Enzyklopadie der Technischen Chemie", Band 19, 4e Aufl. Verlag Chemie, Weinheim 1980, p. 591.

41. "Kirk-Othmer's Encyclopedia of Chemical Technology", Vol. 19, John Wiley & Sons, New York 1978, p. 453.

42. Wesdemiotis, C., Danis, P.O., Feng, R., Tso, J. and McLafferty, F.W. J. Am. Chem. Soc. 1985, 107, 8059.

43. Harada, K. "The chemistry of the carbon nitrogen double bond" (Ed. S. Patai), Interscience Publishers, New York 1970, p. 262.

44. Camia, M., Gherardi, P., Gubitosa, G., Petrera, M. and Pernicone, N. Proc. 8th Int. Cong. on Catal. 1984 (publ. 1985), 4, Vol. IV, p. 747.

45. Aue, D.H., Webb, H.M. and Bowers, M.T. J. Am. Chem. Soc. 1972, 94, 4726.

46. Parker, L.M., Bibby, D.M. and Meinhold, R.H. Zeolites 1985, 5, 384.

CHAPTER VII

AN EXPLORATORY STUDY OF THE HYDROXYALKYLATION OF PHENOL

WITH GLYOXYLIC ACID OVER VARIOUS Al-CONTAINING CATALYSTS.

GLYOXYLATE AS A NEW Al-EXTRACTING AGENT

ABSTRACT

The hydroxyalkylation of phenol with glyoxylic acid over
various Al-containing catalysts in aqueous medium has been
studied. The catalytic activity of Al-containing solid
materials could be traced back to dissolved Al^{III}-ions which
catalyze the reaction of phenol and glyoxylic acid towards
hydroxymandelic acid in a homogeneous way. Dealumination of
zeolite Na-Y by aqueous glyoxylic acid has been studied. An
initial 'zeolite concentration' effect on the Si-concen-
tration in the solution followed by the establishment of an
equilibrium in Si and Al concentrations was observed during
the reaction. Addition of Cu^{II} or phenol to the initial
solution influences the maximum Al-concentration in the
extraction liquid.

INTRODUCTION

The alkylation of aromatic compunds was first described by
Friedel and Crafts (1) while performing an experiment on the
halogenation of benzene under the influence of aluminum
chloride. Nowadays, reactions of the Friedel-Crafts type
are associated with various acid-catalyzed alkylations and
acylations of aromatic and aliphatic compounds (2).

In this Chapter the reaction of phenol and glyoxylic acid
(3) towards hydroxymandelic acid will be considered. It is
known in literature that phenol can react with glyoxylic
acid under acidic as well as under basic conditions.
Generally, acid catalyzed reactions of phenol with aldehydes

or ketones result in bisphenol-type products (see for
example reference 4), which are, amongst others, good
starting materials for the production of epikote resins and
polycarbonate polymer materials. Both Hubacher (5) and the
Nippon Synthetic Chemical Industry Co. Ltd. (6) describe the
acid catalyzed reaction between phenol and glyoxylic acid,
resulting in bis(4-hydroxyphenyl)acetic acid. Here, the
intermediate compound 4-hydroxymandelic acid enters into a
fast consecutive reaction.
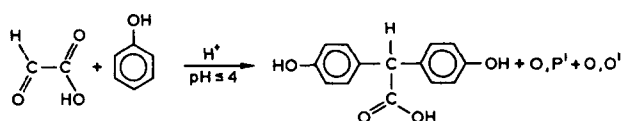
In contrast to the acid-catalyzed reactions, reactions in
alkaline media give 4- and 2-hydroxymandelic acid, the first
compound being an intermediate in the synthesis of
amoxycillin and cephalosphorin type antibiotics and the
latter compound being an intermediate in the synthesis of
some sequestering agents.
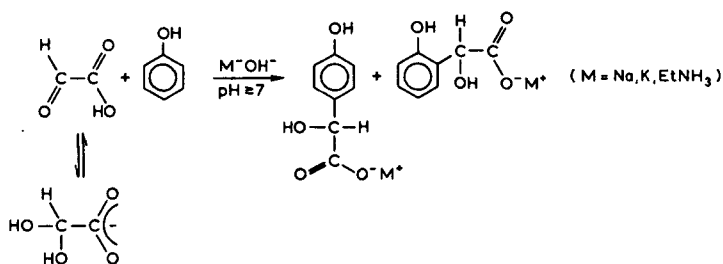
The first preparation of 4-hydroxymandelic acid in an
aqueous alkaline environment has been reported by Riedel-de
Haen (7) in 1936. A disadvantage of the reaction conducted
at high pH is the sensitivity of aldehyde derivatives
towards the Cannizzaro reaction (8): upon heating in water
at pH>7, glyoxylic acid reacts towards oxalic acid and
glycolic acid. This side reaction can be suppressed by
carrying out the reaction at room temperature but then
excessive reaction times are required for the hydroxy-
alkylation. However, Schouteeten and Christidis (9)
describe a procedure using higher temperatures and a

relatively short reaction time at pH>10, yielding mainly
4-hydroxymandelic acid (p/o ratio = 6).

In a search for a new and milder procedure to prepare 4-
(or p-)hydroxymandelic acid, we explored the use of zeolites
as a shape-selective catalyst for this reaction, considering
the well known para-selectivity of medium pore zeolites for
alkylation reactions of aromatics. Also the clay mineral
Hydrotalcite. with basic interlayers (CO_3^{2-}, OH^-) has been
included in this study. However, the results obtained
induced us to focus our attention on the dealuminating
properties of glyoxylic acid as well as on the reaction
towards hydroxymandelic acid, homogeneously catalyzed by the
extracted Al-ions. Both aspects, the reaction towards
hydroxymandelic acid and the exploratory investigation
regarding the dealumination of zeolite Na-Y are presented in
this Chapter.

EXPERIMENTAL

Catalysts: The molecular sieve materials HZSM-5 (Si/Al =
36), Silicalite-1 and HNu-10 (Si/Al = 45) were synthesized
according to procedures described in Chapters III and IV.
The zeolites H-Mordenite (large pore; Zeolon 100, Norton)
and Na-Y (SK40, Union Carbide) were commercially available.
RE-Y (Rare Earth exchanged Y) and amorphous silica-alumina
cracking catalyst LA-LPV (13wt% Al_2O_3) were obtained from
AKZO Chemie. Amsterdam. H-Y was obtained by exchanging Na-Y
with a 1M NH_4NO_3 solution (10ml/g) at 80°C, followed by
calcination at 500°C. NaCu-Y was prepared similarly using a
0.1M $CuCl_2$ solution (10ml/g zeolite).
The clay mineral Hydrotalcite, $[Mg_4Al_2(OH)_{12}]CO_3$, was
prepared as follows (10). Two solutions were made: The first
contained 0.30 mol $Mg(NO_3)_2.6H_2O$ and 0.15 mol $Al(NO_3)_3.9H_2O$
in 700 ml H_2O while the other solution contained 1.13 mol
$Na_2CO_3.0H_2O$ in 1050 ml H_2O. In a 2L beaker 300 ml H_2O was
heated up to 80°C. By addition of a small part of the Na_2CO_3
solution the pH of the solution was brought to 8. Then,
under good stirring both the nitrate and carbonate solutions

were added dropwise to the solution. During the addition, which took about 1 hour, the pH as well as the temperature were kept constant. Subsequently the suspension was stirred for another 30 minutes at 80°C. The precipitate was filtered off over a Buchner funnel, washed with 2 litres of water of 80°C and dried overnight at 80°C.

Phenol alkylation: Experiments involving the preparation of hydroxymandelic acid were performed as follows: an aqueous 0.5M glyoxylic acid (Merck) solution and phenol were mixed in a 1:1 molar ratio. The Al-containing catalyst (2g/100ml) was added and the reaction mixture was stirred. For the homogeneous reactions in the presence of Al^{III} or Mg^{II} the molar ratio glyoxylic acid:M^{n+} was 3:1. NaOH was added to adjust the desired pH value. Details regarding pH, reaction time and temperature are presented in Table 1. Stirring was performed during the reaction.

Dealumination reaction: A 0.20M glyoxylic acid solution, adjusted to pH=3 with NaOH, was used for all experiments. For every experiment 50 to 150 ml of this solution was placed into a water-thermostatted glass reaction vessel equipped with a reflux unit and a magnetic stirrer bar. The temperature of the reaction vessel was kept at 70°C for all dealumination reactions. An amount of Na-Y zeolite was added to the hot solution at t=0. Samples (1 to 2 ml) were taken by using a hypodermic syringe and filtered over a 0.45 μm micropore filter (Gelman Sciences) and subsequently stored in small sample flasks in a refrigerator, awaiting further analyses.

Analyses: Determination of the hydroxyalkylation products was performed by HPLC analysis, using a Waters Associates chromatography pump M-45, differential refractometer RI 401 and a Spectraphysics SP4100 integrator. The following conditions were employed: column C18 Nucleosil RCM 100 Module; eluent $MeOH/H_2O/TFA$ 10/90/0.1 and RI detection. The metal ion concentrations in the aluminum extraction liquids were determined by AAS on a Perkin Elmer 460 Atomic Absorption Spectrophotometer.

RESULTS AND DISCUSSION

- Phenol hydroxyalkylation

   The experimental results are summarized in Table 1. In the
absence of a catalyst hydroxymandelic acids are formed at
high pH values only. The zeolites with a high Si/Al-ratio
(>10) as Silicalite-1, HZSM-5, HNu-10 and with an
intermediate Si/Al-ratio as H-Mordenite show almost no
catalytic effect. They even seem to suppress the reaction
at pH=6.0 when compared to the reaction without catalyst.
The low Si/Al (<5) materials as zeolite Y and LA-LPV as well
as the clay Hydrotalcite did catalyze the hydroxyalkylation
reaction but were also found to dissolve partly during the
experiments. This indicated that dissolved aluminum[III]
coordination compounds might be responsible for the
formation of hydroxymandelic acid. Tests using $Al(NO_3)_3$ as
homogeneous catalyst, confirmed the extraction/reaction
idea.

   Meanwhile it has been ascertained by de Vos Burchart et
al. (11) that the zeolites ZSM-5, Silicalite-1. Nu-10 and
Mordenite are essentially unaffected by glyoxylic acid under
the conditions of Table 1.

   The difference in results obtained for LA-LPV at low and
medium pH values (although carried out at 100°C) indicate a
pH-dependence of the o/p-ratio. The dependence of the o/p
ratio upon the pH as well as the use of other multivalent
metal ions as homogeneous catalyst in the alkylation of
phenol by glyoxylic acid (cf. Table 1 the results obtained
with NaCu-Y and H-Y) were investigated subsequently in more
detail by Hoefnagel et al. (12). Figure 1 illustrates the
product composition vs. time of a reaction mixture
containing Ga^{III} as the homogeneous catalyst at pH 5 and
100°C. Also some disubstituted products are observed. For
Al^{III}, Cu^{II} and Zn^{II} as the catalyst the influence of the pH
on the o/p-ratio is depicted in Figure 2.

Table 1. Reaction conditions and results for the reaction
of phenol (0.5M) and glyoxylic acid (0.5M) towards 4- and
2-hydroxymandelic acid.

Catalyst	pH	Reaction time (min)	temp (°C)	Conversion phenol (%)	o/p ratio
---	2.2	120	70	0	-
---	6.0	180	100	7.8	0.41
---[1]	>10	30	70	80.0	0.11
Silicalite-1	6.0	180	100	0	-
HZSM-5	2.4	30	70	0.5	0.0
HZSM-5	6.0	180	100	1.3	0.43
HNu-10	6.0	180	100	1.8	0.47
H-Mordenite	2.6	30	70	1.0	1.08
H-Mordenite	6.0	180	100	1.8	0.39
Na-Y[2,3]	3.0	145	70	17.4	9.00
H-Y[2]	6.0	180	100	21.8	2.13
NaCu-Y[2,4]	6.0	180	100	66.5	1.69
RE-Y[2]	6.0	180	100	12.6	1.94
LA-LPV[2]	2.6	30	70	20.2	9.00
LA-LPV[2]	6.0	180	100	43.3	3.04
Hydrotalcite[2]	2.1	30	70	44.8	10.11
Hydrotalcite[2]	5.2	30	70	45.2	0.89
Hydrotalcite[2]	7.6	30	70	55.3	0.64
$Al(NO_3)_3$	2.8	30	70	49.9	5.43
$Mg(NO_3)_2$	1.3	30	70	0	-

[1] Reaction according to Schouteeten and Christidis (9).
[2] Catalyst partly dissolved during rection. [3] Molar
ratio (0.2M) glyoxylic acid:phenol 1:3.3. [4] After the
reaction Cu(II) visible in solution.
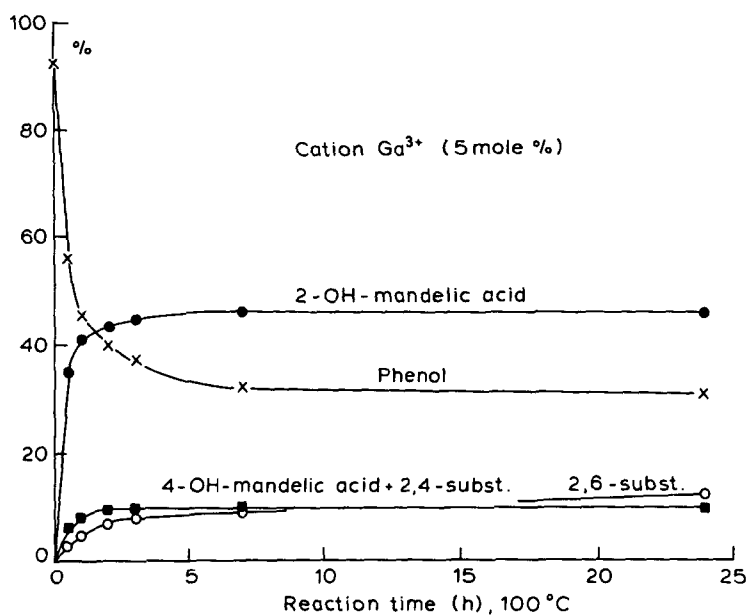
Figure 1. The homogeneously catalyzed hydroxyalkylation of phenol (0.5M) by glyoxylic acid (0.5M) in water with Ga^{III} (0.05M) as the catalyst. Temperature 100°C, pH 5. x = amount of phenol present. Selectivities towards (●) 2-hydroxymandelic acid, (■) 4-hydroxymandelic acid + 2,4-subst. and (o) 2,6 dihydroxymandelic acid.

- Dealumination of zeolite Na-Y by glyoxylic acid

    A literature survey on the dealumination by low molecular weight organic acids revealed the following:

    Dealumination of zeolitic materials by glyoxylic acid has not been described before. By contrast the use of the somewhat related dicarboxylic system, oxalic acid, for the dealumination of zeolites has been reported in the literature (13-15). Also data can be found regarding the association constants of Al-oxalate coordination compounds. For example, Sjoeberg and Oehman (16) describe the equilibria of aluminum^{III}-oxalic acid-hydroxide systems. By means of potentiometric and ^{27}Al NMR measurements these authors determined the successive formation of the complexes [Al(oxalate)$_n$]$^{3-2n}$ with n=1,2,3. These mononuclear
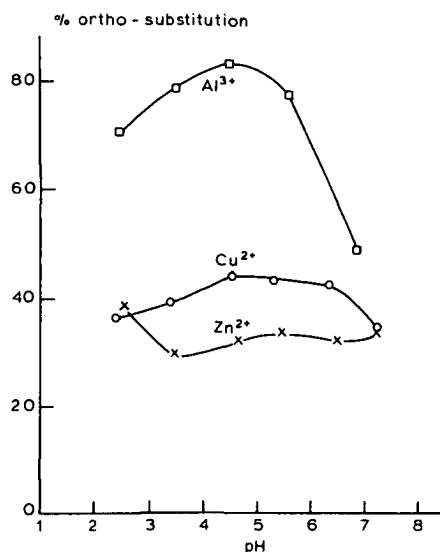
Figure 2. The influence of the pH on the hydroxyalkylation reaction of phenol (0.5M) with glyoxylic acid (0.5M) catalyzed by Zn^{II} (x), Cu^{II} (o) and Al^{III} (□) (0.025M) in water, 100°C.

complexes are found to predominate. Besides the formation of the polynuclear mixed hydroxo-complexes $Al_3(OH)_3^-$ (oxalate)$_3$ and $[Al_2(OH)_2(oxalate)_4]^{4-}$ were established. These authors also describe the increase in 'solubility' of clay minerals such as kaolinite when low concentrations (10^{-5} mol/l) of ligands (L) such as citric acid or oxalic acid are present. For kaolinite this increase is restricted to solutions with 5<pH<9 for oxalic acid and with 4<pH<7 for citric acid and is ascribed to the formation of AlL and AlL$_2$ complexes.

For zeolites Basinskii et al. (13) as well as Urbanovich et al. (14) report the use of oxalic acid in the dealumination of Y-type zeolites. Basinskii et al. investigated the decrease in catalytic activity due to dealumination of NaLa-Y and NaCa-Y by oxalic acid under reflux conditions. Urbanovich et al. treated an ultrastable zeolite Na-Y with 0.05M oxalic acid to remove intrazeolitic (non-framework) Al-species, present after hydrothermal treatments at 550 and 830°C.

Another application is claimed by McVicker et al. (15) in
which metal contaminations present in hydroconversion
catalysts (Al_2O_3, $Al_2O_3-SiO_2$ or zeolite) are removed by
contacting the catalyst at 0-100°C with buffered 0.0001-5M
oxalate solutions (pH 3-10) without dissolving the support.

In view of the results obtained during phenol hydroxy-
alkylation zeolite Na-Y (Si/Al=2.8) was selected to study
the dealuminating properties of glyoxylic acid. The
influence of the glass reaction vessel upon the Si and Al
measurements may be neglected as judged from the following
experiment. A blank reaction under standard conditions in
the absence of zeolite Na-Y shows no increase in Si and Al
concentration after 300 minutes.

The results of a series of dissolution/extraction experi-
ments with different initial amounts of Na-Y are shown in
Figures 3 and 4. It may be noted that complete dissolution
of 1 g Na-Y into 1L of 0.2M glyoxylic acid would result in a
maximum value of 4.1 mmol Al and 7.4 mmol Si (131.6 and
238.7 ppm, respectively).

As can be seen in Figures 3 and 4 both Si and Al are
removed from the zeolite material. Remarkable is the large
increase in Si-concentration at the start of the reaction,
which bears an almost linear relation to the initial 'Na-Y
concentration'. For Al the concentration in solution rises
rapidly to about 370 ppm. At the end of the reaction a
maximum equilibrium of 470 ppm Al seems to be established.
For Si an equilibrium concentration around 200 ppm is
observed, giving a maximum (Si + Al) concentration of about
670 ppm at 70°C and pH=3 after 300 minutes reaction time
(which accounts for a (Si + Al):glyoxylic acid ratio of
1:12.8) showing glyoxylic acid still to be in large excess.
It may also be noted that the pH of the solution does not
change significantly during the reaction. At the start of
the reaction the pH rises to 3.2 and at t=300 minutes a
value of 3.4 is observed.
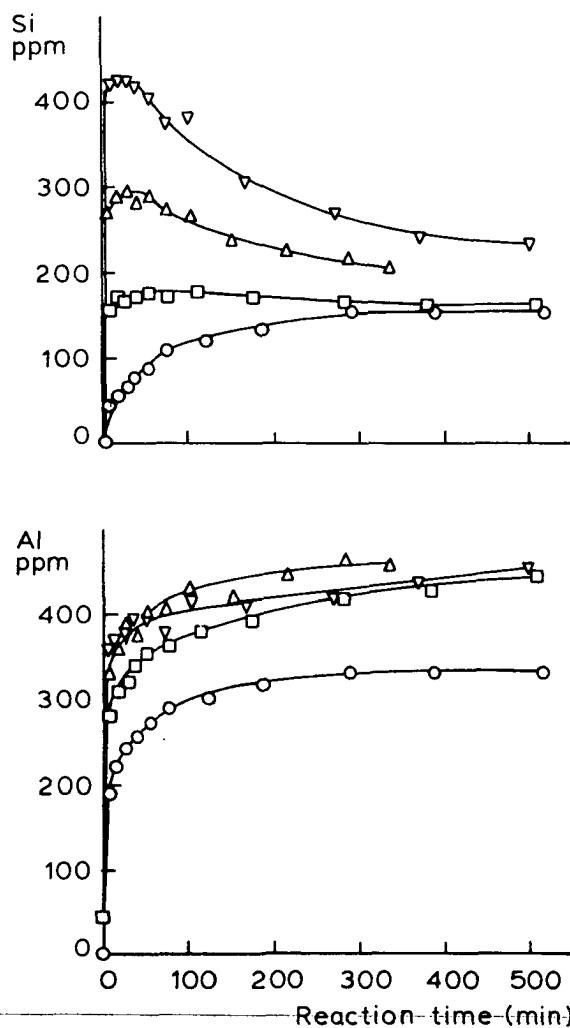
Figure 3. Si and Al concentration versus time of the 0.2M glyoxylic acid solution during dealumination of zeolite Na-Y at 70°C and pH 3. Influence of the initial amount of Na-Y. o=4.8, □=19.7, △=40.6 and ▽=80.0 g Na-Y/l.
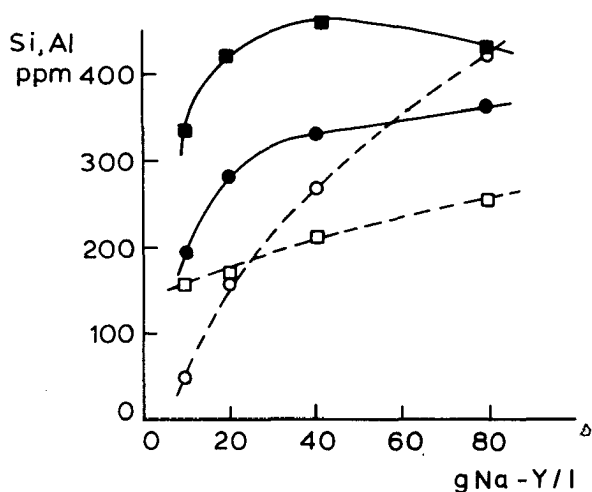
Figure 4. Effect of the initial amount of Na-Y upon the Al (●,■) and Si (o,□) concentration in solution after a reaction time of 6 (●,o) and 300 (■,□) minutes. Conditions: 0.2M glyoxylic acid, pH 3, 70°C.

A comparison with similar dissolution experiments using nitric acid (Table 2) shows that nitric acid is not extracting Al from zeolite Na-Y whilst the Si-dissolution seems to be pH-dependent. For the high concentrations of Si observed in the reactions with glyoxylic acid as extractant. having an initial Na-Y concentration of 40.6 and 80.0 g/l, a possible explanation may be the presence of small amounts of amorphous silica-rich material in the Na-Y zeolite sample.

The decrease in Si concentration in solution measured at Na-Y concentrations above 20 g/l might be explained by the observed flocculation of amorphous material (presumably silica-alumina) during the extraction reaction. The Al-curves do not show such a maximum and are all similar in shape (Figures 3 and 4). De Vos Burchart et al. (11) observed no significant decrease in glyoxylic acid concentration during the reaction excluding precipitation of glyoxalate compounds. Therefore it can be assumed that a maximum Si and Al concentration is allowed in the solution. After this equilibrium has been reached extraction from Si

Table 2. Results for dissolution/extraction experiments
using glyoxylic acid or nitric acid. The initial 'Na-Y
concentration', the acid used, the initial pH and the
reaction time are given below. Reaction temperature was
70°C.

19.7 g Na-Y/l, 0.2M Glyoxylic acid

pH = 3

Reaction time (min)	pH	ppm Si	ppm Al
6	3.3	156	280
17	3.3	171	312
280	3.4$^\triangle$	168	418

25.3 g Na-Y/l, HNO_3[1]				21.1 g Na-Y/l, HNO_3[2]			
pH = 3[1]				pH = 6[2]			
Reaction time (min)	pH	ppm Si	ppm Al	Reaction time (min)	pH	ppm Si	ppm Al
5	3.4[1]	51	<10	6	6.5	<10	<10
10	2.9[1]	82	<10				
235	3.1[1]	132	<10	347	6.9	22	<10

---

[1] Diluted HNO_3 used. After zeolite addition extra HNO_3
added during the course of the reaction to mantain pH 3.
[2] Diluted HNO_3 (pH=3) used as starting material. After
Na-Y addition the pH rose to 6.5.

or Al from the zeolite material causes precipitation of
material of low solubility.

   The relatively high phenol conversion observed when using
NaCu-Y as the catalyst (cf. Table 1) might be due to
homogeneous catalysis by Al^{III} and Cu^{II} ions and induced us
to investigate the effect of Cu^{II} present in the solution or
in the zeolite upon the progress of dealumination. For this
purpose an experiment was carried out in which zeolite Na-Y
(21.4 g/l) was subjected to a solution containing Cu^{II} as
well as 0.2M glyoxylic acid and pH 3 initially. The initial
molar Cu/Al ratio was 0.78. Figure 5 shows the results.
First rapid Cu^{II}-Na^{I} ion exchange is observed, causing the
Cu concentration to decrease below 2300 ppm. The addition
of Cu^{II} has hardly any effect on the Si-extraction when
compared to the treatment of a sample having a similar Na-Y

concentration (19.7 g/l) in the absence of Cu^{II}. The amount
of dissolved Al however, increases substantially in the
presence of Cu^{II}. During zeolite dealumination the exchanged
Cu^{II} cations return again in the solution indicating the
loss of zeolitic anionic sites. The observed decrease in Cu
concentration after 150 minutes might be due to newly
created Cu-binding-sites in the deposited amorphous
silica-alumina.

   In order to study any effect of the presence of phenol in
the dealumination of Na-Y by glyoxylic acid, a reaction
mixture, having a Na-Y concentration of 13.5 g/l and a
phenol:glyoxylic acid (0.2M) molar ratio of 3.3:1, has been
examined. By comparing the amount of dissolved Si (see
Figure 6) with experiments in which phenol is absent it can
be concluded that the Si-extraction is not influenced by the
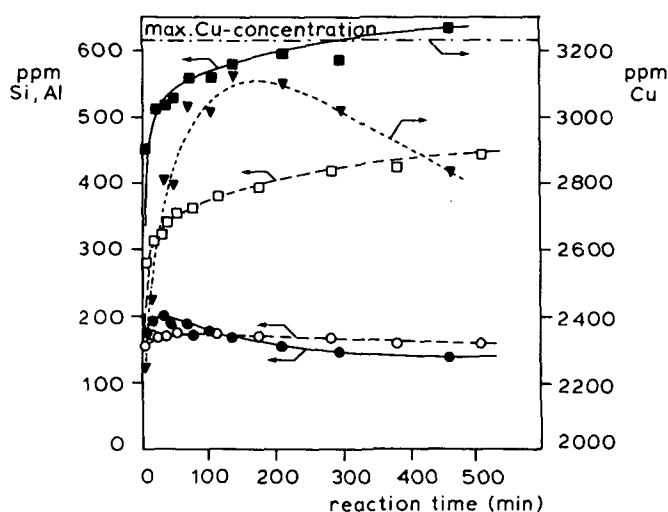
Figure 5. Effect of the addition of Cu^{II} (added as $CuCl_2$) to
the initial reaction mixture on the dealumination of Na-Y by
glyoxylic acid. ●,o = Si concentration; ■,□ = Al concen-
tration for a Cu containing solution (●,■) having an initial
Na-Y concentration of 21.4 g/l and reference solution (o,□)
without Cu^{II}, with an initial Na-Y concentration of 19.7
g/l. ▼ = Cu concentration in the solution; —·—· = initial
Cu concentration.

addition of phenol. By contrast, an increase in
Al-extraction is observed. The phenol conversion towards
hydroxymandelic acid seems to be almost complete after 500
minutes. The o/p ratio of the hydroxymandelic acid formed
was 8.9 and remained constant during the reaction period.

The fact that no effect on the dealumination is observed
during the progress of the phenol alkylation reaction might
be explained by the observations by de Vos Burchart et al.
(11) that 4-hydroxymandelic acid as well as glyoxylic acid
is capable of extracting Si and Al from zeolites.

Hoefnagel et al. (11) propose that metal complexes of
glyoxylate are the key intermediates in the phenol hydroxy-
alkylation reactions. As shown on the next page the ortho
substitution is assumed to involve coordination of both
organic reactants to the metal cation catalyst, explaining
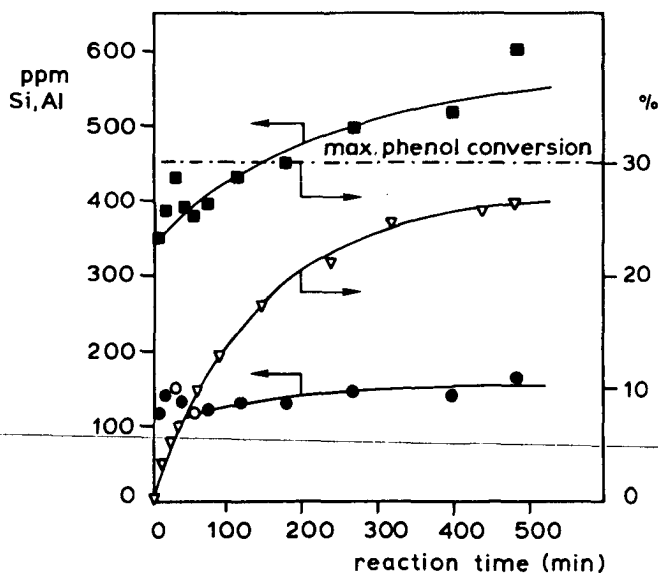
Figure 6. Effect of the addition of phenol to the initial
reaction mixture on the dealumination of Na-Y by glyoxylic
acid. ● = Si concentration; ■ = Al concentration for the
phenol containing solution; ∇ = phenol conversion; —·—· =
maximal phenol conversion.

the high o/p ratio. Though phenol coordination is
relatively weak, ionization of coordinated phenol will
result in a highly active system. Cations with a high
charge density are assumed to be the most effective catalyst
for this reaction.

p-substitution of phenol
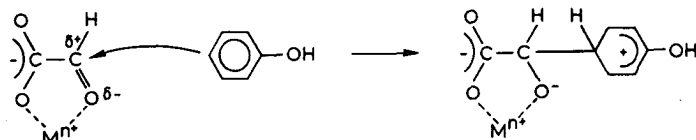
o-substitution of phenol
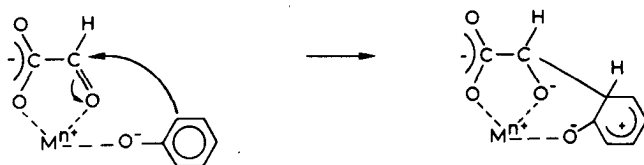
   In conclusion, our experiments show the ability of
glyoxylic acid to extract Al (+ Si) from zeolitic or related
materials with a low Si/Al-ratio. A detailed reaction
mechanism for this dealumination can not be presented at
this moment. Further investigations regarding the
dealumination are in progress in this laboratory (11).

ACKNOWLEDGEMENTS

REFERENCES

1. Friedel. C. and Crafts. C. Compt. Rend. 1877. 84,
    1392.
2. Olah, G.A. "Friedel-Crafts and Related Reactions",
    Vol. I-II, Interscience Publ.. New York, 1963.

3. Trivial names used: glyoxylic = oxoacetic: mandelic =
    α-hydroxybenzeneacetic; glycolic = hydroxyacetic.
4. Pizzi, A. Horak, R.M., Ferreira. D. and Roux, D.G. J.
    Appl. Polymn. Sc. 1979, 24, 1571.
5. Hubacher, M.H. J. Org. Chem. 1959, 24, 1949.
6. JP 8155337 (1981) or Chem. Abstr. 95:203534m.
7. Riedel-de Haen, A.G. DE 621.567 (1936).
8. Boettinger, C. Chem. Ber. 1880, 13, 1931.
9. Schouteeten, A. and Christidis, Y. DE 2944295 (1982).
10. Doesburg et al., E.B.M. "Handleiding voor het 3e jaars
    project 'Bereiding van Nikkel/alumina katalysatoren'",
    Delft University of Technology, Delft 1984.
11. Vos Burchart, E. de, Febre, R.A. le and Bekkum, H.
    van. To be published.
12. Hoefnagel, A.J., Peters, J.A. and Bekkum, H. van.
    Recl. Trav. Chim. Pays-Bas 1988, 107, 242.
13. Basinskii, V.I., Kashkovskii, V.I., Piskun, L.A. and
    Bavika, N.P. Nefteprerab Neftekhim. (Kiev) 1987, 32,
    14 or Chem. Abstr. 107:220116k.
14. Urbanovich, I.I., Russak, M.F., Kozlav, N.S.
    Zareiskii, M.V. and Akulich, N.A. Vestsi Akud. Navuk
    BSSR, Ser. Khim. Navuk 1979, 45 or Chem. Abstr.
    92:79131x.
15. McVicker, G.B.. Carter, J.L.. Murrell. L.L.. and
    Ziemiak, J.J. US 4522928 (1985); DE 3337619 (1984).
16. Sjoeberg, S. and Oehman, L.O. J. Chem. Soc., Dalton
    Trans. 1985, 2665.

CHAPTER VIII

THE GEOMETRY OF TETRAPROPYLAMMONIUM IONS IN CRYSTAL

LATTICES. CRYSTAL AND MOLECULAR STRUCTURE OF BIS-(TETRA-N-

PROPYLAMMONIUM)-BIS(μ-2-CHLORO)-TETRACHLORO-DI-COPPER(II)

ABSTRACT

The conformation of the tetrapropylammonium (TPA) ion in
crystal lattices is reviewed. In the crystal structures
examined two different TPA conformations occur regularly,
both having CCNC torsion angles around 180, 60 and $-60°$.
Eclipsed conformations (CCNC torsion angles of 0, 120 and
$-120°$) are observed exceptionally. A relation between shape
and size of the anion and the conformation of TPA is
proposed. When occluded in the zeolite ZSM-5 TPA exhibits
an energetically unfavourable conformation which is probably
due to interactions of the terminal methyl groups with those
of neighbouring TPA ions.
$(N(C_3H_7)_4)_2Cu_2Cl_6$. $M_r=712.54$. triclinic, P1. a=9.369(1).
b=9.352(1). c=11.866(2) A. $\alpha=106.45(1)$. $\beta=100.05(1)$,
$\gamma=113.30(1)°$. V=866 A^3, Z=1. $D_x=1.37$ g/cm^3, $\lambda(MoK\alpha)=0.71069$
A, $\mu=1.75$ mm^{-1}, F(000)=374. T=290 K. R=0.038 for 3252
observed reflections. The structure consists of dimeric
Cu_2Cl_6 units. Each copper atom shows a distorted
tetrahedral coordination to four chlorine atoms. Both
tetrahedra are linked by sharing an edge.

INTRODUCTION

Since the introduction of the tetrapropylammonium (TPA)
ion as a template for the synthesis of zeolite ZSM-5 (1) its
structure directing role is under discussion (2-4). In
zeolite synthesis TPA. as well as other tetraalkylammonium
ions. seems to direct the topology of the framework and to

stabilize it when formed.

The synthesis of a ZSM-5 single crystal. large enough for
a single crystal X-ray structure determination. has been
described by van Koningsveld et al. (5). In this article
the ZSM-5 framework structure as well as the location and
conformation of the TPA ions are determined accurately and
compared with structural data of TPA-ZSM-5 crystal
structures reported earlier (6-8).

Molecular mechanics calculations on the conformations of
4,4-dipropylheptane (tetrapropylmethane. structural
isomorphous to TPA) by van de Graaf ,(9). show that
4,4-dipropylheptane posesses two structurally different
favourable conformations. Both conformations are very close
in steric energy. having a difference of only 0.24
kcal/mole.

The two essentially iso-energetic conformations can be
conveniently considered by examining the six heptyl chains
present in the system and by numbering the four propyl
grouos of 4,4-dipropylheptane clockwise 1-4.
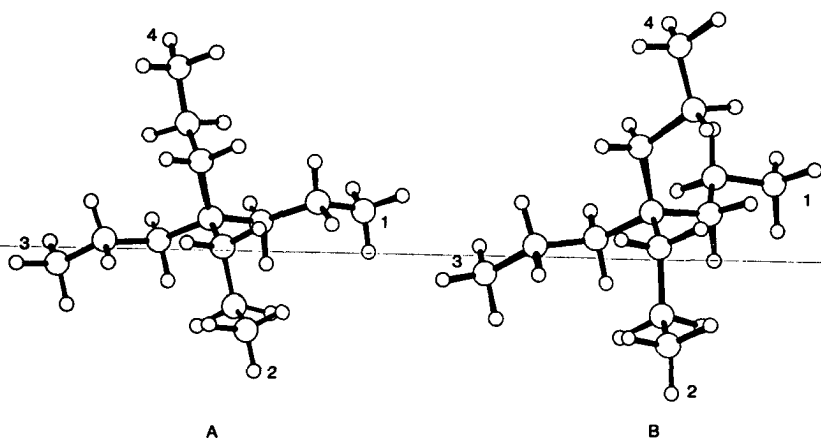
Figure 1. The two energetically favourable conformations of
4,4-dipropylheptane as calculated by van de Graaf (9). The
small circles represent H-atoms.

In conformation A (Figure 1a) two heptyl chains (1-3 and 2-4) are in an all-trans conformation. whereas in each of the other four heptyl chains (1-2. 1-4. 2-3 and 3-4) two gauche butane interactions are present. In conformation B (Figure 1b) all-trans oriented heptane chains are absent: in two heptyl chains (1-4 and 2-3) two gauche interactions are present. whereas in the other four heptyl chains one gauche orientation can be observed. Thus conformations A and B posess the same total (8) of gauche interactions.

It may be noted that conformations around C_2-C_3 and C_4-C_5 are always trans.

The conformations of TPA (as reported by van Koningsveld et al. (5)) in ZSM-5 deviate from the ideal conformations A and B described above. To see if the conformations as described for 4.4-dipropylheptane also exist for TPA and to find out if deviations as reported for TPA-ZSM-5 (%) occur more frequently. a literature search on TPA-containing crystal structures has been undertaken.

As this literature search revealed a possible correlation between the size of dimeric anionic compounds and the TPA-conformation. the crystal structure of the title compound has been solved because we expected it to interpolate in the series of known (dimeric) structures.

EXPERIMENTAL

- $(TPA)_2$-Cu_2Cl_6 preparation and structure refinement

A hot solution of 0.1M TPA-Cl in 96% ethanol was added slowly to an equimolar amount of $CuCl_2$.$2H_2O$ dissolved in 96% ethanol. Yellow-brown crystals of $(TPA)_2$-Cu_2Cl_6 were grown by slow evaporation at room temperature. Approximate crystal size 0.15 x 0.20 x 0.25 mm. In a similar way crystals of TPA-Br and $CuCl_2$.$2H_2O$ were prepared. The latter structure was also solved by Patterson and Fourier techniques. However. this analysis will not be reported because of disorder of the Br- and Cl-atoms.

A single crystal of the title compound was measured on an
Enraf Nonius CAD-4 diffractometer. Mo-Kα radiation,
monochromated by graphite, was used for the determination of
the unit cell parameters as well as for measuring the
reflection intensities. The cell parameters were calculated
from setting angles of 25 reflections with $15 < \theta < 19°$. Range
of hkl: $0 \to 12$, $-12 \to 11$, ± 15. θ_{max} = 28°. 4169 independent
reflections were measured. 3252 reflections with $I > 2.85\sigma(I)$
were used. $\omega/2\theta$ scan, scan width = 0.95 + 0.35$\tan\theta$,
max. recording time 120 s. $\sigma_{count}(I)/I < 0.02$ was requested in
a scan. Three reference reflections showed a decay of 2.0%;
a correction was applied. The data ware not corrected for
absorption.

The structure refinement was carried out using as start
positions the coordinates of the TPA-Br-CuCl$_2$ compound. The
structure proved to be isomorphous. A full-matrix
least-squares refinement was carried out on F with
anisotropic thermal parameters for all non-H atoms. The
H-atoms were located from the difference Fourier map and
refined with fixed isotropic thermal parameters set equal to
those of the parent C-atoms. The model converged with 3252
observations and 239 variables to R=0.038, wR=0.042, w=1,
S=1.13, $(\Delta/\rho)_{max}$=0.8 [z-value H(422)]. The final $\Delta\rho$ is less
than 0.60 eA^{-3} ($\sim$ at Cl(3) position). Scattering and
anomalous-dispersion factors for Cu and Cl were taken from
the International Tables for X-ray Crystallography (10).

All calculations were carried out on the Delft University
Amdahl 470/V7B computer using programs of the XRAY72-system
(11).

- TPA Geometry determination and definitions

To distinguish between the stable conformations as
calculated by van de Graaf (9) we name the TPA ion in which
two heptyl chains (1-3 and 2-4) are in an all-trans
orientation, conformer A (Figure 1a) and the other conformer
B (Figure 1b).
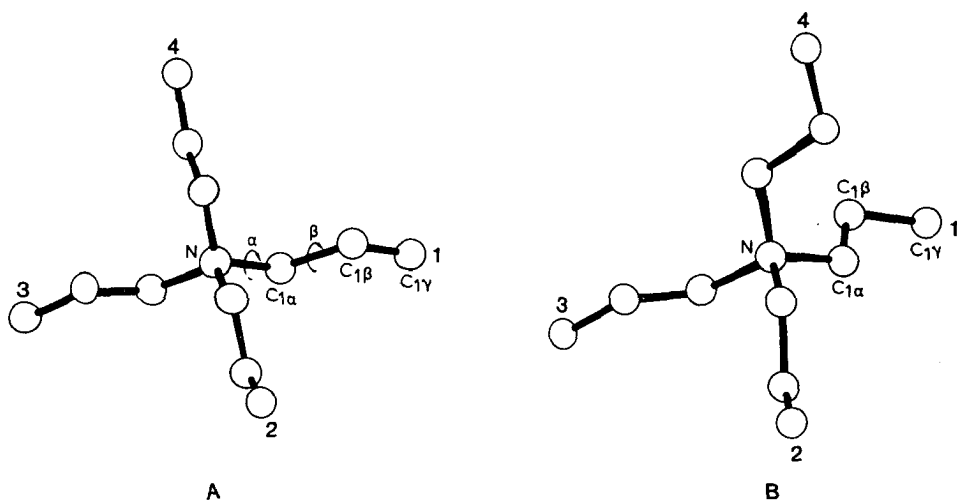
Figure 2. Definition of α. β and ϰ carbons in TPA. The numberings 1. 2. 3. 4 are related to the propyl chains and are used in Figure 3 and in Table 3.

The crystal structure parameters and atom coordinates for all TPA-containing compounds (except for ZSM-5 and the title compound) were obtained from the Cambridge Structural Database (12).

In refinement of the TPA-ZSM-5 structure Waser constraints were applied (5). These coordinates were used in defining the conformation of TPA.

The geometry of the TPA ions in the crystal structures described was determined by calculating the torsion angles of the $C_{i\alpha}$-N bonds as well as of the $C_{i\alpha}$-$C_{i\beta}$ bonds. The torsion angles α and β were calculated as the dihedral angle between the planes formed by the atoms $C_{i\alpha}$-N-$C_{j\alpha}$ and N-$C_{i\alpha}$-$C_{i\beta}$ for α, and by the atoms $C_{i\alpha}$-$C_{i\beta}$-$C_{i\gamma}$ and N-$C_{i\alpha}$-$C_{i\beta}$ for β (see Figure 2). The geometry is defined by twelve α and four β angles.
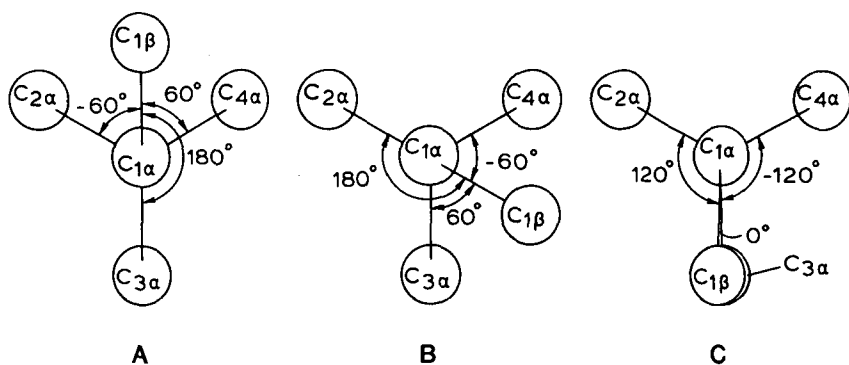
Figure 3. Newman projections of the $C_{1\alpha}$-N bond (a) of conformation A. (b) conformation B and of (c) an eclipsed conformation (E). The numbering is defined in Figure 2.

Figure 3 gives Newman projections of the $C_{1\alpha}$-N bond in conformation A (Figure 3a) of the $C_{1\alpha}$-N bond in conformation B (Figure 3b) and of the $C_{1\alpha}$ bond in case of an eclipsed conformation in the $C_{1\beta}$-$C_{1\alpha}$-N-$C_{3\alpha}$ fragment.

As the numbering of the propyl chains is not essential changes in α can not be used directly for the distinction between conformation A and conformation B. However, for conformation A the 12 α-values assigned to these chains are always pairwise equal when following any heptyl chain vice versa. This does not hold for conformation B. Here in just two of the six heptyl chains (i.c. 1-4 and 2-3, cf. Figure 2) such vice versa equality of α's is encountered.

RESULTS AND DISCUSSION

- $(TPA)_2$-Cu_2Cl_6 crystal structure

The final positional parameters are reported in Table 1. Relevant bond distances and angles are listed in Table 2. Lists of anisotropic temperature factors. H-atom positions and bonds involving H-atoms are included at the end of this Chapter. For reasons of clarity the numbering of the TPA atom parameters differs from those defined in Figure 2.

Table 1. Final fractional coordinates and equivalent iso-
tropic temperature factors (A^2) for the non-hydrogen atoms
with e.s.d.'s in parentheses. $U_{eq} = (U_{11} + U_{22} + U_{33})/3$.

Atom	x/a	y/b	z/c	U_{eq}
Cu	-0.05243(6)	0.55249(5)	0.37898(4)	0.0447(2)
Cu' [1]	0.05243(6)	0.44715(5)	0.62102(4)	0.0447(2)
Cl(1)	0.0653(1)	0.7919(1)	0.3553(1)	0.0695(4)
Cl(2)	-0.1838(1)	0.4189(1)	0.4964(1)	0.0593(3)
Cl(2')[1]	0.1838(1)	0.5811(1)	0.5036(1)	0.0593(3)
Cl(3)	-0.2566(2)	0.4076(2)	0.2028(1)	0.0679(4)
N	0.5101(3)	0.7967(3)	0.2414(3)	0.040(1)
C(11)	0.5423(5)	0.8059(5)	0.3736(3)	0.047(1)
C(12)	0.6135(7)	0.6964(6)	0.4048(5)	0.072(2)
C(13)	0.6390(6)	0.7246(6)	0.5390(4)	0.060(2)
C(21)	0.4359(5)	0.9145(5)	0.2362(3)	0.045(1)
C(22)	0.3980(7)	0.9347(7)	0.1153(4)	0.069(2)
C(23)	0.3168(7)	1.0473(7)	0.1231(5)	0.078(2)
C(31)	0.3954(5)	0.6170(5)	0.1470(4)	0.046(1)
C(32)	0.2286(6)	0.5316(6)	0.1608(5)	0.061(2)
C(33)	0.1250(7)	0.3617(7)	0.0536(6)	0.072(2)
C(41)	0.6686(5)	0.8519(5)	0.2084(4)	0.048(1)
C(42)	0.8013(6)	1.0304(6)	0.2866(5)	0.059(2)
C(43)	0.9388(6)	1.0774(7)	0.2347(6)	0.070(2)

[1] Cu' and Cl(2') are centrosymmetrically related to Cu
and Cl(2), respectively.

The structure contains a nearly symmetrical dimeric
dihalogen-bridged unit as depicted in Figure 4. The Cu atom
is coordinated by Cl in a distorted tetrahedron. The
bridging Cu-Cl distances are 2.321(1) and 2.307(1) A. The
distances of Cu to the terminal Cl atoms are equal within
experimental error (2.195(1) A). Similar TPA-containing
dimeric dihalogen-bridged units are found for example in
crystal structures of $(TPA)_2-Hg_2I_6$ (13), $(TPA)_2-Sb_2Cl_8$ (14)
and $(TPA)_2-Cu_2I_4$ (15).

   The TPA orientation in $(TPA)_2-Cu_2Cl_6$ is clearly in the A
conformation.

   The N...Cl(1) and N...Cl(3) contacts. with Cl(3) on x+1.
y, z are 4.588(4) and 4.892(4) A, respectively. The
difference between these distances (~0.3 A) might explain
the slight preference of Br to occupy the Cl(3) position as

Table 2. Intramolecular bond distances (A) and angles (°)
with e.s.d.'s in parentheses.

Cu − Cl(1)	2.196(1)	C(11) − C(12)	1.516(9)
Cu − Cl(2)	2.312(1)	C(12) − C(13)	1.497(8)
Cu − Cl(3)	2.194(1)	C(21) − C(22)	1.499(7)
Cu − Cl(2')[1]	2.306(1)	C(22) − C(23)	1.504(11)
N − C(11)	1.516(5)	C(31) − C(32)	1.511(7)
N − C(21)	1.527(7)	C(32) − C(33)	1.513(6)
N − C(31)	1.523(4)	C(41) − C(42)	1.507(5)
N − C(41)	1.528(6)	C(42) − C(43)	1.488(9)
Cl(1) − Cu − Cl(2)	145.98(6)	C(21) − N − C(41)	111.2(3)
Cl(1) − Cu − Cl(2')[1]	96.15(5)	C(31) − N − C(41)	105.6(3)
Cl(1) − Cu − Cl(3)	98.91(5)	N − C(11) − C(12)	116.8(4)
Cl(2) − Cu − Cl(3)	97.45(5)	C(11)−C(12)−C(13)	109.0(5)
Cl(2') − Cu − Cl(3)[1]	147.54(6)	N − C(21) − C(22)	116.5(4)
Cl(2') − Cu − Cl(2)[1]	85.47(5)	C(21)−C(22)−C(23)	110.2(5)
Cu − Cl(2) − Cu'[1]	94.53(5)	N − C(31) − C(32)	116.0(4)
C(11) − N − C(21)	105.4(3)	C(31)−C(32)−C(33)	109.3(5)
C(11) − N − C(31)	112.0(3)	N − C(41) − C(42)	115.9(4)
C(11) − N − C(41)	111.3(3)	C(41)−C(42)−C(43)	110.8(4)
C(21) − N − C(31)	111.6(3)		

[1] Cu' and Cl(2') are centrosymmetrically related to Cu
and Cl(2). respectively.
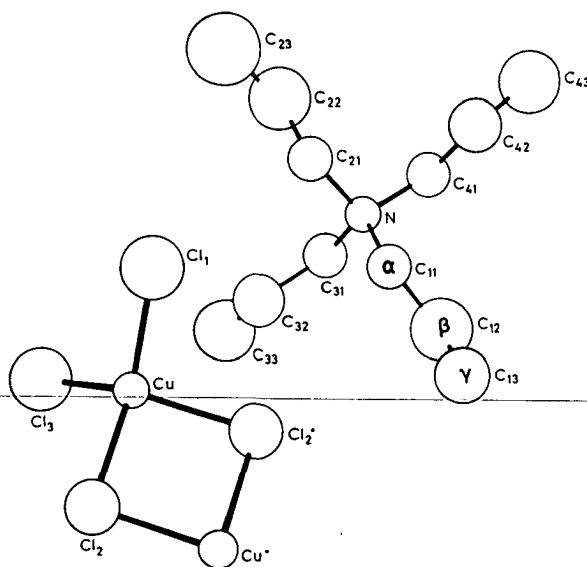
Figure 4. View of the molecular structure of the [TPA−
Cu$_2$Cl$_4$]$^+$ fragment. The thermal ellipsoids correspond to the
50% probability surfaces. The H−atoms nave been left out
for clarity.

observed in the isomorphous TPA–Br–CuCl$_2$ crystal (see:
Experimental). In that structure the Br atoms are
distributed over the Cl(1) and Cl(3) positions.

– TPA geometry

The literature search in the Cambridge Structural Database
contained 45 hits. Two hits referred to TPA in Silicalite–1
(7) which was discussed earlier (5). In five other
structures no TPA-coordinates were given . Four structures
were not usable because of disordered TPA molecules.
Torsion angles of the TPA molecules in the remaining
structures (and the title compound) are listed in Table 3
together with their point symmetry and conformation.

As can be seen in Table 3 the conformations A and B, as
calculated by van de Graaf (9) for tetrapropylmethane appear
in TPA as well. No preference for either conformation is
observed, indicating a small difference in steric energy,
which is to be expected on the basis of the data for
4,4–dipropylheptane.

Except for (TPA)$_4$–Mo$_4$H$_4$(CO)$_{12}$ the value of β is hardly
influenced by the counterion nor by the conformation
geometry (A,B) of the TPA molecule. The average value of β
observed over all structures is $\pm173°$. Observed values of β
below $\pm160°$ are mentioned in Table 3 (footnotes).

In addition to TPA–ZSM–5 some other TPA-containing crystal
structures are found to deviate from conformations A and B.
In (TPA)$_2$–W$_2$Br$_9$ and in (TPA)$_2$–Cu$_5$I$_7$ eclipsed conformations
(E) are present whereas in (TPA)$_2$–Cu$_4$Br$_6$ deviating α-values
of 90° are found (–).

In the two TPA orientations of ZSM–5 as presented by van
Koningsveld et al. (5) orientation 1 resembles conformation
B whereas orientation 2 contains an eclipsed conformation.
However, these remarks should be considered with care,
because of the disordering of the TPA ions: Changing propyl
chain nr. 3 to its mirror-related position leads to a new
set of α-values which still deviate from the A and B

Table 3. α torsion angles (°) for several TPA-containing cry

Structure	Point symmetry + conformation[1]		$C_{1\beta}-C_{1\alpha}-N-C_{i\alpha}$			$C_{2\beta}-C_{2\alpha}-N-C_{i\alpha}$		
			i=2	i=3	i=4	i=1	i=3	i=4
$C(C_3H_7)_4$ (calculated)	$\bar{4}$	A	180	59	−59	180	−59	59
$C(C_3H_7)_4$ (calculated)	$\bar{4}$	B	−174	65	−54	−65	54	174
TPA−Br	$\bar{4}$	A	57	179	−64	57	−64	179
TPA−PBr$_4$	1	A	59	180	−60	57	−59	179
$(TPA)_2-S_7$	1	A	−57	61	−180	−63	178	58
TPA−CuCl$_2$	2	B	173	54	−65	65	−174	−54
$(TPA)_2-UO_2Cl_4$[2]	1	A	54	175	−61	58	−59	177
	1	A	55	176	−63	61	−55	−177
$(TPA)_2-(C(NH_2)_3)Br_3$[2]	1	A	177	51	−58	−175	−52	64
	1	B	−53	169	75	−46	78	−169
$TPA-(C(NH_2)_3)_2Br_3$[2]	1	B	−57	60	−175	63	−47	−172
	1	A	58	178	−64	71	−64	−178
$(TPA)_2-PtCl_4-PtCl_2-$	1	B	72	−167	−48	173	54	−65
$(CH_3NH_2)_2$[2]	1	B	67	−174	−53	165	47	−73
$TPA-(C_6H_4(OH)_2)-Br$	1	B	63	−55	−174	−169	71	48
$TPA-(C_6H_5SiF_4)$	1	A	−59	59	180	−61	179	58
$TPA-Ga(C_2H_5S)_4$	$\bar{4}$	B	65	54	−173	173	−65	54
$TPA-Pb(C_6H_5S)_3$	1	B	−66	54	174	56	176	−63
$TPA-CrCl_4(C_2H_2-$	1	B	68	−51	−170	178	−62	57
$(P(C_6H_5)_2)_2)$								
$TPA-Co(C_{10}H_{13}S)_3(CH_3CN)$	1	B	−60	180	59	−57	63	−177
$TPA-Co(C_{12}H_8N_2)-$	1	A	55	−61	174	55	175	−58
$(C_4N_2S_2)_2$								
$(TPA)_2-Cu_2Cl_6$	1	A	61	−177	−59	62	−59	−177
$(TPA)_2-Ga_2Br_6$[2]	2	B	54	172	−72	−54	−178	64
	2	A	59	180	−53	59	−56	−178
$(TPA)_2-Sb_2Cl_8$[2]	1	B	177	59	−60	72	−169	−48
	1	A	59	−56	−178	64	−175	−54

stal structures.

$C_{3\beta}$-$C_{3\alpha}$-N-$C_{i\alpha}$			$C_{4\beta}$-$C_{4\alpha}$-N-$C_{i\alpha}$			Reference
i=1	i=2	i=4	i=1	i=2	i=3	
59	−59	180	−59	59	180	9
174	.54	−65	−54	65	174	
−179	−57	64	−57	−179	64	16
−177	−55	63	−57	−179	58	17
55	176	−63	180	57	−61	18
54	−65	173	−174	−54	65	19
175	−66	53	−65	177	54	20
−177	−55	63	−54	−177	61	
58	−63	172	−66	54	178	21
−52	−179	63	174	−55	54	
176	−66	59	169	48	−72	22
−178	−49	64	−58	177	47	
−62	56	176	−55	−175	65	23
−60	58	178	−58	−176	62	
−54	−174	65	−65	57	175	24
58	178	−61	−179	60	−58	25
−54	−173	65	−65	54	173	26
−177	62	−58	72	−168	−47	27
−59	−178	61	−66	54	174	28
−73	165	46	176	−62	58	29
174	−66	50	−62	179	58	30
−178	−60	61	−59	−177	62	
172	−72	54	−178	64	−54	31
180	−53	59	−56	−178	59	
51	−68	170	−179	−58	62	14
−61	179	57	177	−62	54	

p.t.o.

(Table 3 cont.)

$(TPA)_2-Cu_2I_4$	1	B	170	50	-69	64	-175	-55
$(TPA)_2-Hg_2I_6$	1	B	69	-168	-51	-66	175	56
$(TPA)_2-W_2Br_9$ [2]	1	E	-15	94	-147	-53	-163	77
	1	-	-178	-52	63	-91	150	26
$(TPA)_2-AgWS_4(CN)$ [2]	1	B	56	-62	177	55	175	-66
	1	B	58	-64	175	46	166	-71
$(TPA)_2-CuMoS_4(CN)$ [2]	1	B	169	-69	49	63	-61	-177
	1	B	172	-67	53	64	-56	-175
$(TPA)_2-CuMoS_4(C_6H_5S)$ [2]	1	A	52	174	-65	58	-59	180
	1	B	-65	177	56	-173	-54	67
$(TPA)_2-P_2S_5(CN)_2$ [2]	1	B	36	162	-82	57	-68	171
	1	B	52	172	-67	58	-62	177
$TPA-P_4S_9N$	1	B	-59	61	179	-51	-169	70
$(TPA)_2-Cu_2MoS_4(C_6H_5S)_2$	1	A	62	-177	-55	61	-58	-178
$TPA-Fe_3Cl_3VS_4(C_4H_{16}P_2)-$	1	B	-56	67	-174	-47	-169	71
$(CH_3CN)_3$								
$(TPA)_2-Cu_5I_7$ [2]	1	E	82	-57	-177	10	134	-100
	1	B	-68	175	57	-173	63	-57
$(TPA)_2-Cu_4Br_6$ [3]	4	A	-179	-57	59	-179	59	-57
	4	B	56	175	-63	56	-63	175
	2	-	169	-52	90	68	-90	164
$(TPA)_4-Mo_4H_4(CO)_{12}$ [4]	1	A	177	54	-61	-179	-55	61
	1	A	56	178	-66	55	-62	178
	1	A	-62	177	59	-51	70	-173
	1	A	-180	-60	60	-175	67	-54
$(TPA)_4-Co_8S_6(C_6H_5S)_8$ [4]	1	A	57	180	-58	58	-60	178
	1	A	-58	-180	58	-58	57	-178
	1	A	59	-180	-59	56	-64	178
	1	B	167	-67	52	82	-33	-164
$(TPA)_4-Rh_{12}C_2(CO)_{23}$ [4]	1	A	68	-173	-52	54	-64	177
	1	A	61	-179	-57	52	-69	175
	1	B	-67	174	56	-168	-53	68
	1	B	-77	42	170	-175	54	-67
$(TPA)_3-Rh_{17}(CO)_{30}$	1	B	-179	-59	61	-60	180	60
$(TPA)_n-(Cu_3I_4)_n$	2	A	54	175	-63	57	-59	179

55	−63	175	−174	−57	64	15
53	174	−65	−60	180	59	13
157	−87	37	−76	154	39	32
−54	65	−169	−178	65	−64	
−170	70	−50	65	−174	−55	33
−174	64	−56	68	−172	−50	
−165	−42	75	55	−67	175	33
−176	−56	64	55	−64	175	
180	−59	58	−64	175	54	34
65	−53	−174	50	170	−71	
48	−178	−59	−164	68	−52	36
64	−173	−56	−171	67	−52	
178	−63	58	−68	171	51	37
179	−60	56	−58	−180	61	34
173	−63	56	−69	170	49	35
−176	63	−58	67	171	−50[5]	38
38	163	−77	70	−50	−171[6]	
−59	57	179	57	−59	179	39
63	175	−56	−175	63	−56	
−52	90	169	−90	164	68[7]	
60	−62	179	−63	58	178	40
179	−61	59	−60	177	54[8]	
176	53	−64	61	176	−57[9]	
−58	60	−179	59	−59	179[10]	
−180	−57	59	−55	−175	61	41
−177	61	−58	57	177	−59[11]	
−180	−57	58	−55	−177	65	
−174	−60	70	53	−57	168[12]	
178	−62	55	−64	174	55	42
174	−64	50	−60	179	63	
64	−55	−176	43	166	−72	
53	169	−71	70	−35	−154	
−57	63	−177	172	52	−68	43
175	−63	54	−59	179	57	44

p.t.o.

(Table 3 cont.)

TPA-ZSM-5[13,14]	1	B	149	45	-76	46	158	-87
	1	E	-61	168	78	-111	-3	115
TPA-ZSM-5[13,15]	1	-	149	79	-76	46	177	-87
	1	-	-61	179	78	-111	-37	115

[1] A=conformation A: B=conformation B (see Figure 2: E=eclips
as well as from B. [2] Two different TPA-molecules present in
present in unit cell. [4] Four different TPA-molecules presen
[6] β for chain nr. 4 is -157°. [7] A C_α-C_α distance of 1.83A is
for chain nr. 3 is -98°. [10] β for chain nr. 2 is -74°. [11] β
nr. 1 is -150°. [13] Two orientations are present. [14] For ZSM-
towards the sinusoidal channels of the zeolite whereas propy
straight channels. [15] Orientations as suggested in this Chap

Table 4. Groups of molecules in which a relation between
anion radius or length and TPA conformation seems to be
present. The chemical formula of the anions is presented
in such a way that the anionic structure becomes visible.
The explanation for the conformation indices A, B, E and
- are given in Table 3.

spherical anions		carbonyl systems	
A	TPA-Br	AAAA	$(TPA)_4-Mo_4H_4(CO)_{12}$
AA	$(TPA)_2-S_7$	AABB	$(TPA)_4-Rh_{12}C_2(CO)_{23}$
AA	$(TPA)_2-UO_2Cl_6$	BBB	$(TPA)_3-Rh_{17}(CO)_{30}$
A	$TPA-PBr_4$		
AB-	$(TPA)_2Cu_4Br_6$		
BE	$(TPA)_2-Cu_5I_7$		
B	$TPA-P_4S_9N$		

binuclear anions		polynuclear anions	
AA	$(TPA)_2-Cl_2CuCl_2CuCl_2$	BB	$(TPA)_2-(CN)S_2PSPS_2(CN)$
AB	$(TPA)_2-Cl_3SbCl_2SbCl_3$	BB	$(TPA)_2-(CN)AgS_2WS_2$
AB	$(TPA)_2-Br_3GaGaBr_3$	BB	$(TPA)_2-(CN)CuS_2MoS_2$
BB	$(TPA)_2-I_2HgI_2HGI_2$	AB	$(TPA)_2-(C_6H_5S)CuS_2MoS_2$
EE	$(TPA)_2-Br_3WBr_3WBr_3$	AA	$(TPA)_2-(C_6H_5S)CuS_2MoS_2Cu(C_6H_5S)$
		A	$(TPA)_n-(Cu_3I_4)_n$

172	60	-65	-53	78	-173	5
-68	176	49	-104	30	145	
-107	-161	49	-53	78	145	
-169	91	-65	-104	30	-173	

ed conformation; -=strong deviation from A
unit cell. [3] Three different TPA-molecules
t in unit cell. [5] β for chain nr. 2 is -156°.
 measured. [8] β for chain nr. 4 is 91°. [9] β
for chain nr. 1 is -158°. [12] β for chain
5 the propyl chains 1 and 2 are located
1 chains 3 and 4 are located towards the
ter.

conformations but does not contain an eclipsed CNCC
fragment.

The occurrence of non-bonded contacts between terminal
methyl groups in neighbouring TPA-ions and the rigid shape
of the ZSM-5 channels might explain the deviations from the
ideal A.B geometry in the α torsion angles of TPA in ZSM-5.
However this can not be the explanation for the deviations
observed for (TPA)$_2$-W$_2$Br$_9$, (TPA)$_2$-Cu$_5$I$_7$ and (TPA)$_2$-Cu$_4$Br$_6$ as
no close anion-cation or cation-cation contacts are observed
for these materials.

In some cases it looks as if the radius or length of the
anion associated with TPA affects the conformation of the
TPA ion. In Table 4. some sets of compunds are arranged
according to increasing radius of the anion. Small anions
seem to prefer conformation A and larger anions conformation
B.

In (TPA)$_2$-Hg$_2$I$_6$ and (TPA)$_2$-W$_2$Br$_9$, having the largest
radius, conformations B and E are observed, respectively.
The smaller radius of (TPA)$_2$-Cu$_2$Cl$_6$ is accompanied with
conformation A. (TPA)$_2$-Sb$_2$Cl$_8$ and (TPA)$_2$-Ga$_2$Br$_6$, having an
intermediate anion radius, show a mixture of both
conformations.

However, a reverse order is observed for polynuclear anions. Relatively short anions have TPA in a B conformation whereas in longer or polymeric anions conformation A is observed.

These observed effects ask for a closer examination. which is beyond the scope of this Thesis.

ACKNOWLEDGEMENTS

REFERENCES

1. Argauer, R.J. and Landolt. S.R. US Patent 3.702.886 (1972).
2. Gaag. F.J. van der, Jansen. J.C. and Bekkum. H. van. Appl. Catal. 1985, 17, 261.
3. Lok, B.M., Cannau, T.R. and Messina. C.A. Zeolites 1983, 3, 282.
4. Nastro, A., Colella, C. and Aiello. R. 'Zeolites: Synthesis. Structure and Technical Applications'. Stud. Surf. Sci. Catal. 1985, 24. 39.
5. Koningsveld, H. van, Bekkum, H. van and Jansen, J.C. Acta Cryst. 1987, B43, 127.
6. Baerlocher, C. Proc. 6th Int. Zeolite Conf. (ed. D. Olson and A. Bisio) Butterworths, Guildford 1984, p. 823.
7. Price, G.D., Pluth, J.J., Smith, J.V., Bennet, J.M. and Patton, R.L. J. Am. Chem. Soc. 1982, 104, 5971.
8. Chao, K.J., Lin, J.C., Wang, Y. and Lee, G.H. Zeolites 1986, 6, 35.
9. Graaf, B. van de. To be published.
10. 'International Tables for X-ray Crystallography, Vol. IV', Kynoch Press, Birmingham 1974. p. 71 (Present distributor D. Reidel, Dordrecht).
11. Stewart, J.M., Kruger, G.J., Ammon. H.L., Dickinson. E.W. and Hall, S.R. 'The XRAY72 system', Tech. Rep. TR-192. Computer Science Center, Univ. of Maryland, College Park, Maryland, U.S.A., 1972.
12. Allen, F.H., Bellard, S., Brice, M.D., Cartwright, B.A., Doubleday, A., Higgs, H., Hummelink, T., Hummelink-Peters, B.G., Kennard, O., Motherwell, W.D.S., Rodgers, J.R. and Watson, D.G. Acta Cryst. 1979, B35, 2331.
13. Contreras, J.G., Seguel, G.V. and Hoenle, W. J. Mol. Struct. 1980, 68, 1.

14. Ensinger, U., Schwartz, W. and Schmidt. A. Z. Naturforsch., Teil B 1982, 37, 1584.
15. Asplund, M. and Jagner, S. Acta Chem. Scand. Ser. A 1984, 38, 411.
16. Zalkin. A. Acta Cryst. 1957, 10, 557.
17. Sheldrick, W.S., Schmidpeter, A., Zwaschka, F., Dillon, K.B., Platt, A.N.G. and Waddington, T.C.W. J. Chem. Soc.. Dalton, 1981, 413.
18. Bottcher. P. and Flamm. W. Z. Naturforsch., Teil B 1986, 41, 1000.
19. Anderson. S. and Jagner, S. Acta Chem. Scand.. Ser. A 1986, 40, 52.
20. Di Sipio, L.. Tondello, C., Pellici. G., Ingletto, G. and Montenero, A. Cryst. Struct. Comm. 1974, 3, 731.
21. Taga, T., Ohashi, Miyajima, K., Yoshida, H. and Osaki, K. Chem. Lett. 1977, 917.
22. Taga, T., Ohashi, M.. Osaki, K., Miyajima, K. and Yoshida, H. Bull. Chem. Soc. Japan 1979, 52, 1851.
23. Brammer, L.. Charnock, J.M., Goggin, P.L., Goodfellow, R.J., Koetze. T.F. and Orpen, A.G. J. Chem. Soc.. Chem. Comm. 1987, 443.
24. Khan, A. J. Mol. Struct. 1986. 145, 203.
25. Schomburg, D. J. Organomet. Chem. 1981, 221, 137.
26. Maelia, L.E. and Koch, S.A. Inorg. Chem. 1986, 25, 1896.
27. Christou. G., Folting. K. and Huffman. J.C. Polyhedron 1984, 3. 1247.
28. Gray, L.R., Hale, A.L., Levason. W., McCullough, F.P. and Webster. M. J. Chem. Soc., Dalton Trans. 1983, 2573.
29. Koch, S.A.. Fikar, R.. Millar, M. and O'Sullivan. T. Inorg. Chem. 1984, 23, 121.
30. Khare. G.P. and Eisenberg. R. Inorg. Chem. 1970, 9, 2211.
31. Cumming, H.J. Hall. D. and Wright. C.E. Cryst. Struct. Comm. 1974, 3, 107.
32. Templeton. J.L.. Jacobson, R.A. and McCarley, R.E. Inorg. Chem. 1977, 16, 3320.
33. Gheller, S.F., Hambley, T.W., Rodgers, J.R., Brownlee, R.T.C, O'Connor, M.J. Snow, M.R. and Wedd, A.G. Inorg. Chem. 1984, 23, 2519.
34. Acott, S.R.. Garner. C.D.. Nicholson, J.R. and Clegg, W. J. Chem. Soc.. Dalton Trans. 1983, 713.
35. Roesky, W., Noltemeyer, M. and Sheldrick. G.M. Z. Naturforsch., Teil B 1986, 41, 803.
36. Roesky, W.. Benmohamed, S.. Noltemeyer, M. and Sheldrick. G.M. Z. Naturforsch.. Teil B 1986. 41, 938.
37. Kovacs. J.A. and Holm. R.H. Inorg. Chem. 1987, 26, 711.
38. Hartl. H. and Mahdjour-Hassan-Abadi. F. Angew. Chem. Int. Ed. E 1984, 23, 378.
39. Asplund, M. and Jagner, S. Acta Chem. Scand.. Ser. A 1984, 38, 725.
40. Lin. J.T. and Ellis, J.E. J. Amer. Chem. Soc. 1983. 105, 6252.
41. Christou. G.. Hagen, K.S., Bashkin. J.K. and Holm. R.H. Inorg. Chem. 1985. 24, 1010.

42. Albano, V.G., Braga, D., Strumolo, D., Seregni, C. and
    Martinengo, S. J. Chem. Soc., Dalton Trans. 1985,
    1309.
43. Ciani, G., Magni, A., Sironi, A. and Martinengo, S. J.
    Chem. Soc., Chem. Comm. 1981, 1280.
44. Hartl, H. and Mahdjour-Hassan-Abadi. F. Z.
    Naturforsch., Teil B 1984, <u>39</u>, 149.

Table 1. (Suppl.). Anisotropic thermal parameters $(A^2 \times 10^3)$ and H-atom positions. E.s.d.'s in parentheses.

Atom	U_{11}	U_{22}	U_{33}	U_{12}	U_{13}	U_{23}
Cu	47.2(3)	39.3(3)	47.6(3)	17.6(2)	17.6(2)	17.0(2)
Cl(1)	76.8(8)	51.1(6)	80.5(8)	25.1(5)	32.9(6)	37.2(5)
Cl(2)	43.3(5)	62.6(6)	72.1(7)	22.4(5)	25.6(5)	36.3(5)
Cl(3)	81.0(8)	68.3(7)	54.5(7)	21.4(6)	2.3(6)	10.2(5)
N	44(2)	36(1)	40(1)	16(1)	18(1)	11(1)
C(11)	52(2)	46(2)	44(2)	25(2)	21(2)	19(2)
C(12)	83(3)	65(3)	67(3)	48(3)	35(2)	32(2)
C(13)	60(3)	56(2)	65(3)	24(2)	8(2)	28(2)
C(21)	48(2)	45(2)	42(2)	23(2)	19(2)	17(2)
C(22)	77(3)	81(3)	48(2)	44(3)	24(2)	30(2)
C(23)	82(4)	87(4)	65(3)	49(3)	23(3)	41(3)
C(31)	53(2)	38(2)	48(2)	11(2)	20(2)	8(2)
C(32)	54(3)	55(3)	75(3)	7(2)	25(2)	14(2)
C(33)	69(3)	56(3)	91(4)	0(2)	17(3)	17(3)
C(41)	47(2)	44(2)	52(2)	17(2)	25(2)	16(2)
C(42)	54(2)	51(2)	70(3)	12(2)	21(2)	10(2)
C(43)	49(3)	76(3)	85(4)	10(2)	18(3)	36(3)

	x/a	y/b	z/c	U[1]
H(11,1)[2]	0.615(5)	0.927(5)	0.427(4)	0.057
H(11,2)	0.457(5)	0.784(5)	0.387(4)	0.057
H(12,1)	0.522(5)	0.567(6)	0.341(4)	0.076
H(12,2)	0.677(6)	0.693(6)	0.375(5)	0.076
H(13,1)	0.697(6)	0.650(6)	0.549(4)	0.089
H(13,2)	0.546(6)	0.687(6)	0.554(6)	0.089
H(13,3)	0.707(6)	0.830(6)	0.594(5)	0.089
H(21,1)	0.350(5)	0.883(5)	0.257(4)	0.057
H(21,2)	0.509(5)	1.028(5)	0.302(4)	0.057
H(22,1)	0.326(6)	0.825(6)	0.046(4)	0.076
H(22,2)	0.477(6)	0.965(6)	0.093(4)	0.076
H(23,1)	0.238(6)	1.012(6)	0.162(5)	0.089
H(23,2)	0.294(6)	1.066(6)	0.042(5)	0.089

Atom	x	y	z	U
H(23,3)	0.376(7)	1.132(7)	0.181(5)	0.089
H(31,1)	0.378(5)	0.619(5)	0.062(4)	0.057
H(31,2)	0.459(5)	0.552(5)	0.158(4)	0.057
H(32,1)	0.244(5)	0.512(5)	0.250(4)	0.076
H(32,2)	0.169(6)	0.584(6)	0.151(4)	0.076
H(33,1)	0.183(6)	0.305(6)	0.064(5)	0.089
H(33,2)	0.037(6)	0.323(6)	0.073(5)	0.089
H(33,3)	0.116(6)	0.367(6)	−0.033(5)	0.089
H(41,1)	0.628(5)	0.831(5)	0.113(4)	0.057
H(41,2)	0.710(5)	0.762(5)	0.216(3)	0.057
H(42,1)	0.848(5)	1.058(6)	0.377(4)	0.076
H(42,2)	0.764(6)	1.104(6)	0.311(4)	0.076
H(43,1)	1.023(6)	1.200(6)	0.287(5)	0.089
H(43,2)	0.899(6)	1.059(6)	0.141(5)	0.089
H(43,3)	0.980(6)	1.005(6)	0.215(5)	0.089

1) U was kept fixed during refinement.

2) H(n,m): H-atom is bonded to C(n).

Table 2. (Suppl.) Bond lengths (Å) and angles (°) concerning the H-atoms. E.s.d.'s in parentheses.

Bond	length		Bond	length
C(11) – H(11,1)	0.99(3)		C(31) – H(31,1)	1.00(5)
C(11) – H(11,2)	0.80(5)		C(31) – H(31,2)	1.02(5)
C(12) – H(12,1)	1.10(4)		C(32) – H(32,1)	1.08(5)
C(12) – H(12,2)	0.74(6)		C(32) – H(32,2)	0.89(6)
C(13) – H(13,1)	1.06(7)		C(33) – H(33,1)	1.03(6)
C(13) – H(13,2)	0.87(6)		C(33) – H(33,2)	0.86(6)
C(13) – H(13,3)	0.89(4)		C(33) – H(33,3)	0.92(7)
C(21) – H(21,1)	0.85(5)		C(41) – H(41,1)	1.06(4)
C(21) – H(21,2)	0.99(3)		C(41) – H(41,2)	1.08(5)
C(22) – H(22,1)	0.98(4)		C(42) – H(42,1)	1.00(5)
C(22) – H(22,2)	0.80(6)		C(42) – H(42,2)	0.89(6)
C(23) – H(23,1)	0.95(6)		C(43) – H(43,1)	1.02(4)
C(23) – H(23,2)	1.03(6)		C(43) – H(43,2)	1.04(6)
C(23) – H(23,3)	0.78(4)		C(43) – H(43,3)	0.90(7)

Angle	value		Angle	value
N –C(11)–H(11,1)	106(3)		N –C(31)–H(31,1)	108(2)
N –C(11)–H(11,2)	107(3)		N –C(31)–H(31,2)	104(2)

H(11,1)-C(11)-H(11,2)	105(4)	H(31,1)-C(31)-H(31,2)	110(4)
C(12) -C(11)-H(11,2)	111(3)	C(32) -C(31)-H(31,1)	108(2)
C(12) -C(11)-H(11,2)	111(4)	C(32) -C(31)-H(31,2)	111(2)
C(11) -C(12)-H(12,1)	104(3)	C(31) -C(32)-H(32,1)	109(2)
C(11) -C(12)-H(12,2)	114(5)	C(31) -C(32)-H(32,2)	113(3)
C(13) -C(12)-H(12,1)	113(3)	C(33) -C(32)-H(32,1)	109(2)
C(13) -C(12)-H(12,2)	122(4)	C(33) -C(32)-H(32,2)	102(2)
H(12,1)-C(12)-H(12,2)	92(4)	H(32,1)-C(32)-H(32,1)	114(5)
C(12) -C(13)-H(13,1)	101(3)	C(32) -C(33)-H(33,1)	103(3)
C(12) -C(13)-H(13,2)	112(3)	C(32) -C(33)-H(33,2)	101(3)
C(12) -C(13)-H(13,3)	107(5)	C(32) -C(33)-H(33,3)	114(3)
H(13,1)-C(13)-H(13,2)	111(5)	H(33,1)-C(33)-H(33,2)	110(6)
H(13,1)-C(13)-H(13,3)	107(5)	H(33,1)-C(33)-H(33,3)	108(5)
H(13,2)-C(13)-H(13,3)	110(5)	H(33,2)-C(33)-H(33,3)	119(5)
N -C(21)-H(21,1)	109(4)	N -C(41)-H(41,1)	104(2)
N -C(21)-N(21,2)	110(3)	N -C(41)-H(41,2)	105(2)
H(21,1)-C(21)-H(21,2)	102(4)	H(41,1)-C(41)-H(41,2)	108(3)
C(22) -C(21)-H(21,1)	110(3)	C(42) -C(41)-H(41,1)	112(2)
C(22) -C(21)-H(21,2)	108(3)	C(42) -C(41)-H(41,2)	111(2)
C(21) -C(22)-H(22,1)	112(3)	C(41) -C(42)-H(42,1)	117(3)
C(21) -C(22)-H(22,2)	112(4)	C(41) -C(42)-H(42,2)	114(2)
C(23) -C(22)-H(22,1)	110(4)	C(43) -C(42)-H(42,1)	109(3)
C(23) -C(22)-H(22,2)	113(5)	C(43) -C(42)-H(42,2)	118(3)
H(22,1)-C(22)-H(22,2)	100(4)	H(42,1)-C(42)-H(42,2)	86(5)
C(22) -C(23)-H(23,1)	107(4)	C(42) -C(43)-H(43,1)	109(3)
C(22) -C(23)-H(23,2)	112(3)	C(42) -C(43)-H(43,2)	112(3)
C(22) -C(23)-H(23,3)	107(5)	C(42) -C(43)-H(43,3)	118(4)
H(23,1)-C(23)-H(23,2)	122(5)	H(43,1)-C(43)-H(43,2)	111(4)
H(23,1)-C(23)-H(23,3)	93(5)	H(43,1)-C(43)-H(43,3)	115(5)
H(23,2)-C(23)-H(23,3)	113(5)	H(43,2)-C(43)-H(43,3)	91(5)

SUMMARY

This Thesis deals with high-silica zeolites and their use as catalyst in organic chemistry.

In Chapter I an introduction on zeolites is given. For example, aspects as structure, chemical composition and catalysis are discussed. In addition the scope of this Thesis is presented.

In Chapter II a frequently observed but never assigned absorption in the 1060-1010 cm^{-1} region of IR spectra of zeolite ZSM-5 is discussed. To examine if this vibration can be correlated to the ZSM-5 framework or to an impurity, the effects of several parameters, such as morphology, particle size and chemical composition were studied. It is concluded that the absorption indicates non-ZSM-5 framework material in the surface layer of particles with an average particle size larger than 2 microns.

Chapter III shows that the Al-gradient present in ZSM-5 influences the rate and selectivity of the dissolution of the zeolite particles in 2M sodium hydroxide. Experiments on ZSM-5 and Silicalite-1 with 1.0M hydrofluoric acid reveal a more homogeneous mechanism to be effective.

Chapter IV discusses the factors affecting the synthesis of the high-silica zeolite Theta-1/Nu-10. In the literature a large variety in synthesis conditions and templates is mentioned. Among the templates used oligo-iminoethylenes are the most suitable. The effects of variation of template concentration, OH^-/SiO_2 ratio and synthesis time on the formation of pure Theta-1/Nu-10 are reported.

Chapter V deals with the reaction of ammonia and ethanol or related compunds towards pyridines using the zeolite Nu-10 as the catalyst. Different proton-introduction procedures of the catalyst result in different catalytic activities and selectivities. It is shown that a combination of ethanol, methylamine and air and Nu-10 or ZSM-5 as the catalyst gives high selectivities towards

pyridine and 4-methyl-pyridine.

In Chapter VI considerations are given regarding the pyridine-formation mechanism out of ethanol and ammonia over high-silica zeolites. Zeolitic acid sites are shown to catalyze the dehydrogenation of ethanol together with condensation, cyclisation and aromatisation, while structural defects probably are responsible for oxidation products as ethanal and formaldehyde, which are thought to play an important role in the reaction. A C_1/C_2-reactant system is presented, showing a selectivity towards pyridine of 80%.

The hydroxyalkylation of phenol with glyoxylic acid over various Al-containing catalysts in aqueous medium is presented in Chapter VII. The catalytic activity of these Al-containing solid materials could be traced back to dissolved Al^{III}-ions which catalyze the reaction in a homogeneous way. In addition, dealumination of zeolite Na-Y by aqueous glyoxylic acid has been studied. Extraction of both Si and Al from the zeolite was observed during the dealumination reaction.

In Chapter VIII the conformation of the tetrapropyl-ammonium (TPA) ion in crystal lattices is reviewed. The crystal structure of $(TPA)_2Cu_2Cl_6$ has been solved because it interpolates in the series of studied structures. In the crystal structures examined, two different TPA conformations occur regularly, both having CCNC torsion angles of 180, 60 and −60°. Eclipsed conformations are observed exceptionally. When occluded in the zeolite ZSM-5, TPA exhibits an energetically unfavourable conformation which is probably due to interactions of the terminal methyl groups with those of neighbouring TPA ions.

SAMENVATTING

Dit Proefschrift behandelt zeolieten met een hoog
silicagehalte en hun gebruik als katalysator in de
organische chemie.

In Hoofdstuk I wordt een algemene inleiding betreffende
zeolieten gegeven. Zo worden bijvoorbeeld aspecten als
structuur, chemische samenstelling en katalyse nader
bekeken. Aansluitend wordt de strekking van dit
proefschrift besproken.

Hoofdstuk II beschrijft een vaak waargenomen (maar tot nu
toe nooit verklaarde) infraroodabsorptie in het gebied
tussen 1060 en 1030 cm^{-1}, in spectra van ZSM-5. Om na te
gaan of er een samenhang bestaat tussen deze vibratie en het
ZSM-5 rooster of de aanwezigheid van een onzuiverheid, is
het effect van diverse parameters zoals morfologie,
deeltjesgrootte en chemische samenstelling bestudeerd. Uit
het onderzoek kwam naar voren dat de absorptie duidt op de
aanwezigheid van niet tot het ZSM-5 rooster behorend
materiaal dat aanwezig is in de oppervlaktelaag van deeltjes
groter dan 2 micron.

Hoofdstuk III laat zien dat de Al-gradient, welke aanwezig
is in ZSM-5, van invloed is op zowel de snelheid als op de
selectiviteit van de oplosbaarheid van zeolietdeeltjes in 2M
natrium hydroxide. Experimenten met ZSM-5 en Silicaliet-1
met 1M fluorwaterstofzuur laten een meer homogeen mechanisme
zien.

Hoofdstuk IV betreft een studie naar de factoren welke van
invloed zijn op de synthese van de hoog-silica zeoliet
Theta-1/Nu-10. In de literatuur worden veel verschillende
synthesecondities en templates genoemd in de literatuur. In
de door ons geteste templates blijken oligo-iminoethylenen
het meest geschikt. De effecten van variatie in template
concentratie, OH^-/SiO_2-verhouding en synthesetijd op de
vorming van zuiver Theta-1/Nu-10 worden gerapporteerd.

Hoofdstuk V beschrijft de reactie van ammonia en ethanol

of verwante verbindingen naar pyridines. met de zeoliet
Nu-10 als katalysator. Verschillende proton-introductie
procedures resulteren in verschillende katalytische
aktiviteiten en selektiviteiten. Een mengsel van ethanol,
methylamine en lucht, met Nu-10 als katalysator. geeft hoge
selektiviteiten naar pyridine en 4-methyl-pyridine.

In Hoofdstuk VI worden een aantal overwegingen gegeven
betreffende het mechanisme van de pyridinevorming uit
ethanol en ammonia over hoog-silica zeolieten. Aangetoond
wordt dat zure plaatsen in de zeoliet de dehydrogenering van
ethanol katalyseren en daarnaast condensatie. cyclisatie en
aromatisering. Voor oxidatieprodukten als ethanal en
formaldehyde daarentegen. waaraan een belangrijke rol in de
reactie wordt toegekend. zijn waarschijnlijk defekten in de
roosterstruktuur verantwoordelijk. Een C_1/C_2-reactanten
systeem wordt gepresenteerd met een selektiviteit naar
pyridines van 80%.

De hydroxylering van fenol met glyoxylzuur. door middel
van diverse Al-bevattende katalysatoren, in een waterige
omgeving wordt gepresenteerd in Hoofdstuk VII. De
katalytische aktiviteit van deze vaste stoffen kan worden
herleid tot opgeloste Al^{III}-ionen, welke de reactie homogeen
blijken te katalyseren. Daarnaast wordt de dealuminering
van de zeoliet NaY met behulp van een waterige
glyoxylzuuroplossing bestudeerd. Gedurende de
dealumineringsreactie wordt extractie van zowel Si als Al
waargenomen.

In Hoofdstuk VIII wordt een overzicht gegeven van de
conformaties van het tetrapropylammonium (TPA) ion in
kristalroosters. In de beschouwde structuren komen
hoofdzakelijk twee verschillende TPA conformaties voor.
beide met CCNC torsiehoeken van 180. 60 en -60°. Eclipsed
conformaties komen slechts bij uitzondering voor. Wanneer
TPA is ingesloten in de zeoliet ZSM-5 dan is de conformatie
energetisch ongunstig. Deze wordt hoogstwaarschijnlijk
veroorzaakt door interacties van de eindstandige
methylgroepen met die van naburige TPA ionen. De
kristalstruktuur van $(TPA)_2Cu_2Cl_6$ is opgelost omdat deze

goed interpoleerbaar is in de serie van bestudeerde structuren.

DANKWOORD

Ik zal altijd met plezier terugdenken aan de periode
waarin ik werkzaam ben geweest aan de TU Delft. Een fijne
werkomgeving en behulpzame (ex-)collega's hebben daartoe
bijgedragen. Een aantal van hen wil ik met name bedanken:
- Herman van Bekkum. voor de onnavolgbare wijze waarop
  hij door zijn enthousiaste begeleiding mij steeds
  opnieuw inspireerde.
- Fred van der Gaag. voor het leren van de basisprincipes
  en de daaropvolgende verhelderende discussies.
- Koos Jansen en Herman Kouwenhoven. voor het uitdiepen
  en in goede banen leiden van bepaalde problemen.
- Henk van Koningsveld. zonder wiens bijdrage Hoofdstuk
  VIII er heel anders zou hebben uitgezien.
- Erik de Vos Burchart. Patrik Voogd en Theo Maesen voor
  de prettige discussies en de collegialiteit.
- J.F. van Lent. voor de snelle en accurate XRD-service.
- Wim Jongeleen. voor de inzet van al zijn vakmanschap om
  mijn hersenschimmen in plaatjes om te zetten.
- Ernst Wurtz. die er voor zorgde dat alles bleef
  draaien.
- Fred Hammers en Piet Duilaart. voor het uitstekende
  fotowerk.
- Robbert Pierik. Jacques van Melis. Bas Schaaf en Eugene
  Straver. voor de prettige samenwerking en al datgene
  wat ik van hen heb kunnen leren.
- De koffieclub. voor de gezellige sociaal-culturele
  werkonderbreking.
- Annelies. voor de broodnodige ondersteuning die een
  promovendus buiten werktijd nodig heeft.
- En last but not least mijn ouders. die het mij mogelijk
  hebben gemaakt te worden wat ik nu ben.

CURRICULUM VITAE

Robert Arie le Febre werd op 17 december 1956 te Leiden geboren. Na het behalen van het HAVO–diploma in 1975 en het VWO–diploma in 1977 aan de Rembrandt Scholengemeenschap te Leiden begon hij in augustus 1977 met de scheikundestudie aan de Rijksuniversiteit te Leiden.

Het kandidaatsexamen (S1a) werd in april 1981 afgelegd. De studie voor het doctoraalexamen stond onder leiding van Prof.dr. J. Reedijk (coordinatiechemie). Dr. R.A.G. de Graaff (rontgendiffractie) en Prof.dr. J. Lugtenburg (kernspinresonantiespectroscopie). Dit examen werd in januari 1984 afgelegd.

Van 1 maart 1984 tot en met 29 februari 1988 was hij als wetenschappelijk assistent in dienst van NWO (SON). Het promotieonderzoek werd uitgevoerd aan de TU Delft onder leiding van Prof.dr.ir. H. van Bekkum.

Sinds 1 januari 1989 is hij werkzaam als analytical supervisor bij ICI Resins b.v. te Waalwijk.

PUBLICATIES UIT DIT PROEFSCHRIFT

- Hoofdstuk II (co-auteurs J.C. Jansen en H. van Bekkum)
- Hoofdstuk IV (co-auteurs H.W. Kouwenhoven en H. van Bekkum)

Nog ter publicatie aan te bieden:

- Hoofdstuk V + Hoofdstuk VI (co-auteur H. van Bekkum)
- Hoofdstuk VII (co-auteurs E. de Vos Burchart, R. Pierik, E.J.M. Straver en H. van Bekkum)
- Hoofdstuk VIII (co-auteurs H. van Koningsveld, B. van de Graaf, J.C. Jansen en H. van Bekkum)

9. Vergeleken met aanduidingen als "tetraedrisch" en "vlak-vierkant" voor twee typen vier-coordinatie. is de aan-duiding "octaedrisch" voor een bepaalde zes-omringing wat minder gelukkig.

10. Wanneer supergeleiding bij hogere temperaturen afhangt van de hoeveelheid afwijkingen en defecten in de mate-rialen wordt het moeiijk zich verbindingen voor te stellen die bij kamertemperatuur naast chemisch stabiel ook nog supergeleidend blijken te zijn.
    W. Hively. American Scientist 1988, 76, 13.

11. De bona fide aanwezigheid van olie onder een raffinade-rij (Rotterdam Charlois) en van mineraalwater onder een limonadefabriek (Bunnik) toont de burger dat het ook anders kan.

12. Het schrijven van een proefschrift is te vergelijken met een zwangerschap. Na een paar maanden kun je het fat-soenshalve niet meer onderbreken.

13. De inhoud van de tenminste zes. aan het proefschrift toegevoegde, niet op het promotieonderwerp betrekking hebbende, wetenschappelijk verantwoorde en verdedigbare stellingen hangt in sterke mate af van de interpretatie van de term "wetenschappelijk verantwoord".
    Promotiereglement TU Delft, p. 7.

14. Het verdient aanbeveling een milieuheffing in te voeren op diervoeders, gerelateerd aan de hoeveelheid en samenstelling van de te verwachten ontlasting.

15. The proposition that the first systems which were able to evolve through natural selection were crystals of clay, leaves a muddy taste.
    A.G. Cairns-Smith. Scientific American 1985, 252, 74.

R.A. le Febre
Delft, 23 maart 1989

STELLINGEN

1. In hun studie betreffende de adsorptie en diffusie van
    glucose en fructose in zeoliet X verzuimen Ching en
    Ruthven aandacht te schenkenaan de mutarotatie-isomeren
    van deze verbindingen.
    C.B. Ching en D.M. Ruthven. Zeolites 1988, 8, 68.

2. De afwezigheid van structuurkarakteristieke absorptie-
    banden in het IR-spectrum van zeoliet ZSM-39 als gegeven
    door Jansen et al. kan wijzen op een onvolledig verlopen
    synthesereactie.
    J.C. Jansen et al. Zeolites 1984, 4, 369.

3. De extra IR-absorptie bij 590 cm^{-1}, in het door Jacobs
    en Martens gepubliceerde IR-spectrum van zeoliet ZSM-22,
    duidt op de aanwezigheid van een verontreiniging.
    *P.A. Jacobs en J.A. Martens, "Synthesis of high-silica
    aluminosilicate zeolites", Stud. Surf. Sci. Catal. 33,
    Elsevier Amsterdam 1987, p. 41.*

4. Het onderzoek van Sulikowsky et al. aan aluminering van
    Silicaliet-1 vs. dealuminering van ZSM-5 zou aan waarde
    gewonnen hebben indien behalve de katalytische aktivi-
    teit van gedealumineerd ZSM-5 ook die van gealumineerde
    Silicaliet-1 gemeten was en vergeleken met een standaard
    ZSM-monster.
    *B. Sulikowsky et al. J. Chem. Soc.. Chem. Commun. 1987,
    1542.*

5. In hun studie betreffende het effect van additieven als
    chloorazijnzuur op de isomeer distributie in de vloei-
    stoffase-chlorering van benzeenderivaten over zeoliet KL
    als katalysator hebben Yazawa et al. verzuimd de reactie
    ook uit te voeren met additief in afwezigheid van
    zeoliet.
    *N. Yazawa. et al. "Preprints of the poster papers of the
    7th Int. Zeolite Conf.". Kodansha Ltd., Tokyo 1986, p.
    285.*

6. De claim van McVicker et al. dat metaalverontreinigingen
    in diverse katalysatoren. als alumina. silica-alumina of
    zeolieten. selektief verwijderd kunnen worden met behulp
    van oxaalzuur zonder oplossen van het dragermateriaal is
    aan twijfel onderhevig.
    *G.B. McVicker et al. US 4522928 (1983); DF 3337619
    (1984). Dit Proefschrift. Hoofdstuk VII.*

7. De uitkomst van een zeolietsynthese is vaak niet alleen
    afhankelijk van de molaire samenstelling van het reac-
    tiemengsel. maar ook van de soort en struktuur van de
    reactanten.
    Dit Proefschrift. Hoofdstuk IV.

8. Het synthetiseren van molekulaire zeven met een basisch
    rooster blijft. hoe zuur 't ook klinkt. voorlopig een
    utopie.